

Accepted Manuscript

Synthesis, crystal structure and effect of indeno[1,2-b]indole derivatives on prostate cancer *in vitro*. Potential effect against MMP-9

Gricela Lobo, Melina Monasterios, Juan Rodrigues, Neira Gamboa, Mario V. Capparelli, Javier Martínez-Cuevas, Michael Lein, Klaus Jung, Claudia Abramjuk, Jaime Charris

PII: S0223-5234(15)00272-X

DOI: [10.1016/j.ejmech.2015.04.023](https://doi.org/10.1016/j.ejmech.2015.04.023)

Reference: EJMECH 7838

To appear in: *European Journal of Medicinal Chemistry*

Received Date: 6 October 2014

Revised Date: 8 April 2015

Accepted Date: 9 April 2015

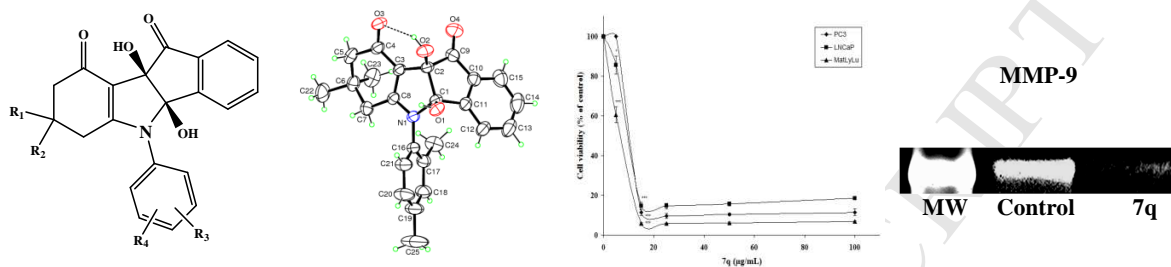
Please cite this article as: G. Lobo, M. Monasterios, J. Rodrigues, N. Gamboa, M.V. Capparelli, J. Martínez-Cuevas, M. Lein, K. Jung, C. Abramjuk, J. Charris, Synthesis, crystal structure and effect of indeno[1,2-b]indole derivatives on prostate cancer *in vitro*. Potential effect against MMP-9, *European Journal of Medicinal Chemistry* (2015), doi: 10.1016/j.ejmech.2015.04.023.

This is a PDF file of an unedited manuscript that has been accepted for publication. As a service to our customers we are providing this early version of the manuscript. The manuscript will undergo copyediting, typesetting, and review of the resulting proof before it is published in its final form. Please note that during the production process errors may be discovered which could affect the content, and all legal disclaimers that apply to the journal pertain.



Synthesis, crystal structure and effect of indeno[1,2-b]indole derivatives on prostate cancer *in vitro*. Potential effect against MMP-9.

Gricela Lobo, Melina Monasterios, Juan Rodriguez, Neira Gamboa, Mario V. Capparelli, Javier Martínez-Cuevas, Michael Lein, Klaus Jung, Claudia Abramjuk, Jaime Charris.



Synthesis, crystal structure and effect of indeno[1,2-b]indole derivatives on prostate cancer *in vitro*. Potential effect against MMP-9.

Gricela Lobo ^a, Melina Monasterios ^a, Juan Rodrigues ^b, Neira Gamboa ^b, Mario V. Capparelli ^c, Javier Martínez-Cuevas ^d, Michael Lein ^{e,f}, Klaus Jung ^{e,f}, Claudia Abramjuk ^{e,g}, Jaime Charris ^{a,*}

^{a,b} Laboratorio de Síntesis Orgánica, Unidad de Bioquímica, Facultad de Farmacia, Universidad Central de Venezuela, Apartado 47206, Los Chaguaramos, 1041-A Caracas, Venezuela. ^cUnidad de Estructura Molecular, Fundación Instituto de Estudios Avanzados (IDEA), Apartado 17606, Caracas 1015-A, Venezuela. ^dServicio de Difracción de Rayos X, Universidad Autónoma de Barcelona, 08193 Barcelona, Spain. ^eDepartment of Urology, University Hospital Charité, Campus Mitte, Schumannstrasse 20/21, 10117 Berlin, Germany. ^fBerlin Institute for Urologic Research, Schumannstrasse 22/21, 10117 Berlin, Germany. ^gDepartment of Experimental Medicine (FEM), University Hospital Charité, Campus Mitte, Charitéplatz 1, 10117 Berlin, Germany.

1. Introduction

Prostate cancer (PCa) represents the second most frequently diagnosed malignancy in men and the sixth leading cause of cancer death worldwide [1]. Many antitumor compounds have been developed, but treatment options in patients with advanced stage of PCa have limited efficacy and are associated with significant side effects and reduced quality of life. Therefore, developing new alternatives for this malignancy is of great importance. The ability of indenoindoles as potential lipid peroxidation inhibitors [2], potassium channel openers [3], DNS intercalators and topoisomerase II inhibitors [4], estrogenic agents [5], or inhibitors of proteins kinase CK2 [6,7], have been reported. They are considered as a novel class of potent inhibitors of the human proteins kinase CK2, which is a second-messenger and phosphorylation independent constitutively active S/T protein kinase. Up to date the literature reports more than 400 potential physiological targets, showing their important roles in a variety of non cancer-related diseases (such as neurodegenerative disorders,

inflammatory processes, angiogenesis-related diseases and viral infections), as well as in different types of cancer (prostate, colon, breast and lung) [8-11].

However, there are no data available about the effect of the indenoindoles structures on the extracellular matrix (ECM). ECM proteins play important roles during proliferation, adhesion, migration and invasion of cancer cells as well as in angiogenesis in developing tumors [12-14]. Each of these events is regulated by the proteolysis of the ECM components and, thus, by matrix metalloproteinases (MMPs). MMP-9, which activity is correlated with the progression and the degree of malignancy, contributes to the invasion and metastatic spread of tumor cells, being recognized as a potential target for the development of new anti-cancer drugs [15,16]. On the other hand , special attention has been focused on the indole structure as responsible of the biological properties of some heterocyclic compounds. Thus, isatin derivatives which contain two carbonyl groups on the indole core have been tested as potential MMPs inhibitors; however, theses analogs did not show important effects on the metalloproteinase activities with no significant inhibitions reported [17].

Despite recent advances in molecular biology and the progress in combinatorial synthetic methodology, the rate of introduction of new pharmaceutical products has decreased markedly over the past two decades. Structural diversity in a focused collection of potential therapeutics is believed to increase the positive hit rate. Most pharmaceutical products in use are still small synthetic organic molecules that often contain a heterocyclic ring. However, the range of easily accessible and suitably functionalized heterocyclic building blocks for the synthesis of structurally diverse libraries is rather limited. The development of new, rapid, and clean synthetic routes toward focused libraries of such compounds is therefore of great importance to both medicinal and synthetic chemists. As part of our

general interest in the preparation of heterocyclic compounds with potential anticancer activities [18-23], herein we report the synthesis of indeno[1,2-b]indole derivatives, and their characterization by X-ray diffraction analysis. Docking simulation was performed using X-ray crystallographic structure of MMP-9 in complex with the most active inhibitor to explore the binding mode of the compound at the active site.

2. Results and discussion

2.1. Synthesis

Among the existing procedures for the preparation of indenoindoles, the Fischer indolization starting with an indanone, via the respective phenylhydrazones, serves as the most common method [24,25]. Recently, two new syntheses by transformation and reduction of 2-nitrobenzylidenephthalide, generated either by intramolecular cyclization of 2-(2-nitrophenylethyl)benzoic acid [26], or by reaction of a phthalidyl-phosphonium bromide with 2-nitrobenzaldehyde [27] and cyclization of the resulting amino compounds, have been published. The formation of *vic*-dihydroxy-indenoindolones by the reaction of ninhydrine **1** with aliphatic, and aromatic amines, or alicyclic, and cyclic enaminones has been reported elsewhere [28-33].

The intermediates **4** and **5** were achieved according to published procedures by refluxing cyclohexane-1,3-dione with aromatic amine and a catalytic amount of *p*-toluensulfonic acid in toluene and removal of water as an azeotrope with a Dean-Stark water trap [34]. To prepare the *vic*-dihydroxy-indenoindiole **6a-q** and **7a-q** derivatives, a solution of equimolar amounts of the corresponding enaminone **4** and **5** and ninhydrin **1** in chloroform, stirred at room temperature for 24 h. TLC (EtAc:Hx 1:1) showed, that only one compound was produced (*cf.* Scheme). Spectroscopic data (¹H and ¹³C NMR) revealed that this was a

cyclization product with two ^1H resonances due to OH functionalities at 5 and 7 ppm and two ^{13}C resonances at 83 and 96 ppm approximately.

2.2. Biological

The effect of compounds **6p-q** and **7p-q**, on cell viability showed a dose-dependent response in all the cancer cell lines tested with inhibition in viability from 5 $\mu\text{g/ml}$ onwards. Compound **7q** showed the maximal cytotoxic effects. The structure-activity relationship studies on these compounds revealed that the presence of a dimethyl at position 7 and dichloro phenyl at position 5 are determinant for the cell viability since compounds which lack these substitutions were less toxic to the tumor cell lines. In addition, the anti-tumor activity is also affected by the presence of the H group at position 7 and methoxy and methyl phenyl groups at position 5. In this context, compound **7q** was selected for further evaluations. This derivative was also active in other human and non-human tumor prostate cell lines, such as LNCaP and MatLyLu (Table I, Figure 1).

Insert Table I here

Insert Figure 1 here

To examine the effect of this compound on the migration/motility properties of the tumor cells, the wound-healing assay was used [35]. Compound **7q**-free cultures of PC-3 cells (control vehicle) largely displayed wound recovery within 24 h and cells migrated to the wound (Figure 2a, 2c). The ability to close the scrape wound was significantly reduced by compound **7q** treatment at its cytotoxic IC_{50} (Figure 2b, 2d). On the other hand, the results of cell invasion assay using the Boyden chamber coated with Matrigel revealed that this compound also decreased the invasion in LNCaP cells after 18 h of incubation (Figure 3).

Insert Figure 2 here

Insert Figure 3 here

As shown in Figure 4, compound **7q** decreased MMP-9 activity in PC-3 cells at its cytotoxic IC₅₀. The inhibition on this metalloprotease would suggest a consequent inhibition on the ability of cells to migrate and invade surrounding areas. No MMP2 activity was reported for these cell lines, as previously shown [36].

Insert Figure 4 here

The anchorage-independent growth is considered an *in vitro* test, which correlates with tumorigenesis *in vivo* [37]. Thus, we examined the ability of PC-3, LNCaP and MatLyLu cells to grow in a semisoft agar medium after **7q** treatment. Cell colonies significantly grew in vehicle-treated agar on day 14 as previously reported [38]. On the other hand, colonies were either reduced in size and number or completely absent in cells treated with compound **7q** (Figure 5, Table II).

Insert Table II here

Insert Figure 5 here

New tissue formation, invasion and tumor cell metastasis all depend on cell motility and migration [39]. Cell migration constitutes an attractive target for the development of potential antitumor compounds and our results showed that the analog **7q** could be considered as an inhibitor of cell migration after 24 hour-incubation, which could lead to further decreases in cell invasion and metastasis prevention. Indeed, the ability of this structure to inhibit cell invasion was also confirmed.

The degree of tumor malignancy is related to the ability of neoplastic cells to invade other tissues and spreading to other organs. An important role is made by different metalloproteinases such as MMP-9 which degrades the extracellular matrix (ECM) that is

required for migration, invasion and metastasis [40]. This secreted gelatinase is highly expressed in cancer cells, making it valuable in finding patients who are at high risk of tumor development [41], thus, compounds that inhibit this protease could represent possible structures against cancer. Our results showed that compound **7q** decreased the activity of this gelatinase, suggesting that this enzyme could be a molecular target of this structure and proposing a possible mechanism for its antitumor action.

On the other hand, a specific feature of tumor cells is that they are able to grow in soft agar. This phenotypic transformation has been positively correlated with the *in vivo* tumor growth and metastasis [42]. Our results indicated that a suspension of PC-3, LNCaP or MatLyLu cells with vehicle successfully developed into relatively large colonies, whereas those cultured with the compound **7q** resulted in fewer and smaller-sized colonies or even a complete abolishment in the development of colonies, indicating a loss of the transformed phenotype and providing possible insights about the behavior of this compound on metastasis *in vivo*.

2.3. X-ray crystallography

To confirm the proposed molecular structures, X-ray single-crystal structure analyses of one compound of each series, viz. **6k** and **7k**, were carried out. The molecular structures are shown in Figure 6 and the relevant bond lengths and angles are given in Table III.

Insert Figure 6 here

Insert Table III here

The two stereocenters (C1 and C2) have the same configurations in **6k** and **7k**. Since both compounds crystallize in centrosymmetric space groups (*cf.* Table V), both crystals consist of equimolar mixtures of the RR and SS diastereomers (Figure 6 shows the RR configurations).

As expected, both compounds display very similar molecular geometries, which are also closely related the methoxy derivative previously reported by us [19]. Actually, **7k** is isostructural with the OMe derivative. Within experimental error (*i.e.* three e.s.d.'s) bond distances are equal in both compounds; the only exception being C5-C6 and C6-C7, which are significantly longer in **7k** due to the C6 methyl substituents (*cf.* Table IV). The tetracyclic systems are V-shaped, with the two 5-membered rings making dihedral angles of $113.75(7)^\circ$ (**6k**) and $114.91(7)^\circ$ (**7k**). The N-bonded phenyl rings are approximately perpendicular to the heterocyclic rings [dihedral angles: $74.85(7)^\circ$ (**6k**) and $78.52(7)^\circ$ (**7k**)]. The phenyl rings are quite planar (r.m.s. deviations: 0.0037- 0.0089 Å) and the two 5-membered rings are approximately planar (r.m.s. deviations: 0.022-0.029 Å). The C3-C4-C5-C6-C7-C8 rings display a semi-sofa conformation (*i.e.* intermediate between boat and sofa), with distances from the C4, C5, C7, C8 mean plane of 0.166(2) Å and 0.142(2) Å for the C3 atoms, and of 0.614(2) Å and 0.599(2) Å for the C6 atoms. The puckering parameters [43] are: $q_2 = 0.4522(16)$ Å, $q_3 = -0.1927(16)$ Å, $\phi_2 = 3.3(2)^\circ$, $Q = 0.4915(17)$ Å for **6k**, and $q_2 = 0.4310(146)$ Å, $q_3 = 0.-1911(14)$ Å, $\phi_2 = 6.15(18)^\circ$, $Q = 0.4715(15)$ Å for **7k**.

The molecules form O-H...O(keto) intramolecular hydrogen bonds (*cf.* Figure 6). In addition, in the crystal structure there are intermolecular hydrogen bonds of the types O-H...O(keto) and (possible) weaker C-H...O(hydroxyl) and C-H...O(keto) (*cf.* Table IV), which link the molecules to form a three dimensional network.

Insert Table IV here

2.4. Molecular docking simulations

In order to seek the structure-activity relationships of these synthetic derivative, molecular docking of the most potent inhibitor **7q** and the inactive compound **6k** into the catalytic domain of the MMP-9 enzyme PDB ID: 1GKC [44] (Figure 7) was performed. The catalytic centre of the active-site includes a zinc ion coordinated by three histidine residues (401, 405 and 411) and a glutamic acid residue (402). The main differences between the catalytic domains of various MMPs occur in the S1' subsite or selectivity pocket (residues 425- 431 in MMP-9). It has been found that chain A is participating in the interactions.

Insert Figure 7 here

The highly active compound **7q** binds in the catalytic domain through three hydrogen bond. Carbonyl group of indene rings acts as receptor of the hydrogen bond formed with the NH group of His 401 (distance 1.88 Å). This interaction is the most important. Furthermore the dichlorophenyl group is placed into the hinge region (residues 420-431) (Figure 8). Also it has a very small overall interaction energy (-12.88 kcal/mol). These indicate that this compound binds to MMP-9 S1' subsite.

Insert Figure 8 here

The binding energy of compound **6k**, which has lower activity, is also smaller (-8.93 kcal/mol). This compound forms several hydrogen bonds but places the phenyl group outside S1' pocket.

Insert Figure 9 here

The docking results revealed that His 401 residue located in the catalytic centre of MMP-9 is important to your interaction with **7q**, which were stabilized by two hydrogen bonds two other residues and hydrophobic interactions to the Pro 430 residue within the S1' pocket. The compound **7q** that binds in the S1' subsite can be a specific inhibitor of MMP-9 mainly through an indirect mechanism by interacting far from the coordinating Zinc atom.

3. Conclusions

In conclusion, compounds were easily synthesized and with highly regiospecificity. The X-ray diffraction studies clearly confirmed the structure of the compounds. All tested compounds proved to be moderately active and, except **7q**, showed cytotoxic effects in different human and non-human prostate cancer cell lines. The mechanism of the antitumor activity of this structure seems to be related to the decrease of migration, invasion and clonogenicity possibly by inhibition of MMP-9. Of notice is the inhibition of the clonogenic potential which might lead to a possible *in vivo* anticancer effect of this compound. The structure-activity relationship studies on these compounds revealed that the presence of a dimethyl at 7 positions and dichloro phenyl at 5 positions are determinant for the cell viability since compounds which lack these substitutions were less toxic to the tumor cell lines. Docking studies shows a set of interactions in specific sites that are important for an inhibitory activity. Further studies will be needed to confirm this hypothesis.

4. Experimental

4.1. Chemistry

Melting points were determined on a Thomas micro hot stage apparatus and are uncorrected. The IR spectra (in KBr pellets) were recorded on a Shimadzu model 470 spectrophotometer. The ^1H NMR, ^{13}C NMR spectra were recorded using a Jeol Eclipse 270 (270 MHz/67.9 MHz) spectrometer using CDCl_3 or DMSO_{d6} , and are reported in ppm downfield from the residual CHCl_3 or DMSO. Elemental analyses were obtained using a Perkin Elmer 2400 CHN elemental analyzer, the results were within $\pm 0.4\%$ of the predicted values. Chemical reagents were obtained from Aldrich Chemical Co, USA. All solvents were distilled and dried in the usual manner. The intermediates **4** and **5** were achieved according to published procedures [34].

4.1.2. General procedure to obtain 5-(substitutedphenyl)-(4bRS,9bRS)-dihydroxy-4b,5,6,7,8,9b-hexahydroindeno[1,2-b]indole-9,10-dione derivatives, 6a-q, 7a-q.

Enaminones (1.35 mmol) and **1** (1.12 mmol) were dissolved in chloroform 5 mL and stirred at rt. (24 h). The solvent was evaporated to dryness under reduced pressure, the solid thus obtained was collected by filtration, washed with diethyl ether and recrystallized from ethanol to afford the title compound.

4.1.2.1. 5-(2-methoxyphenyl)-(4bRS,9bRS)-dihydroxy-4b,5,6,7,8,9b-hexahydro-indeno[1,2-b]-indole-9,10-dione, 6a

Yield: 68% , mp: 234-236 °C, IR cm^{-1} : 3504, 3120 (OH), 1718 (C=O); NMR- ^1H , ppm δ : 1.92 (m, 2H, H_7), 2.12 (m, 2H, H_6), 2.35 (m, 2H, H_8), 3.95 (s, 3H, OCH_3), 5.74 (s, 1H, OH), 6.64 (dd, 1H, H_4 , J: 7.9, 2.3Hz), 6.81(dd, 1H, H_3 , J:7.8, 2.1Hz), 6.90(t, 1H, H_4 , J:7.6, 2.1Hz), 7.12(t, 1H, H_5 , J:7.8, 2.2Hz), 7.8 (m, 3H, OH, Ar), 7.51 (t, 1H, H_2 , J:7.6, 1.8Hz), 7.83 (dd, 1H, H_1 , J: 8.2, 2.1Hz). NMR- ^{13}C , ppm δ : 21.8, 24.1, 37.3, 55.9, 82.7, 96.8, 106.3, 114.7, 115.1, 124.7, 125.2, 127.0, 127.7, 129.8, 131.3, 135.7, 135.4, 149.9, 150.0, 167.7, 193.1, 197.5. Anal. $\text{C}_{22}\text{H}_{19}\text{NO}_5$: C, 70.02; H, 5.07; N, 3.71. Found: C, 69.92; H, 5.10; N, 3.80 %.

4.1.2.2. 5-(3-methoxyphenyl)-(4bRS,9bRS)-dihydroxy-4b,5,6,7,8,9b-hexahydro-indeno[1,2-b]-indole-9,10-dione, 6b

Yield: 80%, mp: 128-130 °C, IR cm^{-1} : 3504, 3152 (OH), 1712 (C=O); NMR- ^1H , ppm δ : 1.90 (m, 2H, H_7), 2.22 (m, 4H, H_6 , H_8), 3.83 (s, 3H, OCH_3), 5.52 (brs, 1H, OH), 6.79(d, 1H, H_4 , J: 7.9Hz), 6.90 (m, 2H, Ar), 7.03(d, 1H, H_6 , J:7.9Hz), 7.13(m, 1H, H_5 , J:2.2), 7.45(m, 2H, H_2 , J:3), 7.81 (d, 1H, H_1 , J: 7.6Hz). NMR- ^{13}C , ppm δ : 21.8, 23.8, 36.7, 55.6, 82.9, 96.3, 106.3, 114.5, 114.6, 124.6, 125.2, 126.4, 127.9, 130.3, 131.0, 135.0, 135.3, 147.8, 159.8,

167.2, 193.1, 197.9. Anal. C₂₂H₁₉NO₅: C, 70.02; H, 5.07; N, 3.71. Found: C, 70.11; H, 5.18; N, 3.97 %.

4.1.2.3. 5-(4-methoxyphenyl)-(4*b*RS,9*b*RS)-dihydroxy-4*b*,5,6,7,8,9*b*-hexahydro-indeno[1,2-*b*]-indole-9,10-dione, **6c**

Yield: 59% , mp: 204 °C, IR cm⁻¹: 3632, 3232 (OH), 1708 (C=O); NMR-¹H, ppm δ: 1.92 (m, 2H, H₇), 2.17 (m, 4H, H_{6,8}), 3.86 (s, 3H, OCH₃), 5.60 (brs, 1H, OH), 6.90(dd, 1H, H₄, J:8.2, 2.1Hz), 6.94 (d, 2H, H_{3',5'}, J:8.2Hz), 7.16(d, 2H, H_{2',6'}, J:78.2Hz), 7.48(t, 1H, H₃, J:7.6Hz), 7.49(s, 1H, OH), 7.50 (t, 1H, H₂, J: 7.6Hz), 7.83(dd, 1H, H₁, J:8.4, 2.0Hz). NMR-¹³C, ppm δ: 21.8, 23.9, 36.8, 55.6, 82.9, 96.4, 106.3, 114.5, 124.6, 125.3, 127.9, 130.0, 135.0, 135.3, 147.8, 159.8, 167.3, 193.1, 197.2. Anal. C₂₂H₁₉NO₅: C, 70.02; H, 5.07; N, 3.71. Found: C, 70.04; H, 5.08; N, 3.75 %.

4.1.2.4. 5-(2,4-dimethoxyphenyl)-(4*b*RS,9*b*RS)-dihydroxy-4*b*,5,6,7,8,9*b*-hexahydro-indeno[1,2-*b*]-indole-9,10-dione, **6d**

Yield: 93%, mp: 188-190 °C, IR cm⁻¹: 3568, 2896 (OH), 1712 (C=O), NMR-¹H, ppm δ: 1.94 (m, 2H, H₇), 2.17 (m, 4H, H_{6,8}), 3.85 (s, 3H, OCH₃), 3.98 (s, 3H, OCH₃), 5.27 (brs, 1H, OH), 6.36(d, 1H, H₃, J:1.9Hz), 6.61 (dd, 1H, H₅, J:7.9, 1.9Hz), 6.74 (m, 2H, Ar), 7.42 (s, 2H, OH, Ar), 7.58 (m, 1H, Ar), 7.81(dd, 1H, H₁, J:8.0, 2.1Hz). NMR-¹³C, ppm δ: 21.7, 23.5, 36.8, 55.2, 55.7, 81.5, 95.5, 99.3, 104.6, 105.9, 116.9, 124.4, 124.6, 129.9, 132.0, 134.8, 135.0, 148.2, 157.0, 161.4, 193.4, 198.0. Anal. C₂₃H₂₁NO₆: C, 67.80; H, 5.20; N, 3.44. Found: C, 67.83; H, 5.26; N, 3.63 %.

4.1.2.5. 5-(3,4-dimethoxyphenyl)-(4*b*RS,9*b*RS)-dihydroxy-4*b*,5,6,7,8,9*b*-hexahydro-indeno[1,2-*b*]-indole-9,10-dione, **6e**

Yield: 87%, mp: 220-222 °C, IR cm⁻¹: 3536, 3105 (OH), 1715 (C=O); NMR-¹H, ppm δ: 1.96 (m, 2H, H₇), 2.28 (m, 4H, H_{6,8}), 3.86 (s, 3H, OCH₃), 3.94 (s, 3H, OCH₃), 6.03 (brs,

1H, OH), 6.74(dd, 1H, H₄, J:8.4, 2.1Hz), 6.90 (d, 1H, H₅, J:8.6Hz), 7.01(s, 1H, H₂), 7.03 (dd, 1H, H₆', J:8.4, 1.5Hz), 7.46 (t, 1H, H₄, J:7.5Hz), 7.48 (s, 1H, OH), 7.51 (t, 1H, H₂, J:7.5Hz), 7.83(dd, 1H, H₁, J:8.3, 1.8Hz). NMR-¹³C, ppm δ : 21.8, 23.9, 36.7, 56.1, 56.3, 83.1, 96.8, 106.2, 110.8, 113.5, 122.2, 124.4, 125.5, 128.1, 130.3, 135.1, 147.9, 149.2, 149.3, 167.3, 193.0, 197.8. Anal. C₂₃H₂₁NO₆: C, 67.80; H, 5.20; N, 3.44. Found: C, 68.04; H, 5.33; N, 3.57 %.

4.1.2.6. 5-(2,5-dimethoxyphenyl)-(4*bRS*,9*bRS*)-dihydroxy-4*b*,5,6,7,8,9*b*-hexahydro-indeno[1,2-*b*]-indole-9,10-dione, **6f**

Yield: 87%, mp: 142-144 °C, IR cm⁻¹: 3504, 3104 (OH), 1712 (C=O); NMR-¹H, ppm δ : 1.93 (m, 2H, H₇), 2.15 (t, 2H, H₆, J: 6.8Hz), 2.36 (t, 2H, H₈, J: 6.7Hz), 3.10 (s, 3H, OCH₃), 3.86 (s, 3H, OCH₃), 4.32 (brs, 1H, OH), 6.72(d, 1H, H₄, J:7.9Hz), 6.75 (d, 1H, H₃, J:8.9Hz), 6.96 (dd, 1H, H₄', J: 8.9, 3.0Hz), 7.00(s, 1H, OH), 7.3 (d, 1H, H₆', J: 3.0Hz), 7.45 (m, 2H, H_{2,3}), 7.83(d, 1H, H₁, J:7.9Hz). NMR-¹³C, ppm δ : 21.7, 23.6, 36.3, 55.6, 56.0, 82.8, 96.3, 106.5, 112.4, 116.0, 116.7, 124.6, 125.0, 130.0, 134.9, 135.0, 148.1, 150.0, 154.0, 169.3, 192.9, 198.0. Anal. C₂₃H₂₁NO₆: C, 67.80; H, 5.20; N, 3.44. Found: C, 67.81; H, 5.35; N, 3.59 %.

4.1.2.7. 5-(3,4,5-trimethoxyphenyl)-(4*bRS*,9*bRS*)-dihydroxy-4*b*,5,6,7,8,9*b*-hexahydro-indeno[1,2-*b*]-indole-9,10-dione, **6g**

Yield: 46%, mp: 140-142 °C, IR cm⁻¹: 3525, 2986 (OH), 1723 (C=O); NMR-¹H, ppm δ : 1.78 (m, 2H, H₇), 2.10 (m, 4H, H_{6,8}), 3.73 (s, 9H, OCH₃), 5.95 (s, 1H, OH), 6.67(s, 2H, H_{2,6}'), 6.93 (d, 1H, H₄, J:7.7Hz), 7.13(s, 1H, OH), 7.55 (t, 1H, H₃, J:7.7Hz), 7.66 (t, 1H, H₂, J:7.7Hz), 7.73(d, 1H, H₁, J:7.6Hz). NMR-¹³C, ppm δ : 22.1, 24.0, 37.6, 56.6, 60.7, 84.0, 97.0, 106.6, 108.2, 123.6, 125.8, 130.7, 131.7, 135.3, 135.4, 137.7, 147.8, 153.1, 165.5,

190.2, 198.1. Anal. $C_{24}H_{23}NO_7$: C, 65.90; H, 5.30; N, 3.20. Found: C, 66.08; H, 5.37; N, 3.47 %.

4.1.2.8. 5-[(2-methylphenyl)]-(4*b*RS,9*b*RS)-dihydroxy-4*b*,5,6,7,8,9*b*-hexahydroindeno[1,2-*b*]indole-9,10-dione, **6h**

Yield: 55%, mp: 219-222 °C, IR cm^{-1} : 3560, 3184 (OH), 1718 (C=O); NMR- 1H , ppm δ : 1.15 (s, 3H, CH_3), 1.78 (m, 2H, H_7), 1.98 (m, 2H, H_6), 2.16 (m, 2H, H_8), 5.91 (s, 1H, OH), 6.62 (d, 1H, H_4 , J: 5.4), 7.27 (m, 2H, OH, Ar), 7.40 (m, 2H, Ar), 7.56 (m, 2H, $H_{2,3}$), 7.65 (m, 2H, Ar), 7.76 (d, 1H, H_1 , J: 8.9). NMR- ^{13}C , ppm δ : 17.0, 21.6, 23.8, 36.0, 83.1, 97.2, 106.4, 124.9, 126.0, 126.2, 127.4, 129.5, 129.7, 130.4, 131.0, 132.0, 135.2, 135.6, 148.0, 168.1, 192.4, 198.0. Anal. $C_{22}H_{19}NO_4$: C, 73.12; H, 5.30; N, 3.88. Found: C, 73.17; H, 5.31; N, 4.07 %.

4.1.2.9. 5-[(3-methylphenyl)]-(4*b*RS,9*b*RS)-dihydroxy-4*b*,5,6,7,8,9*b*-hexahydroindeno[1,2-*b*]indole-9,10-dione, **6i**

Yield: 75%, mp: 211-212 °C, IR cm^{-1} : 3424, 2992 (OH), 1708 (C=O); NMR- 1H , ppm δ : 1.79 (m, 2H, H_7), 2.01 (m, 2H, H_6), 2.11 (m, 2H, H_8), 2.34 (s, 3H, CH_3), 5.95 (s, 1H, OH), 6.65 (d, 1H, H_4 , J: 8.2), 7.08 (d, 1H, Ar, J: 7.7), 7.15 (s, 1H, Ar_2), 7.17 (s, 1H, OH), 7.27 (d, 1H, Ar, J: 7.7), 7.36 (t, 1H, Ar_5 , J: 7.7), 7.55 (m, 2H, $H_{2,3}$), 7.71 (dd, 1H, H_1 , J: 8.2, 1.7).). NMR- ^{13}C , ppm δ : 18.5, 21.4, 24.0, 35.8, 83.5, 97.2, 107.5, 124.7, 125.3, 126.4, 129.1, 129.8, 130.0, 130.5, 134.9, 135.2, 135.4, 139.5, 147.7, 167.6, 191.7, 197.6. Anal. $C_{22}H_{19}NO_4$: C, 73.12; H, 5.30; N, 3.88. Found: C, 73.15; H, 5.38; N, 4.12 %.

4.1.2.10. 5-[(4-methylphenyl)]-(4*b*RS,9*b*RS)-dihydroxy-4*b*,5,6,7,8,9*b*-hexahydroindeno[1,2-*b*]indole-9,10-dione, **6j**

Yield: 73%, mp: 228-231 °C, IR cm^{-1} : 3513, 3184 (OH), 1721 (C=O); NMR- 1H , ppm δ : 1.78 (m, 2H, H_7), 1.93 (m, 2H, H_6), 2.0 (m, 2H, H_8), 2.38 (s, 3H, CH_3), 5.92 (s, 1H, OH),

6.66 (d, 1H, H₄, J: 6.9), 7.14 (s, 1H, OH), 7.18 (d, 2H, Ar_{3,5}, J: 8.2), 7.29 (d, 2H, Ar_{2,6}, J: 8.2), 7.55 (m, 2H, H_{2,3}), 7.71 (dd, 1H, H₁, J: 7.6, 1.2); NMR-¹³C, ppm δ : 21.3, 22.3, 24.2, 37.7, 84.1, 96.9, 107.0, 123.8, 125.5, 129.8, 130.0, 130.7, 133.8, 135.3, 135.4, 138.0, 147.9, 165.4, 190.2, 198.2. Anal. C₂₂H₁₉NO₄: C, 73.12; H, 5.30; N, 3.88. Found: C, 73.19; H, 5.32; N, 4.17 %.

4.1.2.11. 5-[(2,4-dimethylphenyl)]-(4bRS,9bRS)-dihydroxy-4b,5,6,7,8,9b-hexahydroindeno-[1,2-b]indole-9,10-dione, 6k

Yield: 88%, mp: 230-233 °C, IR cm⁻¹: 3567, 3184 (OH), 1715 (C=O); NMR-¹H, ppm δ : 1.11 (s, 3H, CH₃), 1.76 (m, 2H, H₇), 1.98 (m, 2H, H₆), 2.13 (m, 2H, H₈), 2.34 (s, 3H, CH₃), 5.88 (s, 1H, OH), 6.67 (d, 1H, H₄, J: 8.4), 7.05 (s, 1H, Ar₃), 7.21 (m, 2H, OH, Ar), 7.52 (d, 1H, Ar, J: 7.9), 7.58 (m, 2H, H_{2,3}), 7.75 (dd, 1H, H₁, J: 7.2). NMR-¹³C, ppm δ : 17.0, 21.2, 21.6, 23.8, 36.0, 83.0, 97.1, 106.4, 124.9, 125.0, 128.1, 130.4, 130.7, 131.0, 135.1, 135.6, 136.5, 139.6, 148.0, 165.3, 191.8, 198.0. Anal. C₂₃H₂₁NO₄: C, 73.58; H, 5.64; N, 3.73. Found: C, 73.63; H, 5.71; N, 3.97 %.

4.1.2.12. 5-[(2,5-dimethylphenyl)]-(4bRS,9bRS)-dihydroxy-4b,5,6,7,8,9b-hexahydroindeno-[1,2-b]indole-9,10-dione, 6l

Yield: 79%, mp: 227-229 °C, IR cm⁻¹: 3497, 3168 (OH), 1715 (C=O); NMR-¹H, ppm δ : 1.09 (s, 3H, CH₃), 1.76 (m, 2H, H₇), 1.97 (m, 2H, H₆), 2.13 (m, 2H, H₈), 2.36 (s, 3H, CH₃), 5.89 (s, 1H, OH), 6.66 (m, 1H, H₄), 7.12 (d, 1H, Ar₃, J: 7.9), 7.21 (m, 2H, OH, Ar), 7.47 (s, 1H, Ar₆), 7.55 (m, 2H, H_{2,3}), 7.75 (dd, 1H, H₁, J: 8.6, 2.7). NMR-¹³C, ppm δ : 16.5, 21.0, 21.6, 23.8, 35.6, 83.1, 97.2, 100.2, 124.9, 125.0, 130.3, 130.4, 130.7, 131.3, 133.3, 135.0, 135.6, 137.2, 147.9, 165.4, 191.7, 198.0. Anal. C₂₃H₂₁NO₄: C, 73.58; H, 5.64; N, 3.73. Found: C, 73.59; H, 5.67; N, 3.87 %.

4.1.2.13. 5-[(3,4-dimethylphenyl)]-(4*bRS*,9*bRS*)-dihydroxy-4*b*,5,6,7,8,9*b*-hexahydroindeno[1,2-*b*]indole-9,10-dione, **6m**

Yield: 79%, mp: 233-236 °C, IR cm^{-1} : 3562, 3184 (OH), 1718 (C=O); NMR- ^1H , ppm δ : 1.77 (m, 2H, H₇), 2.01 (m, 2H, H₆), 2.10 (m, 2H, H₈), 2.23 (s, 3H, CH₃), 2.28 (s, 3H CH₃), 5.92 (s, 1H, OH), 6.69 (d, 1H, H₄, J: 6.7), 7.01 (m, 1H, Ar₆), 7.10 (s, 2H, OH, Ar), 7.23 (d, 1H, Ar₅, J: 8.2), 7.55 (m, 2H, H_{2,3}), 7.71 (dd, 1H, H₁, J: 7.4, 1.2); NMR- ^{13}C , ppm δ : 19.6, 19.9, 22.2, 24.1, 37.7, 84.0, 96.8, 106.8, 123.7, 125.5, 127.2, 130.3, 130.6, 130.7, 134.0, 135.2, 135.3, 136.7, 137.3, 147.9, 165.4, 190.1, 198.2. Anal. C₂₃H₂₁NO₄: C, 73.58; H, 5.64; N, 3.73. Found: C, 73.72; H, 5.69; N, 4.01 %.

4.1.2.14. 5-[(3,5-dimethylphenyl)]-(4*bRS*,9*bRS*)-dihydroxy-4*b*,5,6,7,8,9*b*-hexahydroindeno[1,2-*b*] indole- 9,10-dione, **6n**

Yield: 60%, mp: 215-217 °C, IR cm^{-1} : 3543, 3200 (OH), 1718 (C=O); NMR- ^1H , ppm δ : 1.78 (m, 2H, H₇), 1.95 (m, 2H, H₆), 2.01 (m, 2H, H₈), 2.29 (s, 6H, CH₃), 5.91 (s, 1H, OH), 6.69 (d, 1H, H₄, J: 6.9), 6.92 (s, 2H, Ar₄), 7.09 (s, 1H, Ar_{2,6}), 7.10 (s, 1H, OH), 7.55 (m, 2H, H_{2,3}), 7.71 (d, 1H, H₁, J: 6.4); NMR- ^{13}C , ppm δ : 21.4, 22.3, 24.3, 37.7, 84.1, 96.9, 107.1, 123.7, 125.6, 127.4, 129.9, 130.7, 135.3, 136.4, 138.5, 147.9, 165.3, 190.3, 198.2. Anal. C₂₃H₂₁NO₄: C, 73.58; H, 5.64; N, 3.73. Found: C, 73.71; H, 5.67; N, 3.91 %.

4.1.2.15. 5-[(4-bromophenyl)]-(4*bRS*,9*bRS*)-dihydroxy-4*b*,5,6,7,8,9*b*-hexahydroindeno[1,2-*b*]indole-9,10-dione, **6o**

Yield: 73%, mp: 200 °C, IR cm^{-1} : 3549, 3184 (OH), 1721 (C=O); NMR- ^1H , ppm δ : 1.75 (m, 2H, H₇), 1.93 (m, 2H, H₆), 2.11 (m, 2H, H₈), 6.00 (s, 1H, OH), 6.67 (d, 1H, H₄, J: 7.2Hz), 7.27 (m, 3H, H_{3,5}, OH), 7.53 (t, 1H, H₃, J: 7.2Hz), 7.68 (d, 2H, H_{2,6}, J: 8.7Hz), 7.72 (d, 1H, H₁, J: 7.2Hz); NMR- ^{13}C , ppm δ : 22.2, 24.0, 37.7, 84.0, 97.0, 107.6, 121.6, 123.8, 125.3,

131.8, 132.5, 135.2, 135.6, 136.0, 147.6, 164.9, 190.4, 198.0. Anal. C₂₁H₁₆BrNO₄: C, 59.17; H, 3.78; N, 3.29. Found: C, 59.23; H, 3.83; N, 3.47 %.

4.1.2.16. 5-[(4-chlorophenyl)]-(4bRS,9bRS)-dihydroxy-4b,5,6,7,8,9b-hexahydroindeno[1,2-b]indole-9,10-dione, 6p

Yield: 73%, mp: 170-172 °C, IR cm⁻¹: 3485, 3184 (OH), 1721 (C=O); NMR-¹H, ppm δ: 1.87 (m, 2H, H₇), 1.96 (m, 2H, H₆), 2.23 (m, 2H, H₈), 4.05 (brs, 1H, OH), 6.91 (d, 1H, H₄, J: 7.6Hz), 7.28 (d, 2H, H_{3,5}, J: 8.9Hz), 7.44 (d, 1H, H_{2,6}, J: 8.9Hz), 7.49 (t, 1H, H₃, J: 7.6Hz), 7.51 (s, 1H, OH), 7.54 (t, 1H, H₂, J: 7.5Hz), 7.82 (d, 1H, H₁, J: 7.6Hz); NMR-¹³C, ppm δ: 21.7, 23.9, 35.3, 82.8, 97.6, 107.7, 119.5, 124.9, 125.1, 129.7, 130.7, 133.8, 134.7, 135.2, 135.7, 147.6, 164.9, 192.7, 197.4. C₂₁H₁₆ClNO₄: C, 66.06; H, 4.22; N, 3.67. Found: C, 66.14; H, 4.29; N, 3.83 %.

4.1.2.17. 5-[(3,4-dichlorophenyl)]-(4bRS,9bRS)-dihydroxy-4b,5,6,7,8,9b-hexahydroindeno[1,2-b]indole-9,10-dione, 6q

Yield: 53%, mp: 160-162 °C, IR cm⁻¹: 3561, 3173 (OH), 1727 (C=O); NMR-¹H, ppm δ: 1.8-2.02 (m, 2H, H₇), 2.25-2.33 (m, 2H, H₆), 2.38-2.46 (m, 2H, H₈), 4.52 (brs, 1H, OH), 6.98 (d, 1H, H₄, J: 7.2Hz), 7.27 (dd, 1H, H₆, J: 8.9, 2.2Hz), 7.47 (d, 1H, H₂, J: 2.2Hz), 7.51-7.60 (m, 4H, H_{2,3,5}, OH), 7.84 (d, 1H, H₁, J: 7.6Hz); NMR-¹³C, ppm δ: 21.6, 23.9, 35.9, 82.9, 97.4, 107.8, 124.9, 125.0, 129.0, 130.7, 131.0, 131.3, 133.3, 133.5, 134.9, 135.0, 135.7, 147.4, 167.0, 192.6, 197.1. C₂₁H₁₅Cl₂NO₄: C, 60.59; H, 3.63; N, 3.36. Found: C, 60.62; H, 3.67; N, 3.61 %.

4.1.2.18. 7,7-dimethyl-5-[(2-methoxyphenyl)]-(4bRS,9bRS)-dihydroxy-4b,5,6,7,8,9b-hexahydroindeno[1,2-b]indole-9,10-dione, 7a

Yield: 81%, mp: 170-172 °C, IR cm⁻¹: 3600, 3104 (OH), 1712 (C=O); NMR-¹H, ppm δ: 0.8 (s, 3H, CH₃), 0.94 (s, 3H, CH₃), 1.95 (d, 2H, H₆, J: 17Hz), 2.00 (d, 2H, H₈, J: 17 Hz), 3.16

(s, 3H, OCH₃), 5.81 (s, 1H, OH), 6.52 (dd, 1H, H₄, J: 8.2, 2.1Hz), 7.05 (t, 1H, H_{4'}, J: 7.9Hz), 7.07 (m, 3H, OH, Ar), 7.12 (t, 1H, H₃, J: 7.6Hz), 7.48 (m, 3H, H₂, Ar), 7.62 (dd, 1H, H_{6'}, J: 8.8, 1.8Hz), 7.69(d, 1H, H₁, J: 8.1Hz); NMR-¹³C, ppm δ : 28.5, 28.6, 33.7, 36.9, 52.0, 55.5, 83.8, 96.6, 105.0, 112.5, 121.1, 123.6, 124.7, 125.0, 130.3, 130.8, 131.8, 134.9, 135.1, 148.4, 156.5, 165.6, 189.5, 198.5. Anal. C₂₄H₂₃NO₅: C, 71.10; H, 5.72; N, 3.45. Found: C, 71.19; H, 5.75; N, 3.68 %.

4.1.2.19. *7,7-dimethyl-5-[(3-methoxyphenyl)]-(4bRS,9bRS)-dihydroxy-4b,5,6,7,8,9b-hexahydroindeno[1,2-b]indole-9,10-dione, 7b*

Yield: 95%, mp: 202-204 °C, IR cm⁻¹: 3552, 2992 (OH), 1715 (C=O); NMR-¹H, ppm δ : 0.8 (s, 3H, CH₃), 0.94 (s, 3H, CH₃), 1.92 (d, 2H, H₆, J: 17Hz), 2.01 (d, 2H, H₈, J: 17 Hz), 3.16 (s, 3H, OCH₃), 5.82 (s, 1H, OH), 6.51 (dd, 1H, H₄, J: 8.3, 2.2Hz), 7.03 (dd, 1H, H_{4'}, J: 8.4, 2.1Hz), 7.08 (s, 1H, OH), 7.12 (t, 1H, H₃, J: 7.6Hz), 7.48 (m, 3H, Ar), 7.63 (dd, 1H, H_{6'}, J: 8.0, 1.5Hz), 7.69(d, 1H, H₁, J: 8.2Hz); NMR-¹³C, ppm δ : 28.5, 28.6, 33.7, 36.7, 51.9, 55.5, 83.8, 96.5, 104.7, 112.5, 121.1, 123.5, 124.7, 125.0, 130.2, 130.7, 131.8, 134.9, 148.3, 156.4, 165.4, 189.3, 198.4. Anal. C₂₄H₂₃NO₅: C, 71.10; H, 5.72; N, 3.45. Found: C, 71.16; H, 5.81; N, 3.59 %.

4.1.2.20. *7,7-dimethyl-5-[(4-methoxyphenyl)]-(4bRS,9bRS)-dihydroxy-4b,5,6,7,8,9b-hexahydroindeno[1,2-b]indole-9,10-dione, 7c*

Yield: 85%, mp: 120-122 °C, IR cm⁻¹: 3440, 3100 (OH), 1715 (C=O); NMR-¹H, ppm δ : 0.91 (s, 3H, CH₃), 1.02 (s, 3H, CH₃), 2.05 (d, 2H, H₆, J: 17Hz), 2.22 (dd, 2H, H₈, J: 16.1, 18Hz), 3.91 (s, 3H, OCH₃), 4.09 (brs, 1H, OH), 6.86 (dd, 1H, H₄, J: 8.3, 2.2Hz), 6.96 (d, 2H, H_{3',5'}, J: 8.7Hz), 7.12 (d, 2H, H_{2',6'}, J: 8.7Hz), 7.48 (m, 3H, OH, Ar), 7.87(d, 1H, H₁, J: 8.0Hz); NMR-¹³C, ppm δ : 27.7, 29.5, 34.3, 37.6, 50.5, 55.6, 82.7, 96.8, 105.3, 114.6,

124.7, 125.2, 128.0, 130.3, 130.8, 135.0, 135.3, 147.7, 159.9, 166.1, 191.5, 197.5. Anal. $C_{24}H_{23}NO_5$: C, 71.10; H, 5.72; N, 3.45. Found: C, 71.27; H, 5.77; N, 3.70 %.

4.1.2.21. 7,7-dimethyl-5-[(2,4-dimethoxyphenyl)]-(4*bRS*,9*bRS*)-dihydroxy-4*b*,5,6,7,8,9*b*-hexahydroindeno[1,2-*b*]indole-9,10-dione **7d** [19]

4.1.2.22. 7,7-dimethyl-5-[(3,4-dimethoxyphenyl)]-(4*bRS*,9*bRS*)-dihydroxy-4*b*,5,6,7,8,9*b*-hexahydroindeno[1,2-*b*]indole-9,10-dione **7e**

Yield: 72%, mp: 156-158 °C, IR cm^{-1} : 3456, 3088 (OH), 1715 (C=O); NMR- 1H , ppm δ : 0.87 (s, 3H, CH₃), 0.95 (s, 3H, CH₃), 1.77 (d, 1H, H₆, J: 17.6Hz), 1.88 (d, 1H, H₈, J: 15.6Hz), 2.10 (d, 1H, H₈, J: 15.6Hz), 2.34 (d, 1H, H₆, J: 17.6Hz), 3.71 (s, 3H, OCH₃), 3.82 (s, 3H, OCH₃), 5.95 (s, 1H, OH), 6.73 (dd, 1H, H_{6'}, J: 8.3, 2.1Hz), 6.80 (d, 1H, H₄, J: 7.2Hz), 6.96 (d, 1H, H_{2'}, J: 2.1Hz), 7.03 (d, 1H, H_{6'}, J: 8.4Hz), 7.15 (s, 1H, OH), 7.53 (t, 1H, H₃, J: 7.2Hz), 7.61 (t, 1H, H₂, J: 7.2Hz), 7.71 (d, 1H, H₁, J: 7.7Hz); NMR- ^{13}C , ppm δ : 28.4, 33.5, 36.7, 51.9, 55.4, 55.9, 83.7, 96.3, 99.4, 104.6, 105.3, 117.2, 123.4, 125.0, 130.1, 132.3, 134.8, 135.0, 148.4, 157.3, 161.1, 165.7, 189.2, 198.4. Anal. $C_{25}H_{25}NO_6$: C, 68.95; H, 5.79; N, 3.22. Found: C, 68.97; H, 5.81; N, 3.41 %.

4.1.2.23. 7,7-dimethyl-5-[(2,5-dimethoxyphenyl)]-(4*bRS*,9*bRS*)-dihydroxy-4*b*,5,6,7,8,9*b*-hexahydroindeno[1,2-*b*]indole-9,10-dione, **7f**

Yield: 80%, mp: 210-212 °C, IR cm^{-1} : 3488, 3056 (OH), 1712 (C=O); NMR- 1H , ppm δ : 0.80 (s, 3H, CH₃), 0.94 (s, 3H, CH₃), 1.92 (d, 2H, H₆, J: 17.5Hz), 2.00 (d, 2H, H₈, J: 17.5Hz), 3.12 (s, 3H, OCH₃), 3.78 (s, 3H, OCH₃), 5.83 (s, 1H, OH), 6.60 (dd, 1H, H₄, J: 8.2, 1.5Hz), 6.97 (d, 1H, H_{3'}, J: 9.2Hz), 7.04 (dd, 1H, H_{4'}, J: 9.2, 2.9Hz), 7.09 (s, 1H, OH), 7.29 (d, 1H, H_{6'}, J: 2.9Hz), 7.49 (t, 1H, H₃, J: 7.2Hz), 7.54 (t, 1H, H₂, J: 7.2Hz), 7.69 (d, 1H, H₁, J: 8.1Hz); NMR- ^{13}C , ppm δ : 28.4, 28.6, 36.9, 52.0, 55.7, 56.1, 56.6, 83.4, 96.7, 105.0,

113.0, 114.9, 118.1, 123.5, 125.2, 130.3, 134.9, 135.1, 148.3, 150.6, 153.4, 165.4, 189.5, 198.3. Anal. $C_{25}H_{25}NO_6$: C, 68.95; H, 5.79; N, 3.22. Found: C, 69.12; H, 5.86; N, 3.30 %.

4.1.2.24. *7,7-dimethyl-5-[(3,4,5-trimethoxyphenyl)]-(4bRS,9bRS)-dihydroxy-4b,5,6,7,8,9b-hexahydroindeno[1,2-b]indole-9,10-dione, 7g*

Yield: 90%, mp: 198 °C, IR cm^{-1} : 3600, 3136 (OH), 1715 (C=O); NMR- 1H , ppm δ : 0.89 (s, 3H, CH_3), 0.96 (s, 3H, CH_3), 1.84 (d, 2H, H_6 , J: 17Hz), 1.89 (d, 1H, H_8 , J: 15Hz), 2.12 (d, 1H, H_8 , J: 15Hz), 3.73 (s, 6H, OCH_3), 3.74 (s, 3H, OCH_3), 6.10 (brs, 1H, OH), 6.90 (d, 1H, H_4 , J: 7.7Hz), 6.63 (s, 2H, $H_{2,6}$), 7.17 (s, 1H, OH), 7.54 (t, 1H, H_3 , J: 6.7Hz), 7.65 (t, 1H, H_2 , J: 6.7Hz), 7.71 (d, 1H, H_1 , J: 7.4Hz); NMR- ^{13}C , ppm δ : 27.0, 30.0, 33.9, 37.4, 51.8, 56.7, 60.8, 84.0, 97.3, 105.6, 108.2, 123.6, 126.9, 130.8, 131.8, 135.3, 135.4, 137.8, 147.7, 153.2, 164.4, 189.7, 198.2. Anal. $C_{26}H_{27}NO_7$: C, 67.09; H, 5.85; N, 3.01. Found: C, 67.12; H, 5.91; N, 3.17 %.

4.1.2.25. *7,7-dimethyl-5-[(2-methylphenyl)]-(4bRS,9bRS)-dihydroxy-4b,5,6,7,8,9b-hexahydroindeno [1,2-b]indole-9,10-dione, 7h*

Yield: 82%, mp: 231-234 °C, IR cm^{-1} : 3424, 2996 (OH), 1712 (C=O); NMR- 1H , ppm δ : 0.89 (s, 3H, CH_3), 0.95 (s, 3H, CH_3), 1.18 (s, 3H, CH_3), 1.86 (s, 2H, H_6), 2.04 (s, 2H, H_8), 5.88 (s, 1H, OH), 6.67 (d, 1H, H_4 , J: 6.2), 7.27 (m, 2H, OH, Ar), 7.37 (m, 2H, $Ar_{4,5}$), 7.57 (m, 2H, $H_{2,3}$), 7.62 (m, 1H, Ar), 7.76 (dd, 1H, H_1 , J: 7.4); NMR- ^{13}C , ppm δ : 17.3, 28.4, 28.6, 33.8, 36.9, 52.0, 84.1, 97.3, 104.7, 124.2, 125.2, 127.2, 129.4, 130.7, 131.3, 132.0, 134.6, 135.4, 135.7, 137.9, 148.7, 164.3, 189.5, 198.7. $C_{24}H_{23}NO_4$: C, 74.02; H, 5.95; N, 3.60. Found: C, 74.11; H, 6.01; N, 3.92 %.

4.1.2.26. *7,7-dimethyl-5-[(3-methylphenyl)]-(4bRS,9bRS)-dihydroxy-4b,5,6,7,8,9b-hexahydroindeno [1,2-b]indole-9,10-dione, 7i*

Yield: 56%, mp: 118-120 °C, IR cm^{-1} : 3524, 3092 (OH), 1718 (C=O); NMR- ^1H , ppm δ : 0.88 (s, 3H, CH_3), 0.95 (s, 3H, CH_3), 1.92 (s, 2H, H_6), 2.10 (s, 2H, H_8), 2.35 (s, 3H, CH_3), 5.96 (s, 1H, OH), 6.65 (d, 1H, H_4 , J: 7.9), 7.02 (d, 1H, Ar_6 , J: 7.7), 7.15 (s, 1H, Ar_2), 7.20 (s, 1H, OH), 7.27 (d, 1H, Ar_4 , J: 7.7), 7.36 (t, 1H, Ar_5 , J: 7.7), 7.54 (m, 2H, $\text{H}_{2,3}$), 7.71 (dd, 1H, H_1 , J: 8.1, 1.9); NMR- ^{13}C , ppm δ : 21.6, 27.1, 30.0, 34.1, 37.7, 51.8, 84.0, 97.3, 106.0, 123.8, 125.6, 127.0, 129.2, 129.3, 130.4, 130.8, 135.3, 135.4, 136.6, 140.0, 147.8, 164.1, 189.8, 198.2. $\text{C}_{24}\text{H}_{23}\text{NO}_4$: C, 74.02; H, 5.95; N, 3.60. Found: C, 74.07; H, 5.98; N, 3.73 %.

4.1.2.27. *7,7-dimethyl-5-[(4-methylphenyl)]-(4bRS,9bRS)-dihydroxy-4b,5,6,7,8,9b-hexahydroindeno [1,2-b]indole-9,10-dione, 7j*

Yield: 99%, mp: 206-207 °C, IR cm^{-1} : 3602, 3214 (OH), 1721 (C=O); NMR- ^1H , ppm δ : 0.95 (s, 3H, CH_3), 1.03 (s, 3H, CH_3), 1.98 (d, 1H, H_6 , J: 17Hz), 2.15 (d, 1H, H_6 , J: 17Hz), 2.20 (d, 1H, H_8 , J: 16Hz), 2.28 (d, 1H, H_8 , J: 16Hz), 2.44 (s, 3H, CH_3), 5.97 (s, 1H, OH), 6.86 (d, 1H, H_4 , J: 8.7), 7.10 (d, 2H, $\text{Ar}_{3,5}$, J: 8.2Hz), 7.26 (d, 2H, $\text{H}_{2,6}$, J: 8.2), 7.48 (m, 3H, $\text{H}_{2,3}$, OH), 7.86 (d, 1H, H_1 , J: 8.6Hz); NMR- ^{13}C , ppm δ : 21.3, 27.6, 30.5, 34.4, 37.6, 51.8, 82.7, 96.8, 105.6, 124.7, 125.2, 129.2, 130.0, 132.9, 134.9, 135.3, 138.8, 147.7, 165.7, 191.7, 197.5. $\text{C}_{24}\text{H}_{23}\text{NO}_4$: C, 74.02; H, 5.95; N, 3.60. Found: C, 63.91; H, 6.13; N, 3.85 %.

4.1.2.28. *7,7-dimethyl-5-[(2,4-dimethylphenyl)]-(4bRS,9bRS)-dihydroxy-4b,5,6,7,8,9b-hexahydroindeno [1,2-b]indole-9,10-dione, 7k*

Yield: 59%), mp: 215-218 °C, IR cm^{-1} : 3583, 3184 (OH), 1718 (C=O); NMR- ^1H , ppm δ : 0.82 (s, 3H, CH_3), 0.94 (s, 3H, CH_3), 1.13 (s, 3H, CH_3), 1.83 (s, 2H, H_6), 2.03 (s, 2H, H_8), 2.33 (s, 3H, CH_3), 5.86 (s, 1H, OH), 6.71 (d, 1H, H_4 , J: 8.2), 7.05 (d, 1H, Ar_3 , J: 1), 7.17 (dd, 1H, Ar_5 , J: 8.2, 1.2), 7.22 (s, 1H, OH), 7.47 (d, 1H, Ar_6 , J: 7.9), 7.57 (m, 2H, $\text{H}_{2,3}$), 7.75 (dd, 1H, H_1 , J: 8.9, 1.2). NMR- ^{13}C , ppm δ : 17.1, 21.2, 28.7, 34.1, 37.1, 50.9, 82.9,

97.0, 104.7, 124.9, 128.0, 130.3, 131.0, 131.6, 135.1, 135.2, 135.5, 139.5, 148.2, 166.5, 191.7, 197.8. C₂₅H₂₅NO₄: C, 74.42; H, 6.25; N, 3.47. Found: C, 74.56; H, 6.30; N, 3.75 %.

4.1.2.29. 7,7-dimethyl-5-[(2,5-dimethylphenyl)]-(4*bRS*,9*bRS*)-dihydroxy-4*b*,5,6,7,8,9*b*-hexahydroindeno[1,2-*b*]indole-9,10-dione, **7l**

Yield: 98%, mp: 173-175 °C, IR cm⁻¹: 3595, 3296 (OH), 1721 (C=O); NMR-¹H, ppm δ: 0.82 (s, 3H, CH₃), 0.94 (s, 3H, CH₃), 1.11 (s, 3H, CH₃), 1.94 (m, 4H, H_{6,8}), 2.35 (s, 3H, CH₃), 5.86 (s, 1H, OH), 6.69 (m, 1H, H₄), 7.12 (d, 1H, Ar₃, J: 7.9), 7.20 (m, 3H, OH, 2Ar), 7.42 (s, 1H, Ar₆), 7.56 (m, 2H, H_{2,3}), 7.74 (m, 1H, H₁). NMR-¹³C, ppm δ: 16.7, 21.0, 28.7, 34.1, 37.2, 50.2, 82.8, 97.1, 105.0, 124.9, 130.4, 130.7, 131.6, 133.4, 133.7, 135.1, 135.5, 137.3, 148.1, 167.0, 191.6, 198.0. C₂₅H₂₅NO₄: C, 74.42; H, 6.25; N, 3.47. Found: C, 74.61; H, 6.39; N, 3.79 %.

4.1.2.30. 7,7-dimethyl-5-[(3,4-dimethylphenyl)]-(4*bRS*,9*bRS*)-dihydroxy-4*b*,5,6,7,8,9*b*-hexahydroindeno[1,2-*b*]indole-9,10-dione, **7m**

Yield: 58%, mp: 185-188 °C, IR cm⁻¹: 3520, 3168 (OH), 1718 (C=O); NMR-¹H, ppm δ: 0.82 (s, 3H, CH₃), 0.90 (s, 3H, CH₃), 1.93 (s, 2H, H₆), 2.06 (s, 2H, H₈), 2.21 (s, 3H, CH₃), 2.25 (s, 3H, CH₃), 5.95 (s, 1H, OH), 6.69 (d, 1H, H₄, J: 6.7), 6.86 (d, 1H, Ar₆, J: 8.2), 7.04 (s, 1H, Ar₂), 7.17 (s, 1H, OH), 7.21 (d, 1H, Ar₅, J: 8.2), 7.53 (m, 2H, H_{2,3}), 7.7 (d, 1H, H₁, J: 7.2); NMR-¹³C, ppm δ: 19.57, 19.95, 27.16, 29.55, 33.86, 37.54, 51.37, 83.75, 97.15, 105.31, 123.81, 125.53, 127.24, 130.43, 130.64, 130.93, 133.65, 134.99, 135.54, 137.11, 137.64, 147.73, 165.08, 190.59, 198.36. C₂₅H₂₅NO₄: C, 74.42; H, 6.25; N, 3.47. Found: C, 74.43; H, 6.27; N, 3.59 %.

4.1.2.31. 7,7-dimethyl-5-[(3,5-dimethylphenyl)]-(4*bRS*,9*bRS*)-dihydroxy-4*b*,5,6,7,8,9*b*-hexahydroindeno[1,2-*b*]indole-9,10-dione, **7n**

Yield: 64%), mp: 143-145 °C, IR cm^{-1} : 3561, 3168 (OH), 1705 (C=O); NMR- ^1H , ppm δ : 0.84 (s, 3H, CH_3), 0.91 (s, 3H, CH_3), 1.94 (s, 2H, H_6), 2.07 (s, 2H, H_8), 2.26 (s, 6H, CH_3), 5.95 (s, 1H, OH), 6.67 (d, 1H, H_4 , J: 6.7), 6.81 (s, 1H, Ar_4), 7.08 (s, 2H, $\text{Ar}_{2,6}$), 7.19 (s, 1H, OH), 7.54 (m, 2H, $\text{H}_{2,3}$), 7.70 (dd, 1H, H_1 , J: 7.4, 2.2); NMR- ^{13}C , ppm δ : 21.3, 27.5, 29.6, 34.5, 37.7, 50.7, 82.7, 96.7, 105.6, 124.7, 125.3, 126.9, 130.4, 130.5, 134.9, 135.2, 135.4, 139.1, 147.7, 165.6, 191.7, 197.6. $\text{C}_{25}\text{H}_{25}\text{NO}_4$: C, 74.42; H, 6.25; N, 3.47. Found: C, 74.47; H, 6.28; N, 3.62 %.

4.1.2.32. *7,7-dimethyl-5-[(4-bromophenyl)]-(4bRS,9bRS)-dihydroxy-4b,5,6,7,8,9b-hexahydroindeno-[1,2-b]indole-9,10-dione, 7o*

Yield: 75%, mp: 140-142 °C, IR cm^{-1} : 3644, 3008 (OH), 1718 (C=O); NMR- ^1H , ppm δ : 0.93 (s, 3H, CH_3), 1.00 (s, 3H, CH_3), 1.96 (d, 1H, H_6 , J:17 Hz), 2.05 (d, 1H, H_6 , J:17 Hz), 2.20 (d, 1H, H_8 , J:15 Hz), 2.29 (d, 1H, H_8 , J: 15Hz), 3.60 (brs, 1H, OH), 6.86 (d, 1H, H_4 , J:6.7 Hz), 7.16 (d, 2H, $\text{H}_{3,5}$, J:8.2 Hz), 7.49 (m, 3H, $\text{H}_{2,3}$, OH), 7.60 (d, 2H, $\text{H}_{2,6}$, J: 8.2 Hz), 7.83 (d, 1H, H_1 , J: 7.6 Hz); NMR- ^{13}C , ppm δ : 27.7, 29.4, 34.4, 37.7, 50.0, 82.8, 123.0, 124.9, 125.1, 128.8, 130.6, 131.0, 132.7, 134.5, 134.6, 134.8, 135.7, 147.5, 191.4, 197.3. $\text{C}_{23}\text{H}_{20}\text{BrNO}_4$: C, 60.81; H, 4.44; N, 3.08. Found: C, 60.93; H, 4.52; N, 3.27 %.

4.1.2.33. *7,7-dimethyl-5-[(4-chlorophenyl)]-(4bRS,9bRS)-dihydroxy-4b,5,6,7,8,9b-hexahydroindeno-[1,2-b]indole-9,10-dione 7p*

Yield: 67%, mp: 147-148 °C, IR cm^{-1} : 3637, 3018 (OH), 1714 (C=O); NMR- ^1H , ppm δ : 0.90 (s, 3H, CH_3), 1.03 (s, 3H, CH_3), 1.98 (d, 1H, H_6 , J:15 Hz), 2.05 (d, 1H, H_6 , J:15 Hz), 2.23 (d, 1H, H_8 , J:17 Hz), 2.31 (d, 1H, H_8 , J: 17Hz), 3.67 (brs, 1H, OH), 6.81 (d, 1H, H_4 , J:6.8 Hz), 7.14 (d, 2H, $\text{H}_{3,5}$, J:8.0 Hz), 7.47 (m, 3H, $\text{H}_{2,3}$, OH), 7.62 (d, 2H, $\text{H}_{2,6}$, J: 8.0 Hz), 7.83 (d, 1H, H_1 , J: 7.6 Hz); NMR- ^{13}C , ppm δ : 28.0, 30.1, 34.7, 36.9, 51.0, 81.7, 122.8,

125.3, 125.9, 128.3, 131.1, 131.7, 132.0, 133.9, 134.7, 135.2, 135.9, 147.7, 191.3, 197.2.

C₂₃H₂₀ClNO₄: C, 67.40; H, 4.92; N, 3.42. Found: C, 67.44; H, 4.99; N, 3.63 %.

4.1.2.34. 7,7-dimethyl-5-[(3,4-dichlorophenyl)]-(4*bRS*,9*bRS*)-dihydroxy-4*b*,5,6,7,8,9*b*-hexahydroindeno[1,2-*b*]indole-9,10-dione **7q**

Yield: 47%, mp: 180-182 °C, IR cm⁻¹: 3568, 2647 (OH), 1724 (C=O); NMR-¹H, ppm δ: 0.96 (s, 3H, CH₃), 1.00 (s, 3H, CH₃), 2.00 (d, 1H, H₆, J: 17Hz), 2.17 (d, 1H, H₆, J: 17Hz), 2.20 (d, 1H, H₈, J: 15Hz), 2.26 (d, 1H, H₈, J: 15Hz), 3.7 (brs, 1H, OH), 6.93 (d, 1H, H₄, J: 7.2Hz), 7.19 (dd, 1H, H₆, J: 8.9, 2.2Hz), 7.48-7.56 (m, 5H, H_{2,5,3,2}, OH), 7.84 (d, 1H, H₁, J: 7.6Hz); NMR-¹³C, ppm δ: 27.5, 29.5, 37.7, 50.1, 82.6, 97.4, 106.7, 124.9, 128.8, 130.7, 131.1, 131.2, 133.4, 134.8, 135.1, 135.7, 147.4, 165.6, 168.9, 191.9, 197.1. C₂₃H₁₉Cl₂NO₄: C, 62.17; H, 4.31; N, 3.15. Found: C, 62.23; H, 4.35; N, 3.41 %.

4.2. Anticancer assays

4.2.1. Cell Culture

Human and non-human prostate tumor cell lines PC-3, LNCaP and MatLyLu were obtained from the German Collection of Microorganisms and Cell Cultures (DSMZ, Braunschweig, Germany). Cells were grown in culture RPMI medium supplemented with fetal bovine serum (FBS, 10%), penicillin (50 units/ml) and streptomycin (50 µg/ml), in a humidified atmosphere (95% air, 5% CO₂, 37°C). Culture medium was purchased from Gibco-In Vitrogen, Karlsruhe, Germany and PAA Laboratories, Pasching, Austria.

4.2.2. Cell Viability Test

5×10³ PC-3, 1.2×10⁴ LNCaP or 1×10⁴ MatLyLu cells were seeded in a 96-well microtiter plate containing 100 µl of culture growth RPMI medium/well. After 24 h of culture, cells were exposed to the compounds previously dissolved in DMSO (72h, 5-100 µg/ml). The final concentration of this solvent in the culture media was always lower than 0.2%, a

concentration that has neither a cytotoxic effect nor causes any interference with the colorimetric detection method. The dose-dependent effects of each compound on were assessed using the XTT test (Roche Applied Science, Mannheim, Germany). After 72 h of exposure with the compounds, cells were incubated with XTT (4h, 37°C) and the formazan was recorded at 492 nm (Microplate reader HT II, Anthos, Salzburg, Austria). The IC₅₀ value was defined as the concentration of tested compound resulting in a 50% reduction in cell viability compared to vehicle-treated cells. Further evaluations of the best compound were performed using this IC₅₀ value [36,45].

4.2.3. Cell Migration and Motility Evaluation

Cell migration and motility was tested using the scrape wound repair assay. 8×10⁴ PC-3 cells were grown to confluence on 24-well plates in RPMI medium (48 h, 37°C). A sterilized micropipette tip was used to introduce a wound across the entire cell monolayer, and the medium was removed. After washing gently with PBS, the most cytotoxic compound on the XTT assay was added (IC₅₀) in fresh medium and incubated for 24 h in the presence of endothelial growth factor (1 pg/ml). Cover slips were mounted onto a light microscope and images of the wounds were captured on a computer system using a digital camera immediately following wounding (0 h) and after 24 h of compound or vehicle incubation. The wound area in each image was measured using the ImageJ program for Windows (<http://rsb.info.nih.gov/ij/>) and quantified by following the change in wound area over time compared with the original wound area. The results were expressed as the percentage of wound closure [35].

4.2.4. Invasion Assay.

Human tumor LNCaP cells (1×10⁵ cells/ml) were pretreated with the compound (cytotoxic IC₅₀, 24h). Cells then were seeded into the upper part of a Boyden chamber membrane

coated with Matrigel (Becton Dickinson Biosciences, Heidelberg, Germany) in 50 μ L of serum-free medium and incubated (18 h, 37°C). The bottom of the chamber contained 0.5 mL of standard medium (20% FBS). Invaded cells at the lower surface of the chamber were reacted with calcein (4 μ g/ml) in Hank's Buffered Salt Solution (1 h, 37°C). The fluorescence of invaded cells was read at 485/530 nm (Fluoroskan Ascent, Thermo Labsystems Oy, Helsinki, Finland) [22,36].

4.2.5. *Measurement of Clonogenic Potential*

The ability of cells to grow in an anchorage-independent manner was tested in cells grown in agar (0.6%). In short, 1 mL of a mixture of 1.2% Noble agar (Gibco-In Vitrogen, Karlsruhe, Germany) and RPMI medium (1:1) was added into each well of a six-well plate. PC3, LNCaP and MatLyLu cells (1×10^5) suspended in completed RPMI medium (FBS 20%) containing Noble agar (0.3%) were overlaid on the semisolid bottom layer. The plates were kept at room temperature for 15 min and incubated for 24 h (37°C, 95% O₂, 5% CO₂). The following day, 1 mL of medium with the compound at its IC₅₀ concentrations was added to each well. After 2 weeks of incubation cells were stained with crystal violet (0.01%) for 18 h at 37°C. Pictures were taken under light microscopy, and the total number of colonies and the relative colony size were determined [22,46].

4.2.6. *MMP Zymography*

To measure MMP-2 and MMP-9 activities, PC-3 and LNCaP cells (80% confluent in six-well plates) were washed twice with PBS and treated with the compound at its respective IC₅₀ concentration in serum-free medium (2.5 mL, 24 h, 37°C) in a humidified atmosphere (95% O₂, 5% CO₂). 22 μ L of a mixture composed of the conditioned medium and sample buffer (without mercaptoethanol, 0.75:0.25) were subjected to electrophoresis on 10% SDS-polyacrylamide gels gelatin-copolymerized (1 mg/mL). MMP-2 and MMP-9

gelatinolytic activity in the conditioned culture medium was assayed as previously described [22,47]. Bands quantification was performed by using ImageJ Software for Windows. Pure human MMP-9 and MMP-2 protein were used as a positive control.

4.3. X-ray crystallography

Crystals of **6k** and **7k** suitable for X-ray diffraction were obtained by slow evaporation of a solution in ethanol. Crystal data, intensity data collection parameters and final refinement results are summarised in Table V. Diffraction data were measured on a Bruker Smart-Apex diffractometer using graphite-monochromated Mo-K α radiation ($\lambda = 0.71070$ Å). The structure was solved by direct methods and refined on F^2 by full-matrix least-squares, using all reflections and weights $w = [\sigma^2(F_o^2) + (a P)^2 + b P]^{-1}$, with $P = (F_o^2 + 2 F_c^2)/3$. The C-bonded H atoms were placed in calculated positions and refined using a riding atom model with fixed C-H distances (0.93 Å for CH, 0.97 Å for CH₂, 0.96 Å for CH₃), and with $U_{iso} = p U_{eq}(\text{parent atom})$ ($p = 1.2$ for CH and CH₂, 1.5 for CH₃). The O-bonded H atoms were placed at idealized tetrahedral geometries, with fixed O-H distances (0.82 Å) and $U_{iso} = 1.5 U_{eq}(\text{parent atom})$.

The following computer programs were used: data collection, SMART [48]; cell refinement and data reduction, SAINT [49]; absorption correction, SADABS [50]; structure solution and refinement, SHELXL-97 [51]; molecular graphics, ORTEP-3 [52]; geometrical calculations, PLATON [53]; The structure solution, the refinement and the drawings were carried out with the aid of the WinGX [54] suite of programs. Comprehensive crystallographic data (excluding structure factors) for the structural analysis of **6k** and **7k** have been deposited with the Cambridge Crystallographic Data Centre. Copies of the data (CIF files) can be obtained, free of charge, on application to CCDC, 12 Union Road,

Cambridge CB2 1EZ, UK, fax: +44-(0)1223-336033, or from www.ccdc.cam.ac.uk/data_request/cif, quoting deposition No. CCDC 1022641 (**6k**) and CCDC 1022819 (**7k**).

4.4. Molecular docking methodology

The three dimensional structure of MMP-9 was downloaded from the Protein Data Bank (<http://www.rscb.org/pdb>) server with PDB code: 1GKC. Internal ligands and the crystallographic water molecules were removed from the protein and missing Hydrogens were added. Ligands were built with the molecular editor of CAChe 6.0 [55] using the crystallographic data structures **7k** and **6k** as reference. They were geometrically optimized by using MM3 [56] force field by CAChe 6.0 and PM3 of the Arguslab 4.0.1 [57] with RMSD 0.0001. The active site of the enzyme was defined and the ligand was placed in a box with dimensions of $X = 20 \text{ \AA}$, $Y = 20 \text{ \AA}$, $Z = 20 \text{ \AA}$ and a resolution of the grid of 0.4000 \AA . Docking was performed using Arguslab 4.0.1 employing genetic algorithm to generate the poses of the ligands at the binding site, allowing flexibility of the ligand. The results of docking were quantified in terms of the score and minimized energy.

Acknowledgments

We thank the IIF and CDCH-UCV (grants IIF.01-2014, PG. 06-8627-2013/1) programs for financial support, and Professor Milagros Avendaño for her help in the Molecular Docking Simulations.

References

- [1] A. Jemal, F. Bray, M. Center, J. Ferlay, E. Ward, D. Forma, Global cancer statistics, CA Canc. J. Clin. 61 (2011) 69-90, DOI: 10.3322/caac.20107.

- [2] D. Brown, P. Graupner, M. Sainsbury, H. Shertzer, New antioxidants incorporating indole and indoline chromophores, *Tetrahedron*, 47 (1991) 4383-4408, DOI:10.1016/S0040-4020(01)87108-8.
- [3] J. Butera, S. Antane, B. Hirth, J. Lennox, J. Sheldon, N. Norton, D. Warga, T. Argentieri, Synthesis and potassium channel opening activity of substituted 10H-Benzo[4,5]furo[3,2-b]indole- and 5,10-dihydro-indeno[1,2-b]indole-1-carboxylic acid, *Bioorg. Med. Chem. Lett.* 11 (2001) 2093-2097, DOI:10.1016/S0960-894X(01)00385-7.
- [4] C. Bal, B. Baldeyrou, F. Moz, A. Lansiaux, L. ColsoKraus-Berthier, S. Léonce, A. Pierre, M. Boussard, A. Rousseau, M. Wierzbicki, C. Bailly, Novel antitumor indenoindole derivatives targeting DNA and antitopoisomerase II, *Biochem. Pharmacol.* 68 (2004) 1911-1922, DOI: 10.1016/j.bcp.2004.07.008.
- [5] C. Miller, M. Collini, B. Tran, Indenoindoles and benzocarbazoles as estrogenic agents, US 6107292 A, (2000).
- [6] H. Hemmerling, C. Götz, J. Jose, Substituierte indeno [1,2-b] indoldrivative also neue hemmstoffe der protein kinase CK2 und ihre verwendung als tumor therapeutika, cytostatike und diagnostika, WO 2008040547 A1, (2008).
- [7] C. Hundsdörfer, H. Hemmerling, C. Götz, F. Totzke, P. Bednarski, M. Borgne, J. Jose, Indeno[1,2-b]indole derivatives as a novel class of potent human protein kinase CK2 inhibitors, *Bioorg. Med. Chem.* 20 (2012) 2282-2289. DOI:10.1016/j.bmc.2012.02.017.
- [8] M. Salvi, S. Sarno, L. Cesaro, H. Nakamura, L. Pinna, Extraordinary pleiotropy of protein kinase CK2 revealed by weblogo phosphoproteome analysis, *Biochim.*

- Biophys. Acta (BBA)-Mol. Cell. Res. 1793 (2009) 847-859, DOI: 10.1016/j.bbamcr.2009.01.013.
- [9] B. Guerra, O. Issinger, Protein kinase CK2 in human diseases, *Curr. Med. Chem.* 15 (2008) 1870-1886, DOI: 10.2174/092986708785132933.
- [10] M. Ruzzene, L. Pinna, Addiction to protein kinase CK2: a common denominator of diverse cancer cells?, *Biochem. Biophys. Acta, Proteins Proteomics*, 1804 (2010) 499-504, DOI: 10.1016/j.bbapap.2009.07.018.
- [11] K. Ahmed, G. Wang, G. Unger, J. Slaton, K. Ahmed, Protein Kinase CK2 - A key suppressor of apoptosis, *Adv. Enzyme Regul.* 48 (2008) 179-187, DOI:10.1016/j.advenzreg.2008.04.002.
- [12] L. Yang, W. Zeng, D. Li, R. Zhou, Inhibition of cell proliferation, migration and invasion by DNAzyme targeting MMP-9 in A549 cells, *Oncol. Rep.* 22 (2009) 121-126, DOI: 10.3892/or_00000414.
- [13] M. Burg-Roderfeld, M. Roderfeld, S. Wagner, C. Henkel, J. Grotzinger, E. Roeb, MMP-9-hemopexin domain hampers adhesion and migration of colorectal cancer cells, *Int. J. Oncol.* 30 (2007) 985-992, DOI: 10.3892/ijo.30.4.985.
- [14] J. Nemeth, R. Yousif, M. Herzog, M. Che, J. Upadhyay, B. Shekarri, S. Bhagat, C. Mullins, R. Fridman, M. Cher, Matrix metalloproteinase activity, bone matrix turnover, and tumor cell proliferation in prostate cancer bone metastasis, *J. Nat. Canc. Inst.* 94 (2002) 17-25, DOI: 10.1093/jnci/94.1.17.
- [15] W. Stetler-Stevenson, A. Yu, Proteases in invasion: matrix metalloproteinase, *Semin. Canc. Biol.* 11 (2001) 143-152, DOI:10.1006/scbi.2000.0365.
- [16] M. Chen, S. Cui, Y. Cheng, L. Sun, B. Li, W. Xu, S. Ward, W. Tang, X. Qu, Galloyl cyclic-imide derivative CH1104I inhibits tumor invasion through

- suppressing matrix metalloproteinase activity, *Anticancer Drugs*, 19 (2008) 957-965, DOI:10.1097/CAD.0b013e328313e15b.
- [17] S. Sjoli, A. Solli, O. Akselsen, Y. Jiang, E. Berg, T. Hansen, I. Sylte, J. Winberg, PAC-1 and isatin derivatives are weak matrix metalloproteinase inhibitors, *Biochim. Biophys. Acta*, 1840 (2014) 3162-3169, DOI: 10.1016/j.bbagen.2014.07.011.
- [18] R. Ferrer, G. Lobo, N. Gamboa, J. Rodrigues, C. Abramjuk, K. Jung, M. Lein, J. Charris, Synthesis of 7-chloroquinolinyl-4-aminophenylchalcones: potential antimalarial and anticancer agents, *Sci. Pharm.* 77 (2009) 725-741, DOI:10.3797/scipharm.0905-07.
- [19] G. Lobo, E. Zuleta, K. Charris, M. Capparelli, A. Briceno, J. Angel, J. Charris, Synthesis and crystal structure of (4bRS, 9bRS)-5-(2,4-dimethoxyphenyl)-4b,9b-7,7-dimetyldihydroxy-4b,5,6,7,8,9b-hexahydroindeno[1,2-b]indole-9,10-dione, *J. Chem. Res.* 35 (2011) 222-224, DOI:10.3184/174751911-X13015834294266.
- [20] J. Rodrigues, J. Charris, R. Ferrer, N. Gamboa, J. Angel, B. Nitzsche, M. Höepfner, M. Lein, K. Jung, C. Abramjuk, Effect of quinolinyl acrylate derivatives on prostate cancer in vitro and in vivo, *Invest. New Drugs*, 30 (2012) 1426-1433, DOI:10.1007/s10637-011-9716-3.
- [21] J. Rodrigues, J. Charris, J. Camacho, A. Barazarte, N. Gamboa, B. Nitzsche, M. Höepfner, M. Lein, K. Jung, C. Abramjuk, N'-Formyl-2-(5-nitrothiophen-2-yl)benzothiazole-6-carbohydrazide as a potential anti-tumor agent for prostate cancer in experimental studies, *J. Pharm. Pharmacol.* 65 (2013) 411-422, DOI: 10.1111/j.2042-7158.2012.01607.x.

- [22] J. Rodrigues, J. Charris, J. Camacho, A. Barazarte, N. Gamboa, F. Antunes, Cytotoxic Effects of N'-Formyl-2-(5-nitrothiophen-2-yl)benzothiazole-6-carbohydrazide in Human Breast Tumor Cells by Induction of Oxidative Stress, *Anticancer Res.* 32 (2012) 2721-2726.
- [23] J. Rodrigues, R. Ferrer, N. Gamboa, J. Charris, F. Antunes, Potential antitumor and pro-oxidative effects of (E)-methyl 2-(7-chloroquinolin-4-ylthio)-3-(4-hydroxyphenyl) acrylate (QNACR), *J. Enz. Inh. Med. Chem.* 28 (2013) 1300-1306, DOI: 10.3109/14756366.2012.736385.
- [24] B. Robinson, *The Fischer indole synthesis*, John Wiley & Sons, Chichester, (1982).
- [25] J. Wang, Q. Ji, J. Xu, X. Wu, Y. Xie, Facile synthesis of novel indeno[1,2-*b*]indol-10-one derivatives by oxidation with DDQ, *Synth. Commun.* 35 (2005) 581-588, DOI:10.1081/SCC-200049795
- [26] F. Robredo, M. Treus, J. Estévez, L. Castedo, R. Estévez, Nitro-facilitated '5-*Exo-dig*' Intramolecular Cyclisation of 2-(2-Nitrophenyl-ethynyl)benzoic Acids: A New Total Synthesis of Indeno[1,2-*b*]indoles, *Synlett*, 06 (2002) 999-1001, DOI: 10.1055/s-2002-31896.
- [27] C. Bal, B. Baldeyrou, F. Moz, A. Lansiaux, P. Colson, L. Kraus-Berthier, S. Leonce, A. Pierre, M. Boussard, A. Rousseau, M. Wierzbicki, C. Bailly, Novel antitumor indenoindole derivatives targeting DNA and topoisomerase II, *Biochem. Pharmacol.* 68 (2004) 1911-1922, DOI:10.1016/j.bcp.2004.07.008.
- [28] D. Black, M. Bowyer, G. Condie, D. Craig, N. Kumar, Reactions of ninhydrin with activated anilines: Formation of indole derivatives, *Tetrahedron*, 50 (1994) 10983-10994, DOI:10.1016/S0040-4020(01)85709-4.

- [29] J. Azizian, F. Hatamjafari, A. Karimi, M. Shaabanzadeh, Multi-component reaction of amines, alkyl propiolates, and ninhydrin: An efficient protocol for the synthesis of tetrahydro-dihydroxy-oxoindeno[1,2-b]pyrrole derivatives, *Synthesis*, (5) (2006) 765-767, DOI: 10.1055/s-2006-926327.
- [30] H. Hemmerling, A. Merschenz-Quack, H. Wunderlich, 1,2-Deoxygenation of *vic*-Dihydroxyindenoimidazoles: Optimization of a Novel Deoxygenation Reagent, *Z. Naturforsch.* 59b (2004) 1143-1152.
- [31] H. Hemmerling, G. Reiss, Partially saturated indeno[1,2-b]indole derivatives via deoxygenation of heterocyclic α -hydroxy-N,O-hemiaminals, *Synthesis*, (6) (2009) 985-999, DOI: 10.1055/s-0028-1087983.
- [32] F. Rostami-Charati, Z. Hossaini, M. Khalilzadeh, H. Jafaryan, Solvent-free synthesis of pyrrole derivatives, *J. Heterocyclic Chem.* 49 (2012) 217-220, DOI: 10.1002/jhet.785.
- [33] I. Sadarangani, S. Bhatia, D. Amarante, I. Lengyel, R. Stephani, Synthesis, resolution and anticonvulsant activity of chiral N-1'-ethyl,N-3'-(1-phenylethyl)-(R,S)-2'H,3H,5'H-spiro-(2-benzofuran-1,4'-imidazolidine)-2',3,5'-trione diastereomers, *Bioorg. Med. Chem. Lett.* 22 (2012) 2507-2509. DOI:10.1016/j.bmcl.2012.02.005.
- [34] A. Yapi, M. Mustofa, A. Valentin, O. Chavignon, J. Teulade, M. Mallie, J. Chapat, Y. Blache, New potential antimalarial agents: synthesis and biological activities of original diaza-analogs of phenanthrene, *Chem. Pharm. Bull.* 48 (2000) 1886-1889.
- [35] L. Rodríguez, X. Wu, J. Guan, Wound-healing assay, *Meth. Mol. Biol.* 294 (2005) 23-29, DOI:10.1385/1-59259-860-9:023.

- [36] J. Rodrigues, C. Abramjuk, L. Vasquez, N. Gamboa, J. Domínguez, B. Nitzsche, M. Hopfner, R. Georgieva, H. Baumler, C. Stephan, K. Jung, M. Lein, A. Rabien, New 4-maleamic acid and 4-maleamide peptidyl chalcones as potential multitarget drugs for human prostate cancer, *Pharm. Res.* 28 (2011) 907-919, DOI 10.1007/s11095-010-0347-8.
- [37] V. Freedman, S. Shin, Cellular tumorigenicity in nude mice: correlation with cell growth in semi-solid medium, *Cell.* 3 (1974) 355-359, DOI:10.1016/0092-8674(74)90050-6
- [38] U. Kelavkar, J. Nixon, C. Cohen, D. Dillehay, T. Eling, K. Badr, Overexpression of 15-lipoxygenase-1 in PC-3 human prostate cancer cells increases tumorigenesis, *Carcinogenesis*, 22 (2001) 1765-1773, DOI: 10.1093/carcin/22.11.1765.
- [39] D. Chodniewicz, R. Klemke, Guiding cell migration through directed extension and stabilization of pseudopodia, *Exp. Cell. Res.* 301 (2004) 31-37, DOI: 10.1016/j.yexcr.2004.08.006.
- [40] A. Folgueras, A. Pendás, L. Sánchez, C. López-Otin, Matrix metalloproteinases in cancer: from new functions to improved inhibition strategies, *Int. J. Dev. Biol.* 48 (2004) 411-424.
- [41] R. Bendardaf, A. Buhmeida, M. Hilska, M. Laato, S.; Syrjanen, K. Syrjanen, Y. Collan, S. Pyrhonen, MMP-9 (gelatinase B) expression is associated with disease-free survival and disease-specific survival in colorectal cancer patients. *Canc. Investig.* 28 (2010) 38-43, DOI: 10.3109/07357900802672761.
- [42] M. Cifone, I. Fidler, Correlation of patterns of anchorage independent growth with in vivo behavior of cells from a murine fibrosarcoma. *Proc. Natl. Acad. Sci. USA.* 77 (1980) 1039-1043.

- [43] D. Cremer, J. Pople, General definition of ring puckering coordinates, *J. Am. Chem. Soc.* 97 (1975) 1354-1358, DOI: 10.1021/ja00839a011.
- [44] S. Rowsell, P. Hawtin, C. Minshull, H. Jepson, S. Brockbank, D. Barratt, A. Slater, W. McPheat, D. Waterson, A. Henney, R. Pauptit, Crystal structure of human MMP9 in complex with a reverse hydroxamate inhibitor, *J. Mol. Biol.* 319 (2002) 173-181, DOI:10.1016/S0022-2836(02)00262-0.
- [45] F. Denizot, R. Lang, Rapid colorimetric assay for cell growth and survival. Modifications to the tetrazolium dye procedure giving improved sensitivity and reliability, *J. Immunol. Methods.* 89 (1986) 271-277, DOI:10.1016/0022-1759(86)90368-6.
- [46] A. Powell, S. Akare, W. Qi, P. Herzer, S. Jean-Louis, A. Feldman, J. Martinez, Resistance to ursodeoxycholic acid-induced growth arrest can also result in resistance to deoxycholic acid-induced apoptosis and increased tumorigenicity, *BMC Cancer*, 6 (2006) 219, DOI:10.1186/1471-2407-6-219.
- [47] X. Qu, Y. Yuan, W. Xu, M. Chen, S. Cui, H. Meng, Y. Li, M. Makuuchi, M. Nakata, W. Tang, Caffeoyle pyrrolidine derivative LY52 inhibits tumor invasion and metastasis via suppression of matrix metalloproteinase activity, *Anticancer Res.* 26 (2006) 3573-3578.
- [48] Bruker, *SMART*, version 5.630. Bruker AXS Inc., Madison, Wisconsin, USA, (2002).
- [49] Bruker, *SAINT*, version 6.22. Bruker AXS Inc., Madison, Wisconsin, USA, (2001).
- [50] Bruker, *SADABS*, version 2.05. Bruker AXS Inc., Madison, Wisconsin, USA, (2003).

- [51] G. Sheldrick, A short history of *SHELX*, Acta Cryst. A64 (2008) 112-122, DOI:10.1107/S0108767307043930.
- [52] L. Farrugia, *ORTEP-3* for Windows - a version of *ORTEP-III* with a graphical user interface (GUI), J. Appl. Cryst. 30 (1997) 565, DOI:10.1107/S0021889897003117.
- [53] A. Spek, Single-crystal structure validation with the program *PLATON*, J. Appl. Cryst. 36 (2003) 7, DOI:10.1107/S0021889802022112.
- [54] L. Farrugia, *WinGX* suite for small-molecule single-crystal crystallography, J. Appl. Cryst. 32 (1999) 837, DOI:10.1107/S0021889899003039.
- [55] CACheReference, version 6.0. Fujitsu Limited CAChe (2003).
- [56] N. Allinger, Y. Yuh, J. Lii, Molecular mechanics. The MM3 force field for hydrocarbons. 1, J. Am. Chem. Soc. 111 (1989) 8551-8556, DOI: 10.1021/ja00205a001.
- [57] Thompson MA. Arguslab 4.0.1. Planaria Software LLC, Seattle, WA. (2004).

Table 1. Selected bond lengths (Å) and angles (°) for **6k** and **7k**.

	6k	7k
C1-C2	1.5796(16)	1.5765(15)
C1-C11	1.5032(17)	1.5060(17)
C1-N1	1.5011(16)	1.4994(14)
C2-C3	1.5009(17)	1.4978(16)
C2-C9	1.5462(17)	1.5440(18)
C3-C4	1.4108(17)	1.4117(16)
C3-C8	1.3710(17)	1.3657(16)
C4-C5	1.5082(19)	1.5099(19)
C5-C6	1.516(2)	1.535(2)
C6-C7	1.532(2)	1.5440(18)
C7-C8	1.4861(18)	1.4870(16)
C9-C10	1.4765(18)	1.4753(19)
N1-C8	1.3427(16)	1.3443(14)
N1-C16	1.4341(15)	1.4310(14)
O1-C1	1.3788(14)	1.3803(14)
O2-C2	1.4126(15)	1.4118(14)
O3-C4	1.2524(16)	1.2500(16)
O4-C9	1.2081(15)	1.2043(17)
C2-C1-C11	105.29(9)	105.19(10)
C2-C1-N1	102.20(9)	102.21(8)
C2-C1-O1	117.03(10)	117.00(9)
C11-C1-N1	109.24(10)	110.02(9)
C11-C1-O1	110.52(10)	110.24(9)
N1-C1-O1	111.97(10)	111.70(10)
C1-C2-C3	103.62(9)	103.66(9)
C1-C2-C9	103.84(9)	104.10(9)
C1-C2-O2	112.31(9)	112.04(9)
C3-C2-C9	111.91(10)	112.27(10)
C3-C2-O2	114.39(10)	114.27(10)
C9-C2-O2	110.12(10)	109.92(10)
C2-C3-C4	126.45(11)	126.84(11)
C2-C3-C8	109.72(10)	109.91(10)
C4-C3-C8	121.58(12)	121.38(11)
C3-C4-C5	116.97(12)	116.93(11)
C3-C4-O3	122.59(12)	122.61(12)
C5-C4-O3	120.31(11)	120.31(11)
C4-C5-C6	113.58(11)	116.39(10)
C5-C6-C7	111.84(12)	109.31(11)
C6-C7-C8	108.88(12)	111.12(11)

C3-C8-C7	123.23(11)	123.57(11)
C3-C8-N1	112.47(11)	112.39(10)
C7-C8-N1	124.18(12)	123.85(10)
C2-C9-C10	108.37(10)	108.15(10)
C2-C9-O4	124.33(12)	124.40(13)
C10-C9-O4	127.24(12)	127.42(13)
C9-C10-C11	110.23(11)	110.57(11)
C1-C11-C10	111.82(10)	111.72(11)
C1-N1-C8	111.55(10)	111.48(9)

Table 2. Crystal data, intensity data collection parameters and final refinement results for **6k** and **7k**

Compound	6k	7k
CCDC deposit No.	CCDC 1022641	CCDC 1022819
<i>Crystal Data</i>		
Formula	C ₂₃ H ₂₁ NO ₄	C ₂₅ H ₂₅ NO ₄
MW	375.31	403.46
Color	pale yellow	pale yellow
Morphology	prism	prism
Specimen size (mm)	0.55x0.52x0.16	0.50x0.48x0.43
T (K)	296(2)	296(2)
a (Å)	10.5702(6)	9.6597(4)
b (Å)	14.0438(7)	18.0974(8)
c (Å)	13.4084(7)	12.2889(5)
β (°)	110.1540(10)	93.7970(10)
V (Å ³)	1868.55(17)	2143.57(16)
Crystal system	monoclinic	monoclinic
Space group (No.)	P2 ₁ /c (No. 14)	P2 ₁ /n (No. 14)
Z	4	4
D _c (g cm ⁻³)	1.334	1.250
F(000)	792	856
μ (Mo-K α) (mm ⁻¹)	0.091	0.084
θ range (°) for cell	2.57-25.69	2.25-28.67
No. refls. for cell	5024	7826
<i>Data Collection</i>		
θ range (°)	2.05-28.77	2.01-28.82
h range	-14, 13	-13, 13
k range	-18, 18	-23, 24
l range	-17, 15	-15, 16
Mean ΔI for checks (%)	-0.3	-0.1
No. refls. measured	9865	17049
No. refls. unique	4447	5250
No. refls. I > 2 σ (I)	3582	4287
Abs. correction	multi-scan	multi-scan
Trans. coeff. (T _{min} , T _{max})	0.937-0.969	0.951-0.973
R _{int}	0.0140	0.0161

Refinement (last cycle)

Weighting scheme (a,b)	0.0638, 0.3320	0.0822, 0.3249
No. params. refined	257	277
R1 [$I > 2\sigma(I)$]	0.0437	0.0471
R1 (all data)	0.0538	0.0572
wR2 [$I > 2\sigma(I)$]	0.1156	0.1299
wR2 (all data)	0.1231	0.1388
S (g.o.f.) (all data)	1.032	1.027
Δ/σ max.	0.001	0.001
Δ/σ mean	<0.0005	<0.0005
$\Delta\rho_r$ (min., max.) ($e \text{ \AA}^{-3}$)	-0.18, 0.30	-0.18, 0.31

Table 3. Possible hydrogen bonds for **6k** and **7k** (Å and °).

6k				
D-H...A	D-H	H...A	D...A	DHA
O1-H1...O3 ⁱ	0.82	1.96	2.7715(13)	173.3
O2-H2...O3	0.82	2.18	2.8528(14)	139.4
C12-H12...O1 ⁱⁱ	0.93	2.52	3.4039(16)	158.5
C15-H15...O4 ⁱⁱⁱ	0.93	2.54	3.3893(17)	151.2
7k				
D-H...A	D-H	H...A	D...A	DHA
O1-H1...O3 ^{iv}	0.82	1.97	2.7839(14)	175.2
O2-H2...O3	0.82	2.22	2.8811(14)	138.5
C5-H5B...O2 ^{iv}	0.97	2.57	3.2341(17)	125.8

Symmetry codes: i) 1-x, 2-y, 1-z; ii) -x,2-y,1-z; iii) 1-x, 2-y, 2-z; iv) -x, -y, 1-z

Table 4. Cytotoxic effects of compounds on human and non-human tumor cells.

Compound	R ₁ , R ₂	R ₃	PC-3	LNCaP	MatLyLu
6p	H	4Cl	67.91 ± 4.37	79.17 ± 2.73	>100
7p	H	3,4-Cl	76.59 ± 5.41	66.25 ± 2.16	>100
6q	CH₃	4Cl	47.77 ± 3.11	53.92 ± 3.88	75.17 ± 2.35
7q	CH₃	3,4-Cl	10.70 ± 0.07**	9.57 ± 0.55**	5.96 ± 0.28
DQ			24.60 ± 2.22	4.94±0.66	10.33±2.17

6a-o, 7a-o: > 100 µg/mL

Results are expressed as the mean ± SEM of the half inhibitory concentration or IC₅₀ (µg/mL). Each experiment was performed three times in five different wells. DQ: control dequalinium. ***p*<0.01 compared to DQ.

Table 5. Inhibition of clonogenic potential by compound **7q**.

Cell line	Colony formation (% of control)		Relative colony size	
	Control	7q	Control	7q
PC-3	100±17.6	0	1±0.3	0
LNCaP	100±18.3	0	1±0.3	0
MatLyLu	100±17.6	6.35±1.98**	1±0.05	0.16±0.04***

Colony growth relative to vehicle-treated controls PC-3, LNCaP and MatLyLu cells were quantified by light microscopy. The results are given as means \pm SEM. of three independent experiments. ** $p < 0.01$ and *** $p < 0.001$ compared to control vehicle.

Figure Captions

Scheme. The general reaction protocols leading to compounds **6a-q** and **7a-q**.

Figure 1. Molecular structures of compounds (a) **6k** and (b) **7k** showing the atomic numbering. The displacement ellipsoids are drawn at 50% probability. Dashed lines indicate intramolecular hydrogen bonds.

Figure 2. Effect of compound **7q** on PC-3, LNCaP and MatLyLu cell viability. Results are expressed as the mean \pm SEM of three different experiments. * $p < 0.05$, ** $p < 0.01$ and *** $p < 0.001$ compared to the previous concentration at the same cell line.

Figure 3. Effect of compound **7q** on PC-3 wound closure. (a) Representative images of PC-3 cells were captured at the time of wounding (a) and (b), and 24 h following the wound (c) and (d), to illustrate recovery from scrape wound. (e) The percentage of wound area closed at 24 hours post-treatment is plotted for cell monolayer with or without **7q**. Data shown in (a), (b), (c) and (d) are from a representative experiment carried out independently three times. Data in (e) represents the mean \pm SEM. ** $p < 0.01$ compared to control vehicle.

Figure 4. Effect of compound **7q** in the invasion of LNCaP cells. Cells treated with the compound or vehicle were seeded onto a Matrigel coated 0.8 μ m porous membrane for 18 h, and the inhibition of invasion relative to the control vehicle treated cells was determined. The results represent the mean \pm SEM of three independent experiments. ** $p < 0.01$ compared to control vehicle.

Figure 5. Activity of MMP-9 metalloproteinase by gelatin zymography in PC-3 cells when exposed to compound **7q** for 24h. (a) Conditioned medium prepared from subconfluent cultures were collected, resolved in non-reducing gels containing gelatin (1 mg/ml) and processed for zones of gel degradation activity. (b) Results were quantified in relation to control vehicle and are presented as the mean \pm SEM of percentage of activity in three different experiments. *** $p < 0.001$ compared to control vehicle.

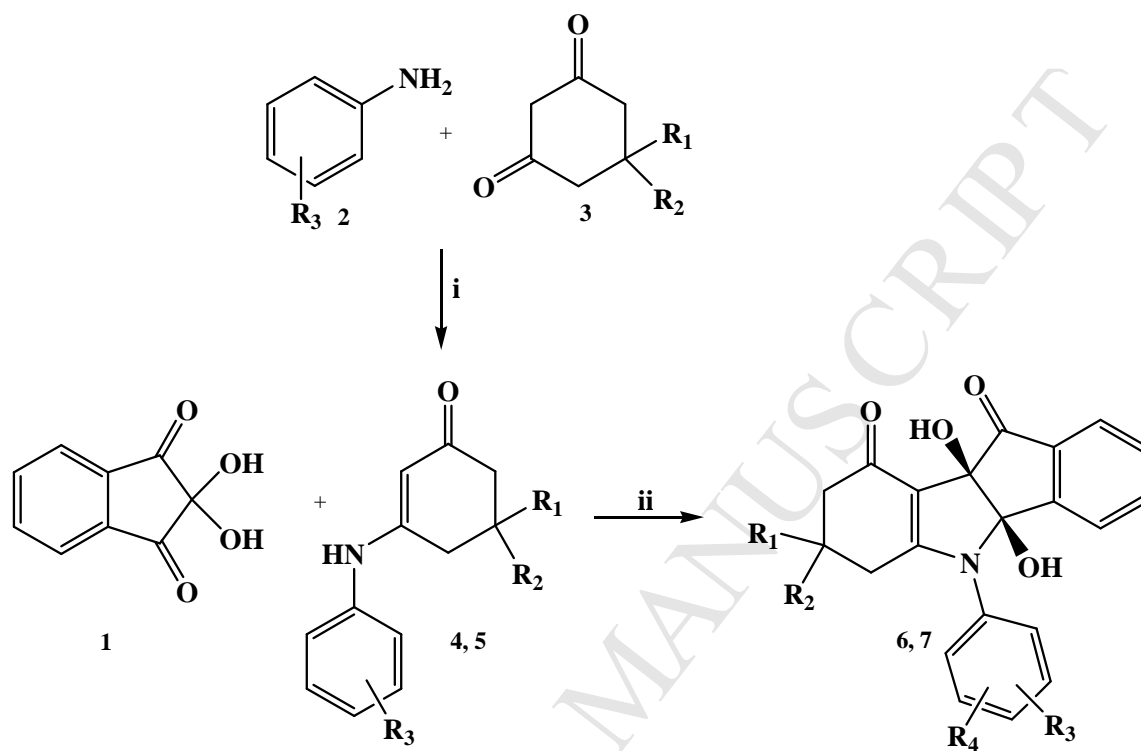
Figure 6. Effect of compound **7q** on the formation of tumor colonies in soft agar. PC-3 (a), LNCaP cells (b) and MatLyLu cells (c) were plated over a semi-solid layer of soft agar and treated with the compound **7q** or vehicle (control) and incubated for 14 days. The results represent standard images of three different experiments.

Figure 7. Catalytic centre and S1'subsite of the enzyme MMP-9 human (PDB ID: 1GKC).

Figure 8. Binding mode of highly active compound **7q** at the catalytic centre and S1'subsite of the enzyme MMP-9 human.

Figure 9. Binding mode of **6k** at the catalytic centre and S1' subsite of the enzyme MMP-9 human.

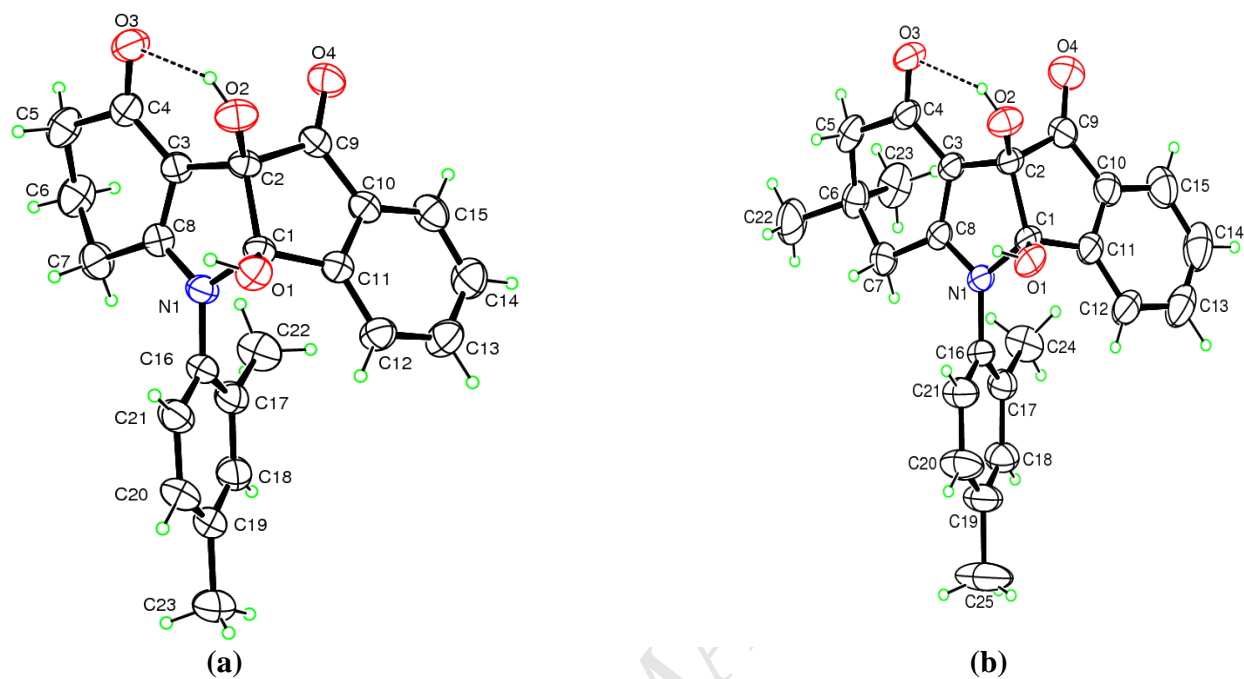
Scheme.



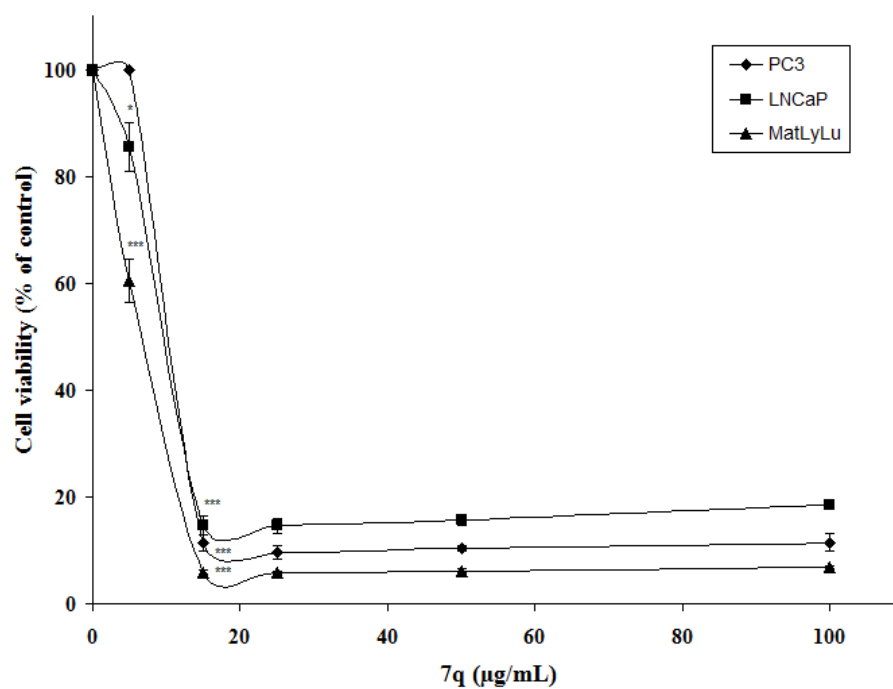
i: cat. p-TsOH, PhMe, Δ ; ii: CHCl_3 , rt.

R_1, R_2 : H; R_1, R_2 : CH_3 ; R_3, R_4 : $\text{CH}_3, \text{OCH}_3, \text{Br}, \text{Cl}$.

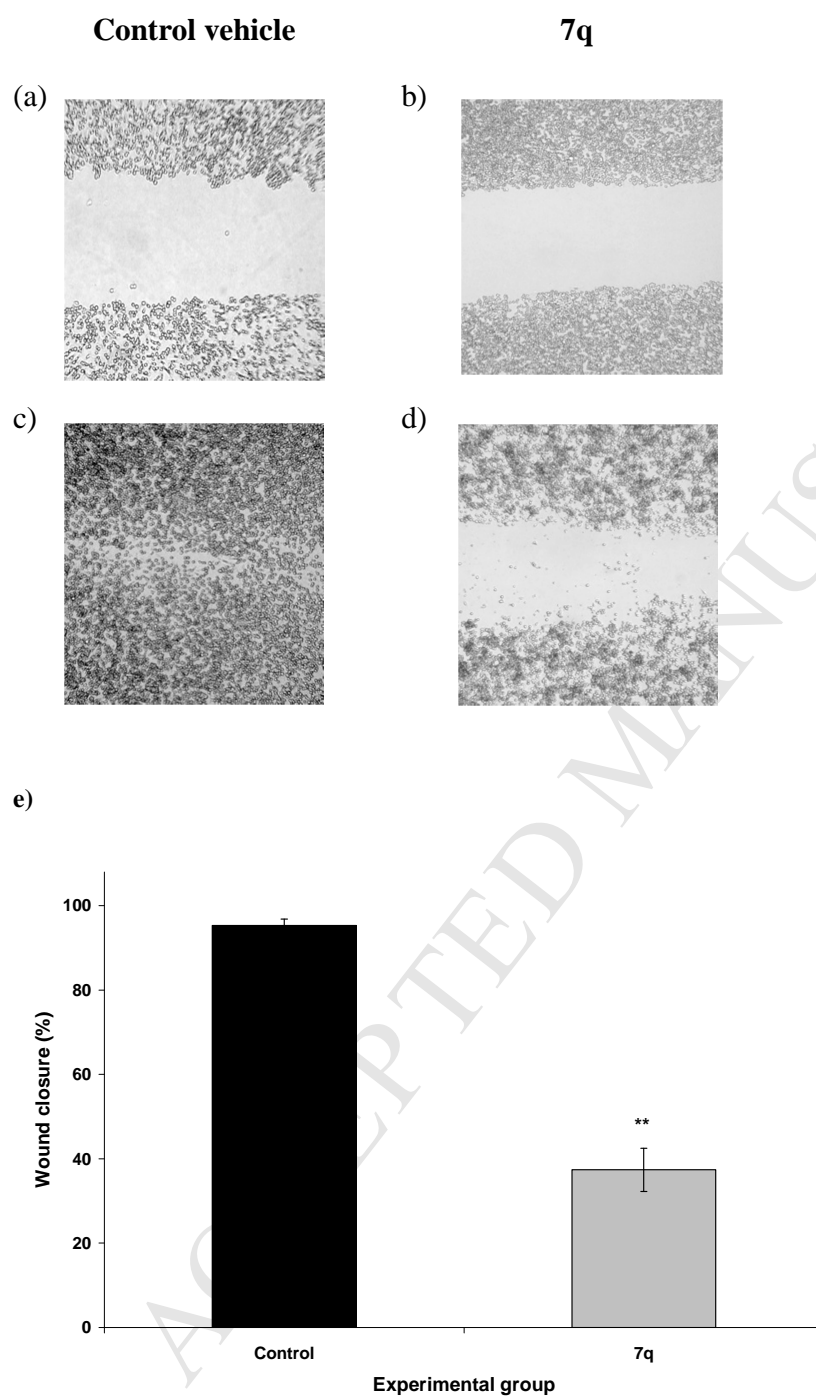
6a-q R_1, R_2 : H. 7a-q R_1, R_2 : CH_3

Figure 1.

The displacement ellipsoids are drawn at 50% probability. Dashed lines indicate intramolecular hydrogen bonds.

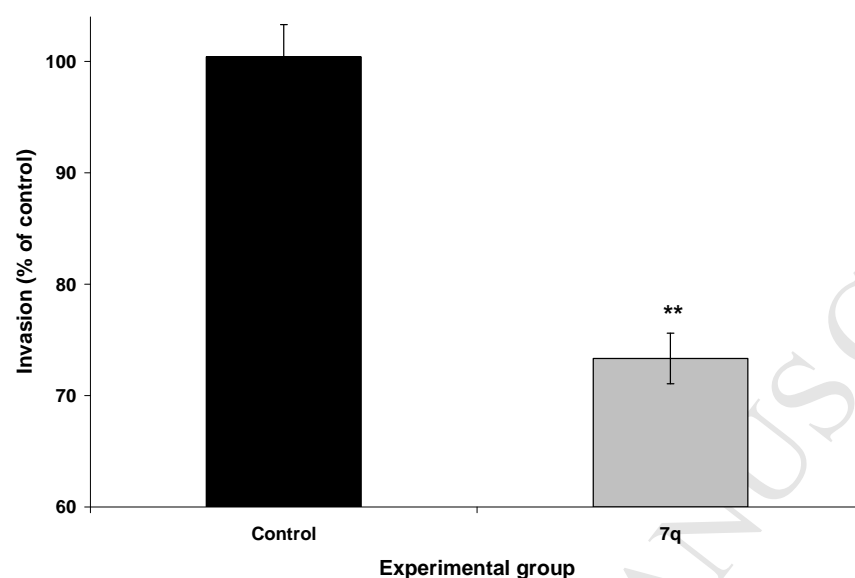
Figure 2.

Results are expressed as the mean \pm SEM of three different experiments. * $p < 0.05$, ** $p < 0.01$ and *** $p < 0.001$ compared to the previous concentration at the same cell line.

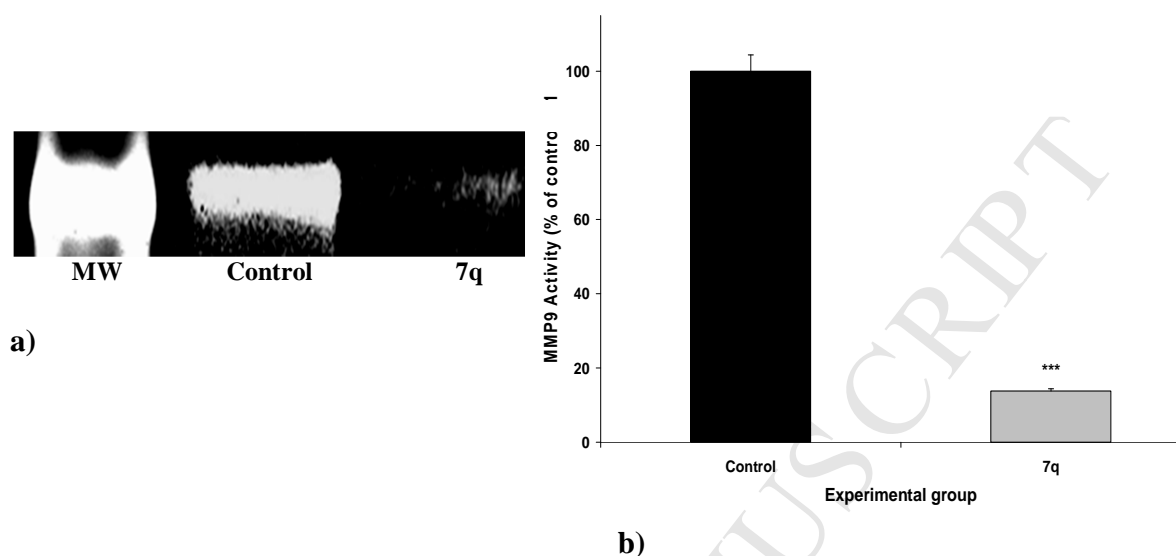
Figure 3.

(a) Representative images of PC-3 cells were captured at the time of wounding (a) and (b), and 24 h following the wound (c) and (d), to illustrate recovery from scrape wound. (e) The percentage of wound area closed at 24 hours post-treatment is plotted for cell monolayer with or without **7q**. Data shown in (a), (b), (c) and (d) are from a representative experiment

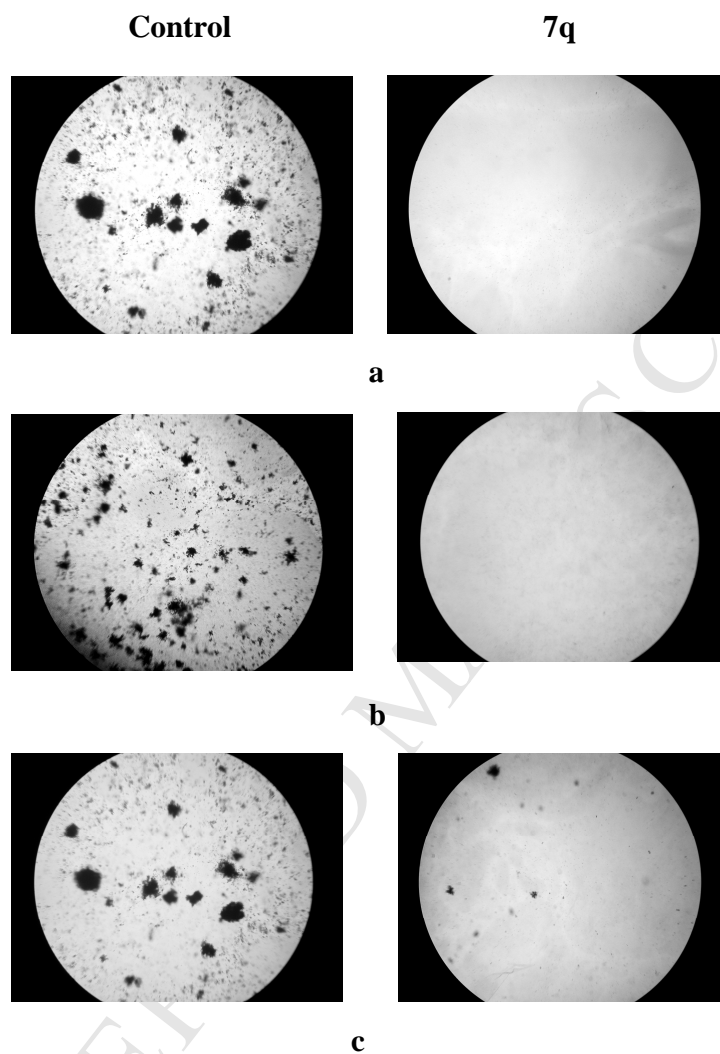
carried out independently three times. Data in (e) represents the mean \pm SEM. $**p<0.01$ compared to control vehicle.

Figure 4.

Cells treated with the compound or vehicle were seeded onto a Matrigel coated 0.8 μ m porous membrane for 18 h, and the inhibition of invasion relative to the control vehicle treated cells was determined. The results represent the mean \pm SEM of three independent experiments. ** $p < 0.01$ compared to control vehicle.

Figure 5.

(a) Conditioned medium prepared from subconfluent cultures were collected, resolved in non-reducing gels containing gelatin (1 mg/ml) and processed for zones of gel degradation activity. (b) Results were quantified in relation to control vehicle and are presented as the mean \pm SEM of percentage of activity in three different experiments. *** $p < 0.001$ compared to control vehicle.

Figure 6.

(a) PC-3, (b) LNCaP and (c) MatLyLu cells were plated over a semi-solid layer of soft agar and treated with the compound **7q** or vehicle (control) and incubated for 14 days. The results represent standard images of three different experiments.

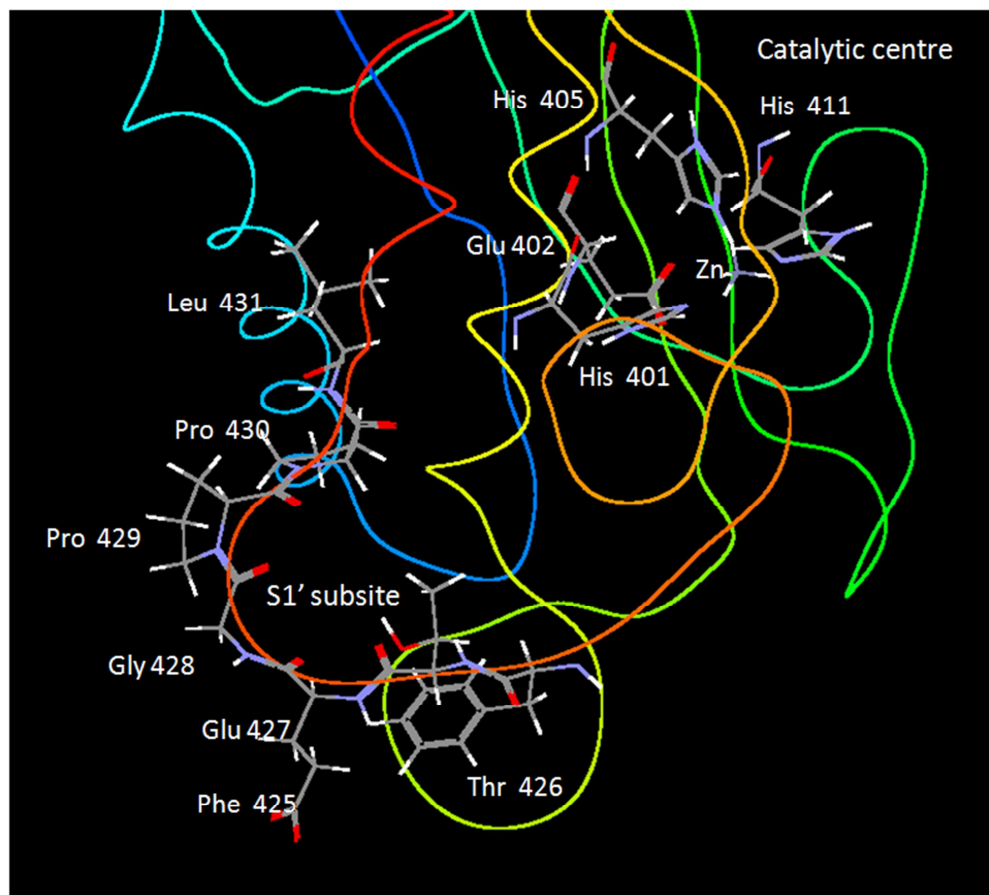
Figure 7.

Figure 8.

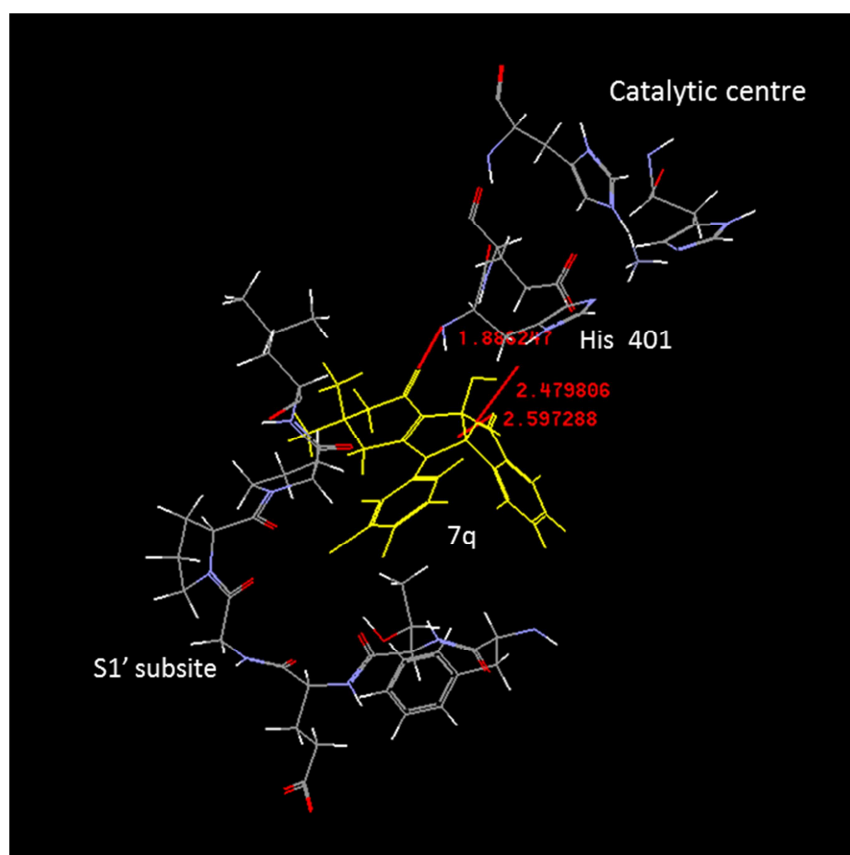
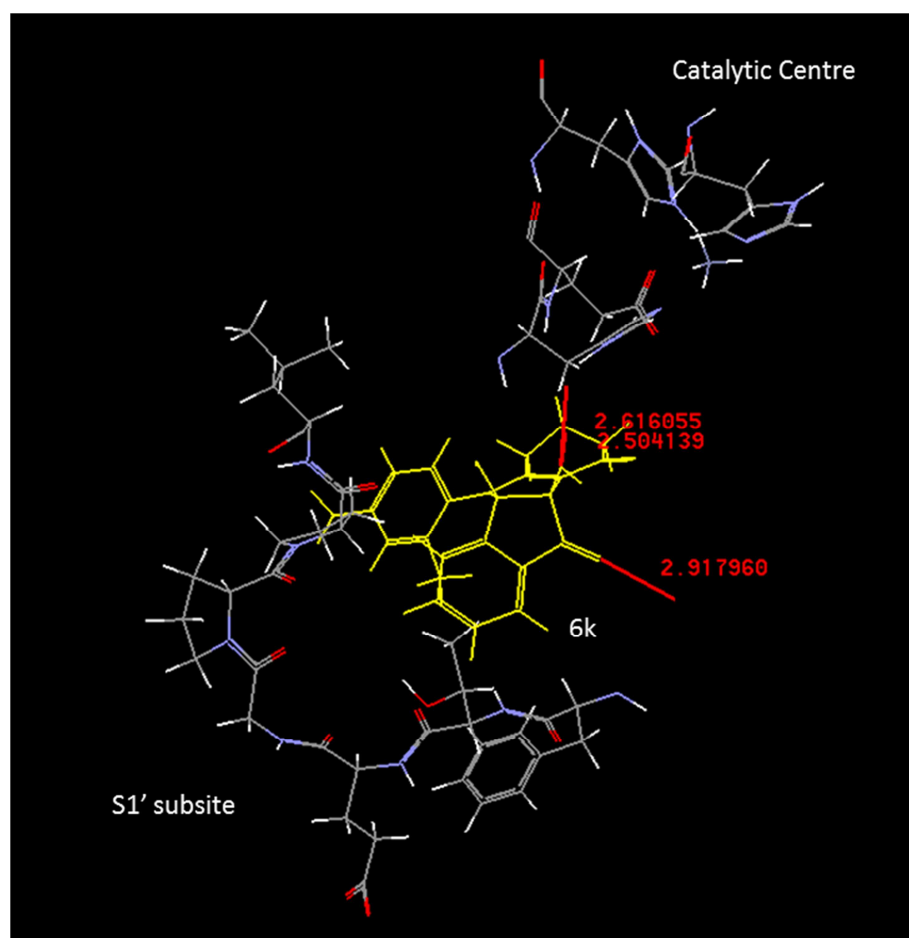
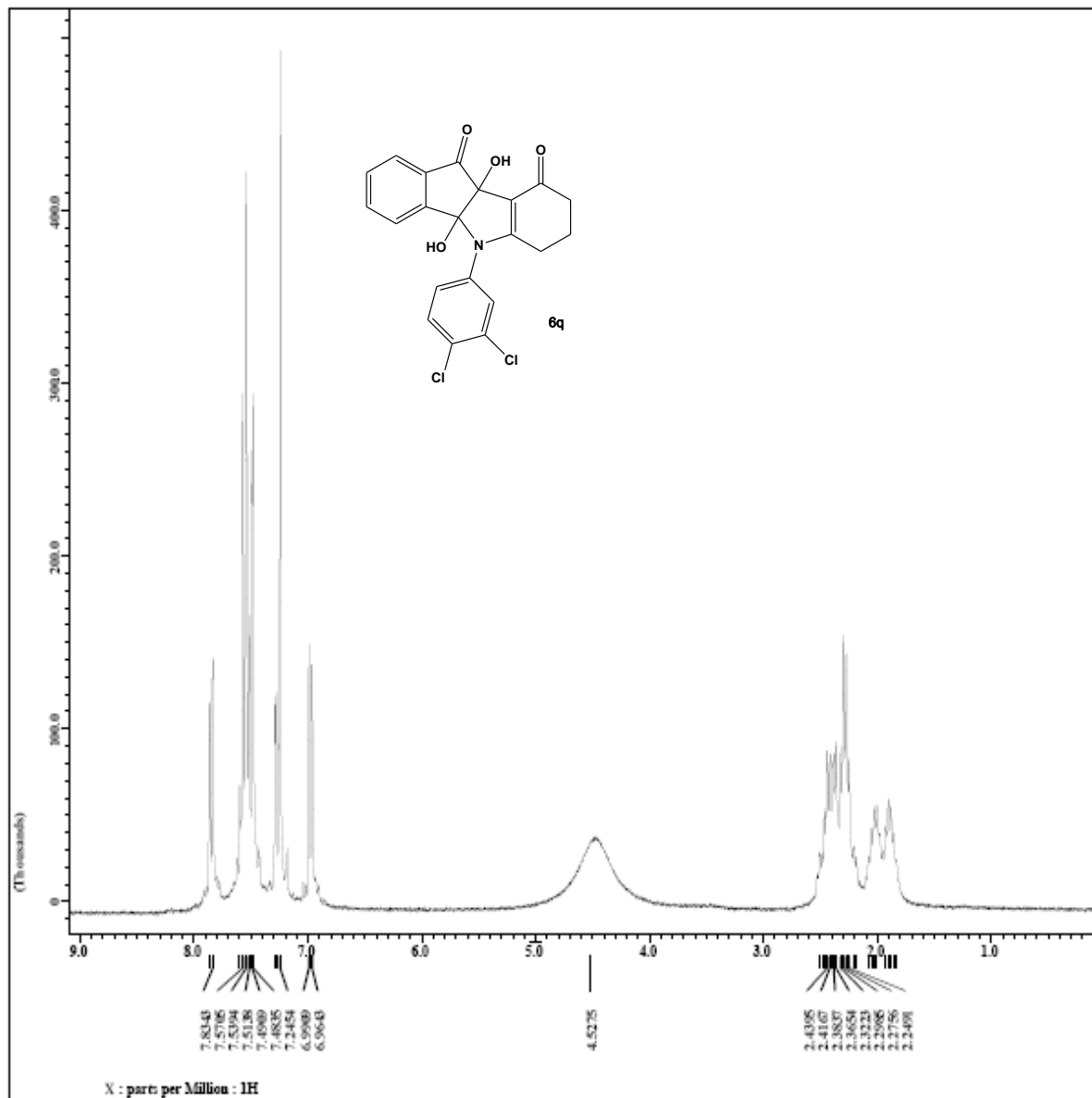


Figure 9.

- Compounds were easily synthesized and with highly regiospecificity.
- Crystals consist of equimolar mixtures of the RR and SS diastereomers.
- All tested compounds proved to be moderately active, except one.
- The antitumor activity seems to be related with inhibition of MMP-9.
- Docking studies shows a set of interactions in specific sites.



Filename = JcharrisGL205-1H-4.jd
 Author = rxnlab
 Experiment = single pulse.exp
 Sample id = JcharrisGL205
 Solvent = CHLOROFORM-D
 Creation time = 30-DEC-2013 20:16:49
 Revision time = 2-MAR-2015 17:04:54
 Current time = 2-MAR-2015 17:05:06

Content = Single Pulse Experiment
 Data format = 1D COMPLEX
 Dim size = 16384
 Dim title = 1H
 Dim units = [ppm]
 Dimensions = 1
 Site = Eclipse4 400
 Spectrometer = DELTA_HMR

Field strength = 6.345446 [T] (270[MHz])
 I acq duration = 4.0419328[s]
 I domain = 1H
 I freq = 270.16608844[MHz]
 I offset = 5[ppm]
 I points = 16384
 I prescans = 0
 I resolution = 0.24740639 [Hz]
 I sweep = 4.05350628 [kHz]
 Clipped = FALSE
 Mod return = 1
 Scans = 8
 Total scans = 8

I 90 width = 11.7[us]
 I acq time = 4.0419328[s]
 I angle = 45[deg]
 I pulse = 5.85[us]
 Initial wait = 1[s]
 Phase preset = 3[us]
 Recvr gain = 15
 Relaxation delay = 4[s]
 Temp get = 20.2 [dC]
 Onblnk time = 2[us]

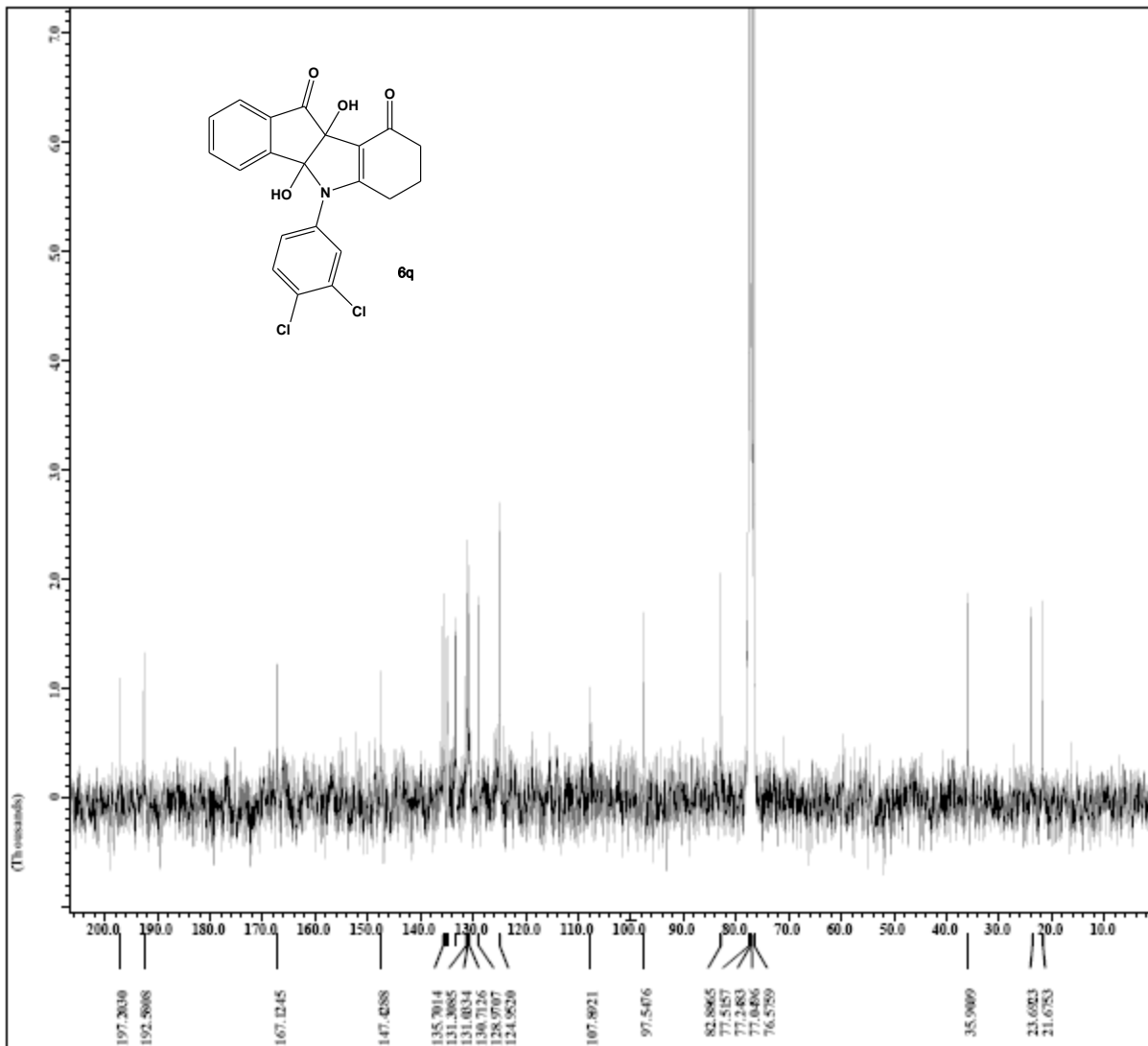
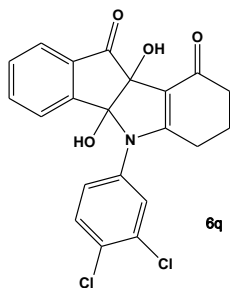


Filename = Jcharris2L205-13C-3.j
 Author = runlab
 Experiment = single pulse dac
 Sample_id = Jcharris2L205
 Solvent = CHLOROFORM-D
 Creation time = 31-DEC-2013 00:58:23
 Revision time = 2-MAR-2015 17:06:58
 Current_time = 2-MAR-2015 17:07:06

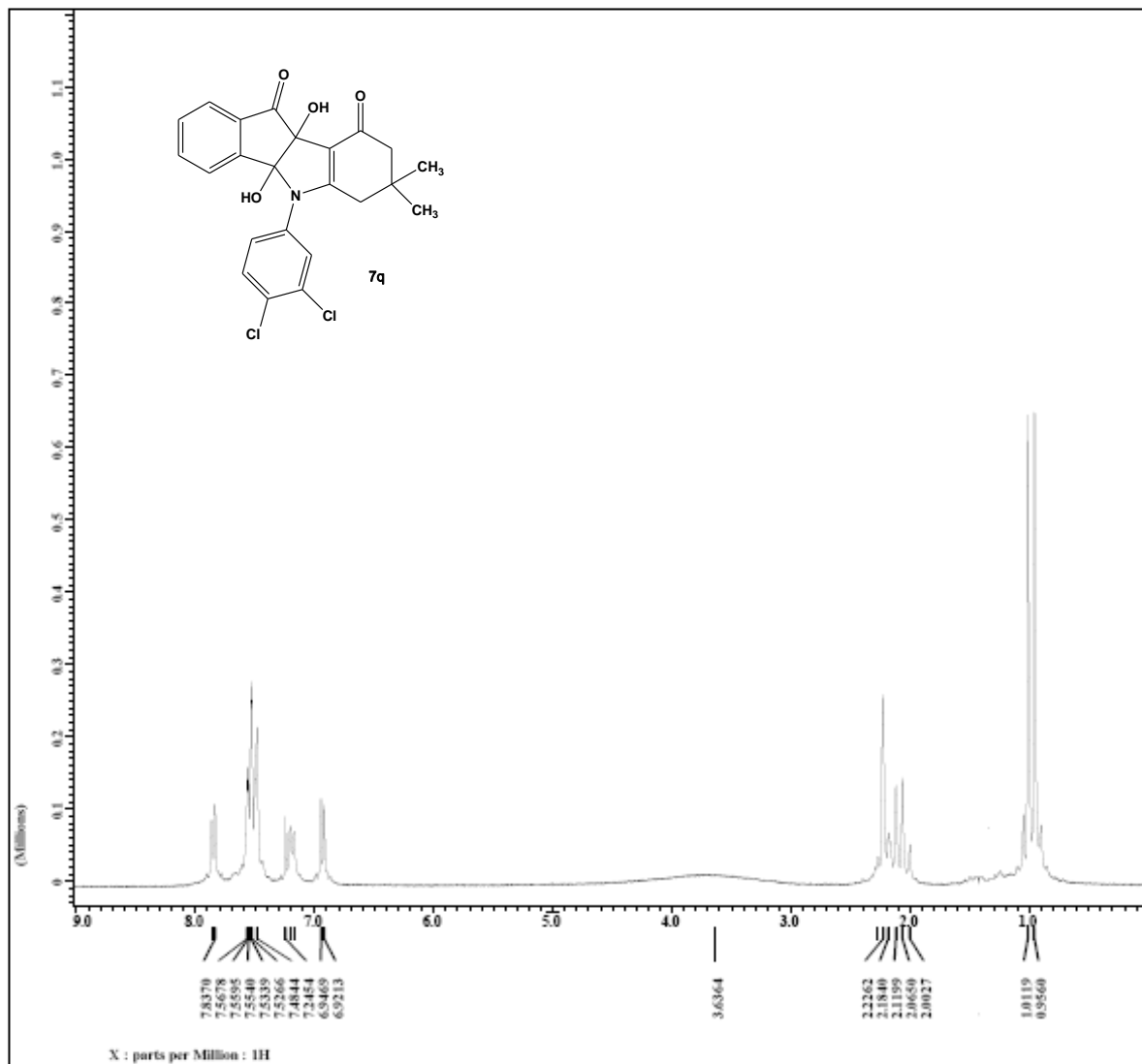
Content = Single Pulse with Bro
 Data format = 1D COMPLEX
 Dim Size = 32768
 Dim title = 13C
 Dim units = [ppm]
 Dimensions = 1
 Site = Solipses+ 400
 Spectrometer = DELTA_NMR

Field strength = 6.345446 [T] (270[MHz])
 F1_acq_duration = 1.9267584 [s]
 F1_domain = 13C
 F1_freq = 87.93330993 [MHz]
 F1_offset = 160 [ppm]
 F1_points = 32768
 F1_prescans = 4
 F1_resolution = 0.51900643 [Hz]
 F1_sweep = 17.06680272 [kHz]
 F1_domain = 1H
 F1_freq = 270.16608844 [MHz]
 F1_offset = 5 [ppm]
 Clipped = FALSE
 Mod Return = 1
 Scans = 5762
 Total_scans = 5762

F2_90_width = 7.8 [us]
 F2_acq_time = 1.9267584 [s]
 F2_angle = 30 [deg]
 F2_pulse = 2.6 [us]
 F2_initial_wait = 1 [s]
 Phase pFset = 3 [us]
 Decvr_gain = 15
 Relaxation_delay = 1 [s]
 Temp_get = 27.1 [dC]
 Onblank_time = 2 [us]



X : part per Million : 13C

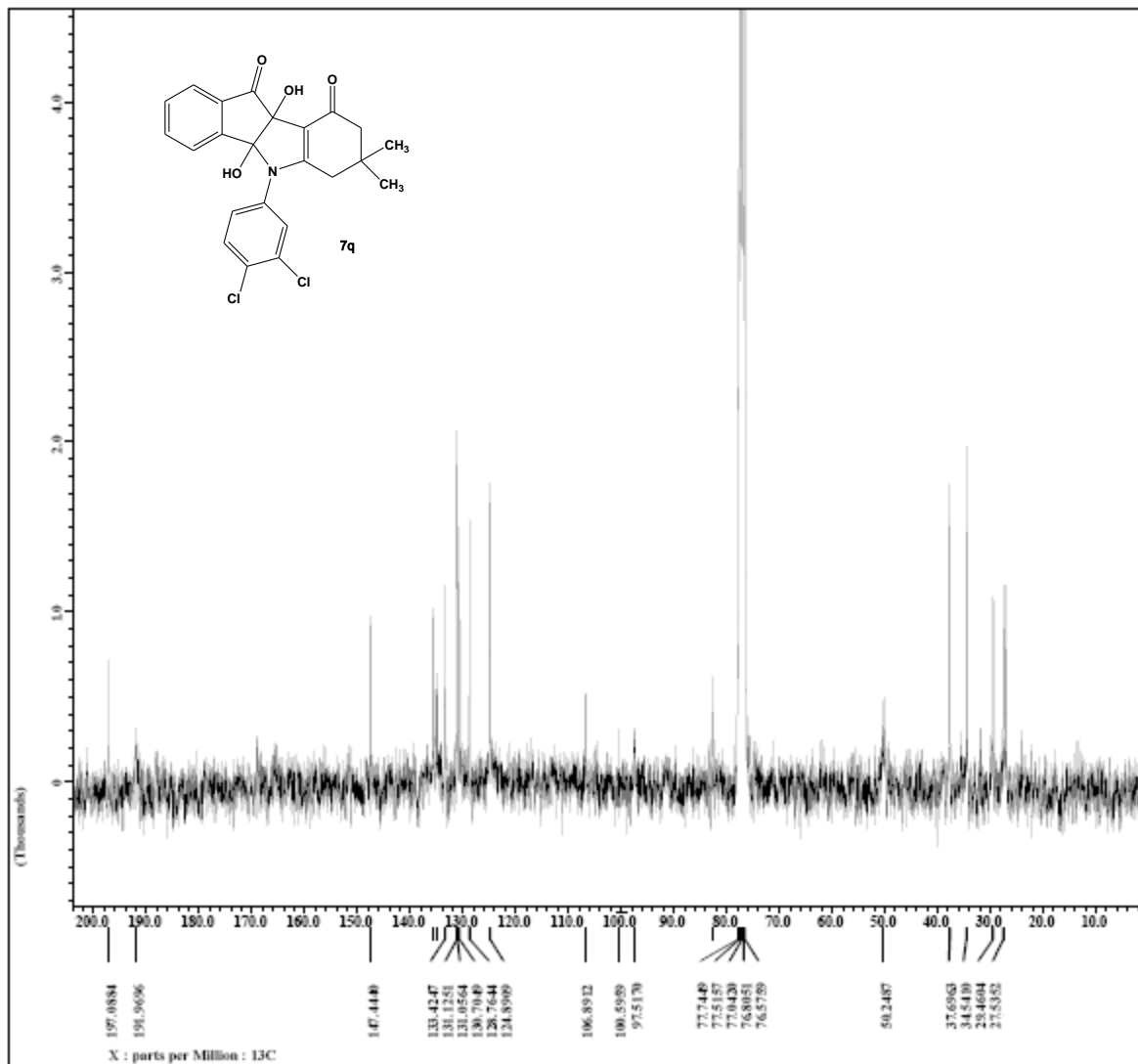


filename = jcharriscu208-1h-3.jd
 Author = rmlab
 Experiment = single pulse.exp
 sample id = jcharriscu208
 solvent = CHLOROFORM-D
 Creation time = 31-MAR-2013 01:05:33
 Revision time = 2-MAR-2015 17:08:31
 Current time = 2-MAR-2015 17:08:40

Content = single pulse experiment
 Data format = 1D COMPLEX
 Dim Size = 16384
 Dim title = 1h
 Dim units = [ppm]
 Dimensions = X
 Site = Eclipse+ 400
 Spectrometer = DELTA 400

Field strength = 6.345446 [T] (270 [kHz])
 X acq duration = 4.0419328 [s]
 X decoupling = 1h
 X freq = 270.16608944 [kHz]
 X offset = 5 [ppm]
 X points = 16384
 X prescans = 0
 X resolution = 0.24740639 [Hz]
 X sweep = 4.05350628 [kHz]
 Clipped = FALSE
 Mod return = 1
 Scans = 8
 Total scans = 8

X 90 width = 11.7 [us]
 X acq time = 4.0419328 [s]
 X angle = 45 [deg]
 X pulse = 5.85 [us]
 Initial wait = 1 [s]
 Phase preset = 3 [us]
 Recvr gain = 15
 Relaxation delay = 4 [s]
 Temp set = 20.5 [deg]
 Unblank time = 2 [us]

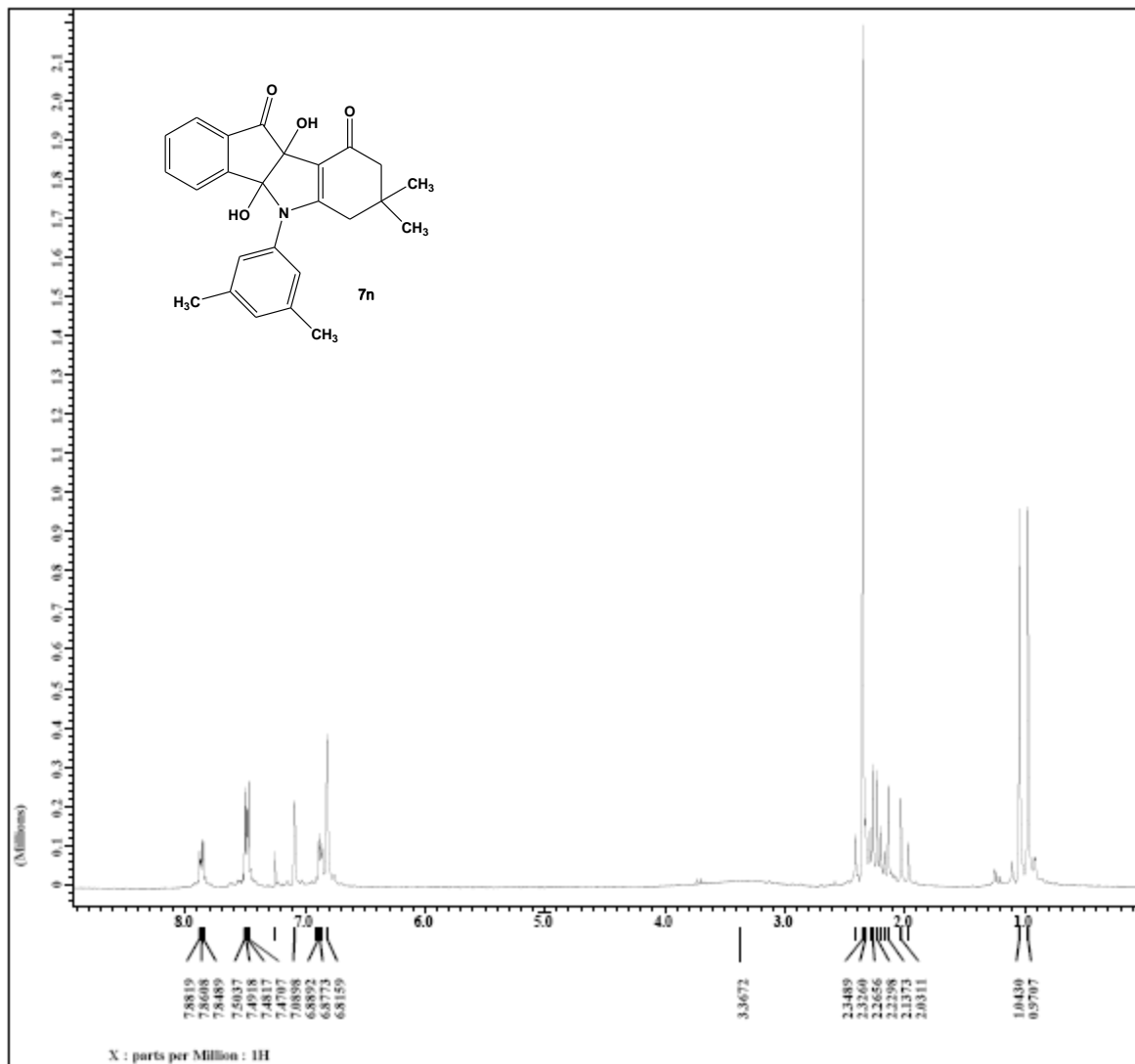


filename = jcharrison208-13c-3.j
 author = rmlab
 experiment = single pulse dec
 sample_id = jcharrison208
 solvent = CHLOROFORM-D
 creation_time = 31-MAR-2013 10:51:25
 revision_time = 2-MAR-2015 17:09:58
 current_time = 2-MAR-2015 17:10:12

content = single pulse with ero
 data_format = 1d cmv1mx
 data_size = 32768
 data_title = 13c
 data_units = [ppm]
 dimensions = x
 site = Eclipse+ 400
 spectrometer = MSL-400

field_strength = 6.345446 [T] (270 [kHz])
 x_acq_duration = 1.9267584 [s]
 x_domain = 13c
 x_freq = 67.93330993 [kHz]
 x_offset = 100 [ppm]
 x_points = 32768
 x_prescans = 4
 x_resolution = 0.51900643 [Hz]
 x_sweep = 17.00680272 [kHz]
 ifr_domain = 1s
 ifr_freq = 270.16608944 [kHz]
 ifr_offset = 5 [ppm]
 clipped = FALSE
 mod_return = 1
 scans = 12000
 total_scans = 12000

x_90_width = 7.8 [us]
 x_acq_time = 1.9267584 [s]
 x_angle = 30 [deg]
 x_pulse = 2.6 [us]
 initial_wait = 1 [s]
 phase_reset = 3 [us]
 recvr_gain = 15
 relaxation_delay = 1 [s]
 temp_get = 26.2 [deg]
 unblank_time = 2 [us]

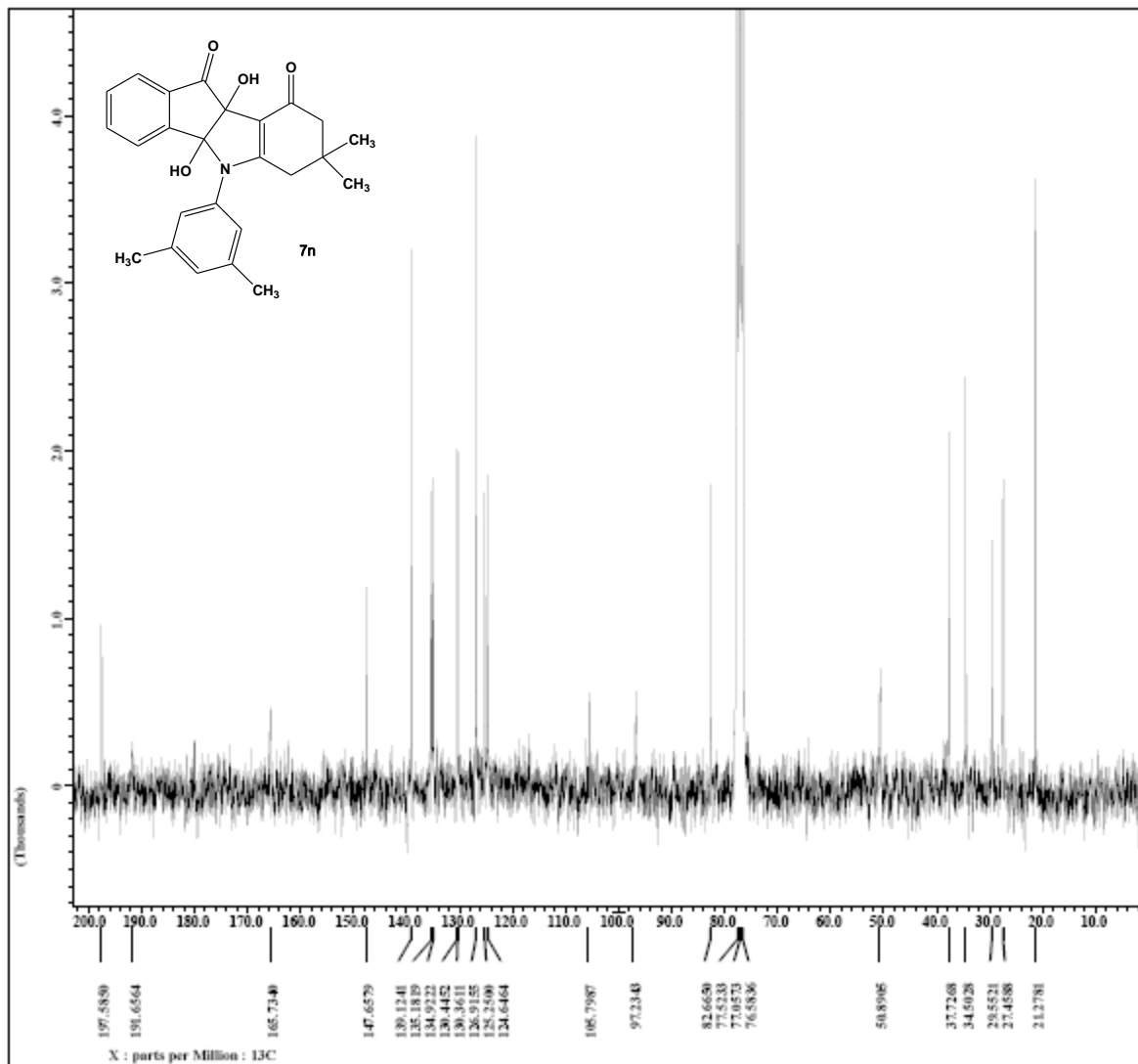


filename = jcharrismz5729-1n-3.j
 author = rmlab
 experiment = single_pulse.exp
 sample_id = jcharrismz5729
 solvent = CDCl3
 creation_time = 24-MAR-2013 20:24:25
 revision_time = 2-MAR-2015 17:37:41
 current_time = 2-MAR-2015 17:37:57

content = single_pulse_experiment
 data_format = 1D_COSY_1H
 bin_size = 16384
 bin_title = 1n
 bin_units = [ppm]
 dimensions = 2
 site = Eclipse+ 400
 spectrometer = JEOL

field_strength = 6.345446 [T] (270 [kHz])
 x_acq_duration = 4.0419328 [s]
 x_domain = 1n
 x_freq = 270.16608944 [kHz]
 x_offset = 5 [ppm]
 x_points = 16384
 x_proscans = 0
 x_resolution = 0.24740639 [Hz]
 x_sweep = 4.05350628 [kHz]
 clipped = FALSE
 mod_return = 1
 scans = 16
 total_scans = 16

x_90_width = 11.7 [us]
 x_acq_time = 4.0419328 [s]
 x_angle = 45 [deg]
 x_pulse = 5.65 [us]
 initial_wait = 1 [s]
 phase_preset = 3 [us]
 recvr_gain = 15
 relaxation_delay = 4 [s]
 temp_get = 25.2 [deg]
 unblank_time = 2 [us]

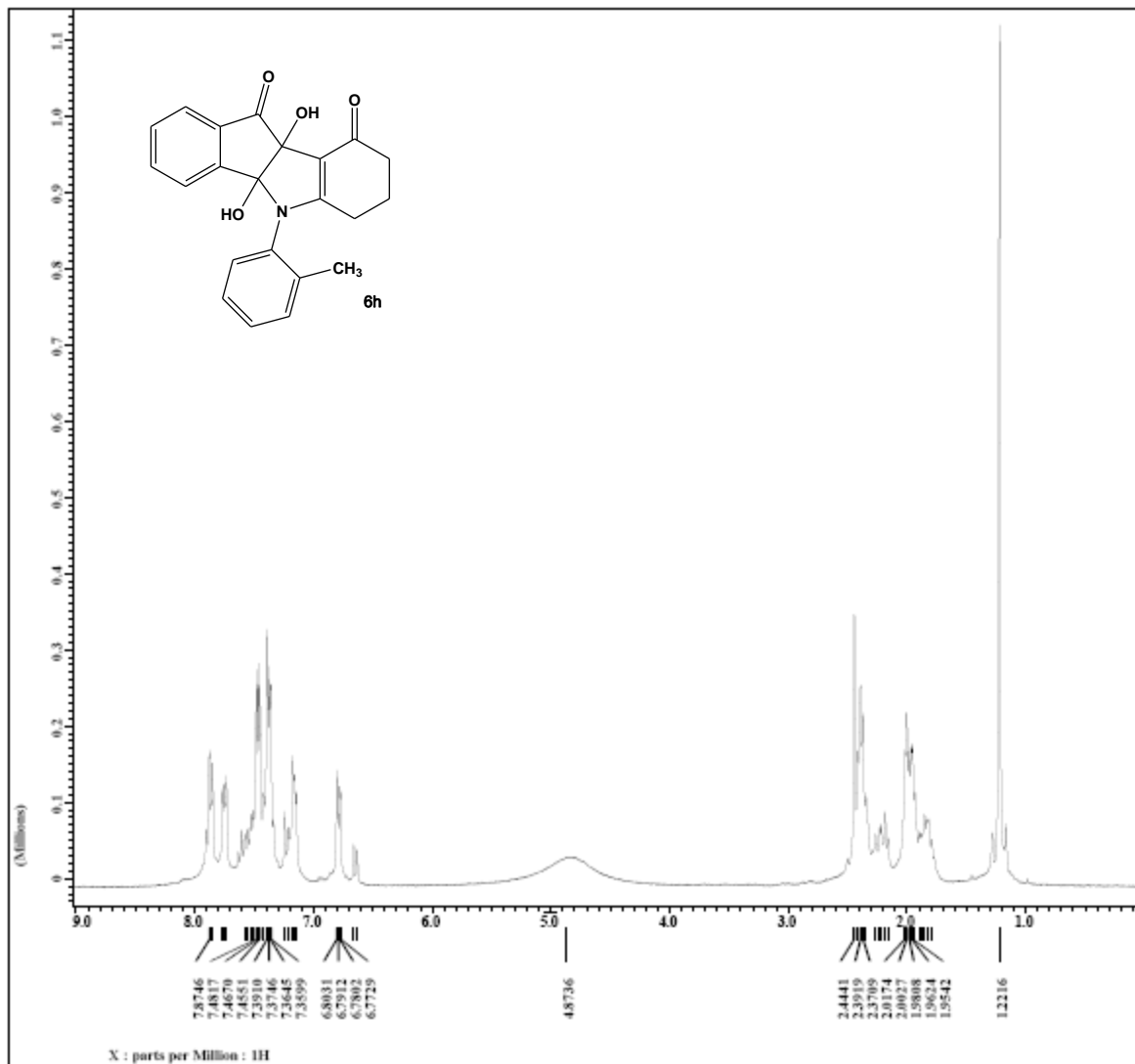


filename = jcharris5729-13c-3.
 author = rmlab
 experiment = single pulse dec
 sample_id = jcharris5729
 solvent = CDCl3
 creation_time = 24-MAR-2013 20:21:56
 revision_time = 2-MAR-2015 17:39:22
 current_time = 2-MAR-2015 17:39:39

content = single pulse with exc
 data_format = 1d cmv1mx
 bin_size = 32768
 bin_title = 13c
 bin_units = [ppm]
 dimensions = x
 site = Eclipse+ 400
 spectrometer = MSL-400

field_strength = 6.345446 [T] (270 [kHz])
 x_acq_duration = 1.9267584 [s]
 x_domain = 13c
 x_freq = 67.93330993 [kHz]
 x_offset = 100 [ppm]
 x_points = 32768
 x_procscans = 4
 x_resolution = 0.51900643 [Hz]
 x_sweep = 17.00680272 [kHz]
 ifr_domain = 1s
 ifr_freq = 270.16608944 [kHz]
 ifr_offset = 5 [ppm]
 clipped = FALSE
 mod_return = 1
 scans = 8395
 total_scans = 8395

x_90_width = 7.8 [us]
 x_acq_time = 1.9267584 [s]
 x_angle = 30 [deg]
 x_pulse = 2.6 [us]
 initial_wait = 1 [s]
 phase_preset = 3 [us]
 recvr_gain = 15
 relaxation_delay = 1 [s]
 temp_get = 27 [deg]
 unblank_time = 2 [us]

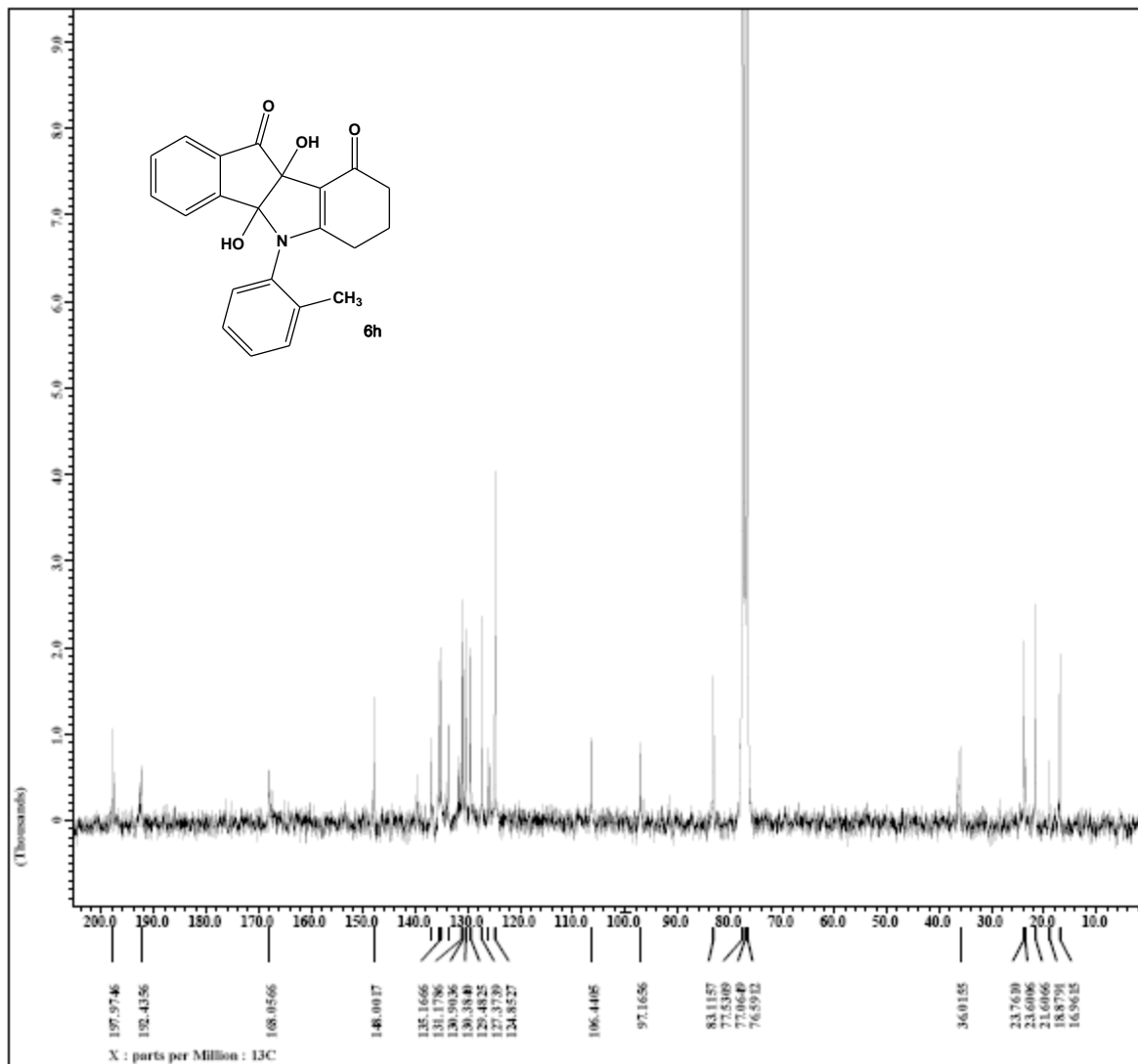


filename = jcharrism2015-1h-4.j
 author = rmlab
 experiment = single pulse exp
 sample id = jcharrism2015
 solvent = CDCl3
 creation time = 16-MAR-2015 13:38:03
 revision time = 2-MAR-2015 17:50:33
 current time = 2-MAR-2015 17:50:45

content = single pulse experiment
 data format = 1d cmv1.mz
 bin size = 16384
 bin title = 1h
 bin units = [ppm]
 dimensions = x
 site = Eclipse 400
 spectrometer = JEOL

field strength = 6.345446 [T] (270 [kHz])
 x acq duration = 4.0419328 [s]
 x domain = 1h
 x freq = 270.16608944 [kHz]
 x offset = 5 [ppm]
 x points = 16384
 x prescans = 0
 x resolution = 0.24740639 [Hz]
 x sweep = 4.05350628 [kHz]
 clipped = FALSE
 mod return = 1
 scans = 16
 total scans = 16

x 90 width = 11.7 [us]
 x acq time = 4.0419328 [s]
 x angle = 45 [deg]
 x pulse = 5.65 [us]
 initial wait = 1 [s]
 phase preset = 3 [us]
 recvr gain = 15
 relaxation delay = 4 [s]
 temp set = 17.3 [deg]
 unblank time = 2 [us]



filename = jcharrism2015-13c-3.
 author = rmlab
 experiment = single pulse dec
 sample id = jcharrism2015
 solvent = CDCl₃
 creation time = 16-MAR-2015 20:21:17
 revision time = 2-MAR-2015 17:51:39
 current time = 2-MAR-2015 17:51:52

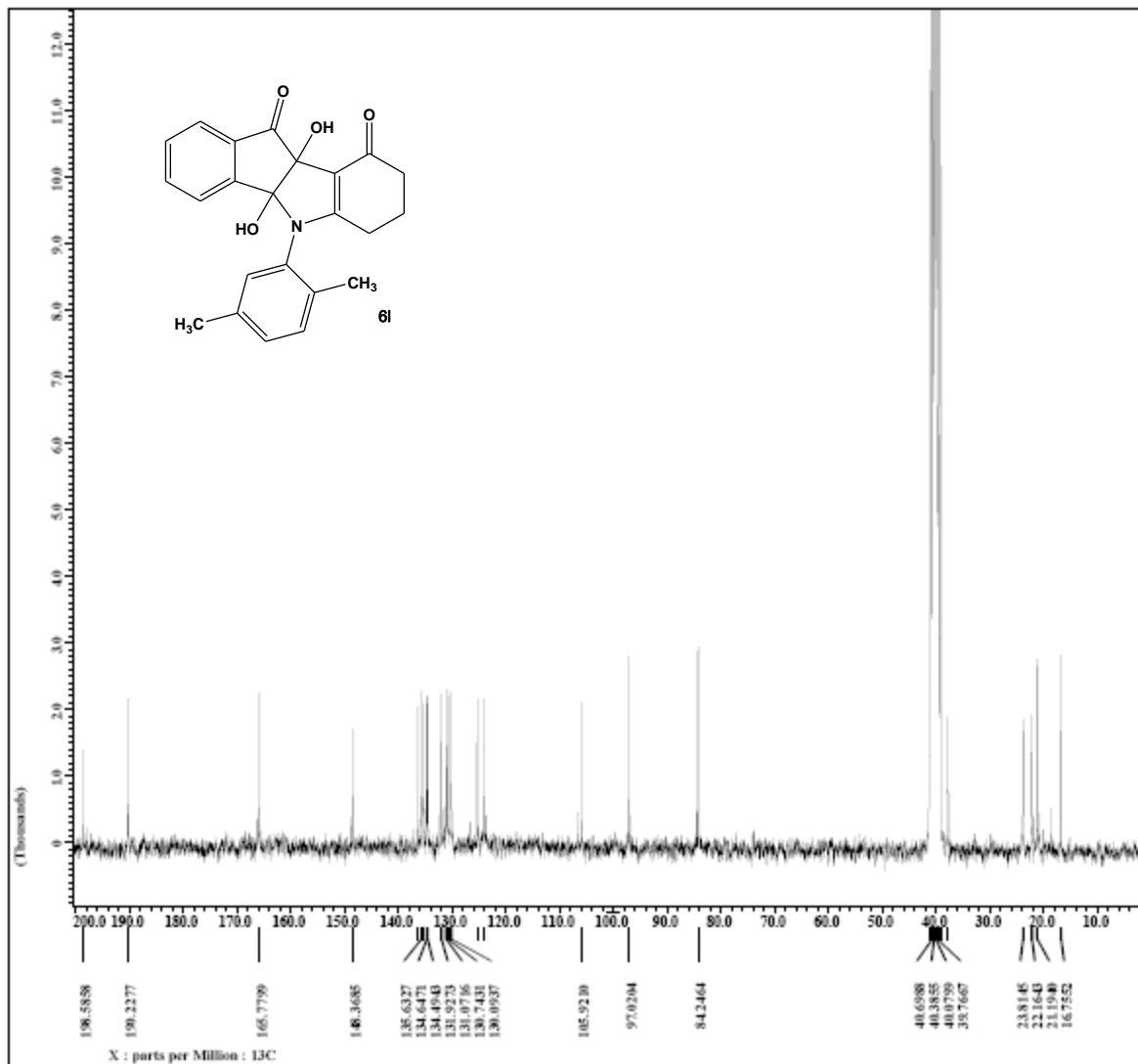
content = single pulse with arc
 data format = 1d cmv1mx
 bin size = 32768
 bin title = 13c
 bin units = [ppm]
 dimensions = x
 site = Eclipse+ 400
 spectrometer = MSL-400

field strength = 6.345446 [T] (270 [kHz])
 x acq duration = 1.9267584 [s]
 x domain = 13c
 x freq = 67.93330993 [kHz]
 x offset = 100 [ppm]
 x points = 32768
 x prescans = 4
 x resolution = 0.51900643 [Hz]
 x sweep = 17.00680272 [kHz]
 ifr domain = 1s
 ifr freq = 270.16608944 [kHz]
 ifr offset = 5 [ppm]
 clipped = FALSE
 mod return = 1
 scans = 8242
 total scans = 8242

x 90 width = 7.8 [us]
 x acq time = 1.9267584 [s]
 x angle = 30 [deg]
 x pulse = 2.6 [us]
 initial wait = 1 [s]
 phase preset = 3 [us]
 recvr gain = 15
 relaxation delay = 1 [s]
 temp gat = 25.7 [deg]
 unblank time = 2 [us]



```
x_90_width      = 11.7 [us]
x_acq_time      = 4.0419328 [s]
x_angle         = 45 [deg]
x_pulse         = 5.65 [Us]
initial_wait    = 1[s]
phase_preset    = 3[us]
recvr_gain      = 19
relaxation_delay = 4[s]
temp_get        = 20.3 [dc]
unblank_time    = 2[us]
```

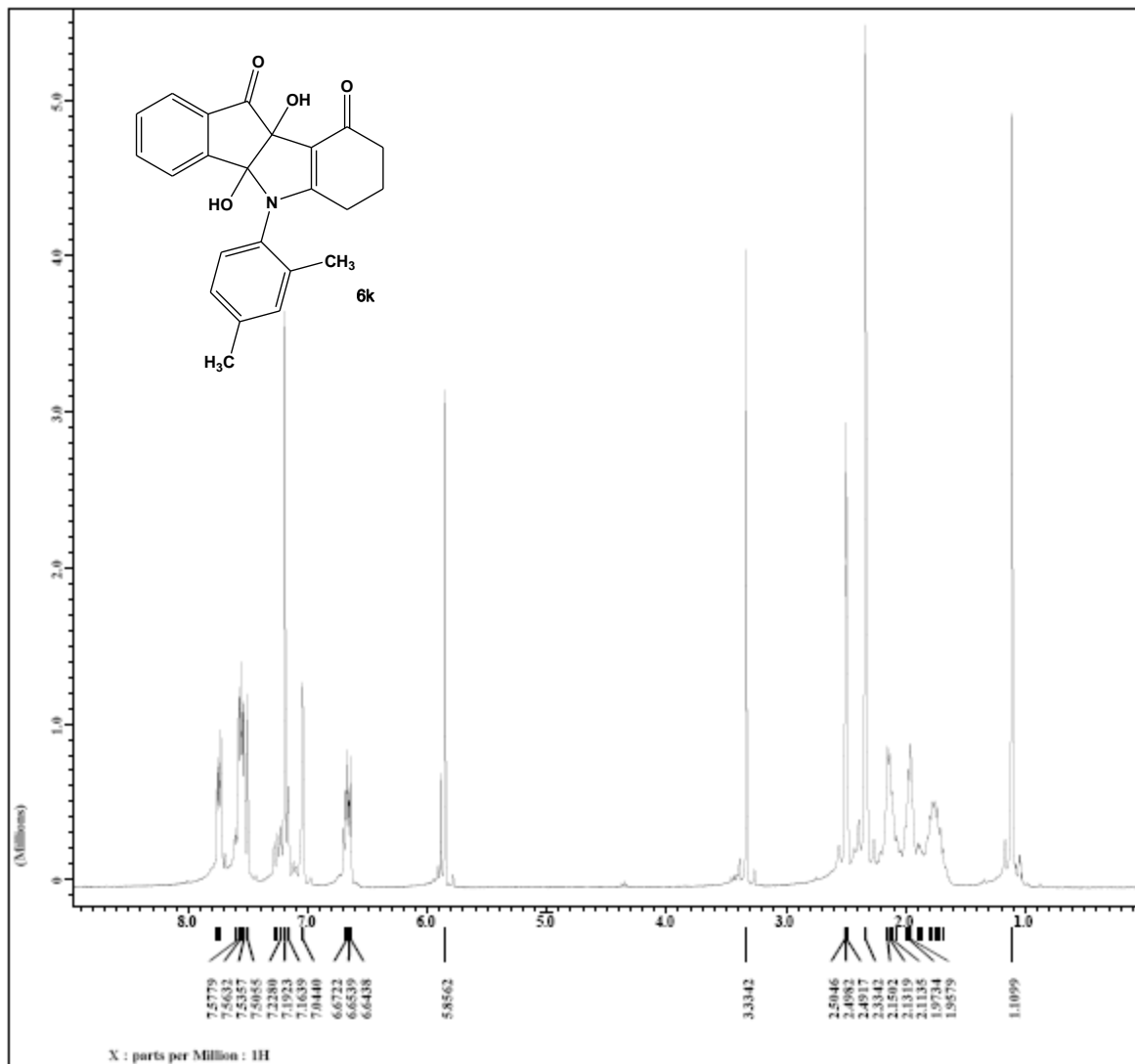


filename = jcharrism-2111-13c-2
 author = allrica
 experiment = single pulse dec
 sample_id = jcharrism-2111
 solvent = dmso-d6
 creation_time = 26-MAR-2009 02:08:29
 revision_time = 2-MAR-2015 18:00:06
 current_time = 2-MAR-2015 18:00:26

content = single pulse with arc
 data_format = 1d cmv1mx
 data_size = 32768
 data_title = 13c
 data_units = [ppm]
 dimensions = x
 site = eclipse+ 400
 spectrometer = delta_400

field_strength = 6.345446 [T] (270 [kHz])
 x_acq_duration = 1.9267584 [s]
 x_domain = 13c
 x_freq = 67.93330993 [kHz]
 x_offset = 100 [ppm]
 x_points = 32768
 x_preprocs = 4
 x_resolution = 0.51900643 [Hz]
 x_sweep = 17.00680272 [kHz]
 ifr_domain = 1s
 ifr_freq = 270.16608944 [kHz]
 ifr_offset = 5 [ppm]
 clipped = false
 mod_return = 1
 scans = 6000
 total_scans = 6000

x_90_width = 7.8 [us]
 x_acq_time = 1.9267584 [s]
 x_angle = 30 [deg]
 x_pulse = 2.6 [us]
 initial_wait = 1 [s]
 phase_reset = 3 [us]
 recvr_gain = 15
 relaxation_delay = 1 [s]
 temp_gat = 21.2 [deg]
 unblank_time = 2 [us]

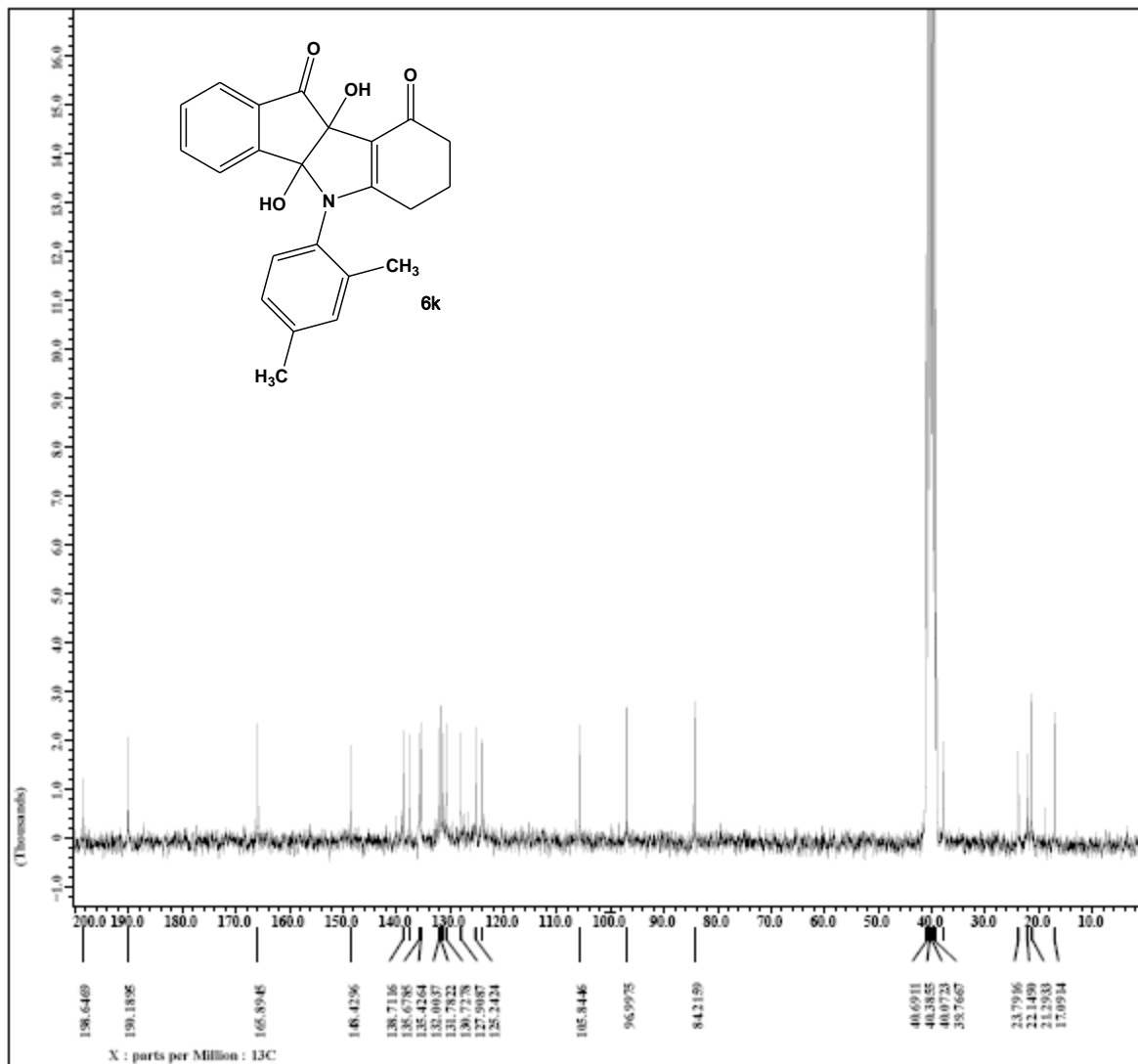


filename = jcharrism-2513-in-3.
 author = allrica
 experiment = single pulse exp
 sample_id = jcharrism-2513
 solvent = DMSO-d6
 creation_time = 25-MAR-2009 15:44:57
 revision_time = 2-MAR-2015 18:02:08
 current_time = 2-MAR-2015 18:02:15

content = single pulse experiment
 data_format = 1D COMET.MX
 bin_size = 16384
 bin_title = 1H
 bin_units = [ppm]
 dimensions = 1
 site = Eclipse+ 400
 spectrometer = DUEVA.MX

field_strength = 6.345446 [T] (270 [kHz])
 x_acq_duration = 4.0419328 [s]
 x_domain = 1H
 x_freq = 270.16608944 [kHz]
 x_offset = 5 [ppm]
 x_points = 16384
 x_preprocs = 0
 x_resolution = 0.24740639 [Hz]
 x_sweep = 4.05350628 [kHz]
 clipped = FALSE
 mod_return = 1
 scans = 16
 total_scans = 16

x_90_width = 11.7 [us]
 x_acq_time = 4.0419328 [s]
 x_angle = 45 [deg]
 x_pulse = 5.65 [us]
 initial_wait = 1 [s]
 phase_offset = 3 [us]
 recvr_gain = 19
 relaxation_delay = 4 [s]
 temp_get = 20.7 [deg]
 unblank_time = 2 [us]



filename = jcharrism-2513-13c-2
 author = allrica
 experiment = single pulse dec
 sample_id = jcharrism-2513
 solvent = dmso-d6
 creation_time = 25-MAR-2009 18:12:18
 revision_time = 2-MAR-2015 18:02:48
 current_time = 2-MAR-2015 18:03:02

content = single pulse with ero
 data_format = 1d cmv64mx
 bin_size = 32768
 bin_title = 13c
 bin_units = [ppm]
 dimensions = x
 site = eclipse+ 400
 spectrometer = delta_400

field_strength = 6.345446 [T] (270 [kHz])
 x_acq_duration = 1.9267584 [s]
 x_domain = 13c
 x_freq = 67.93330993 [kHz]
 x_offset = 100 [ppm]
 x_points = 32768
 x_procscans = 4
 x_resolution = 0.51900643 [ms]
 x_sweep = 17.00680272 [kHz]
 ifr_domain = 1s
 ifr_freq = 270.16608944 [kHz]
 ifr_offset = 5 [ppm]
 clipped = false
 mod_return = 1
 scans = 3000
 total_scans = 3000

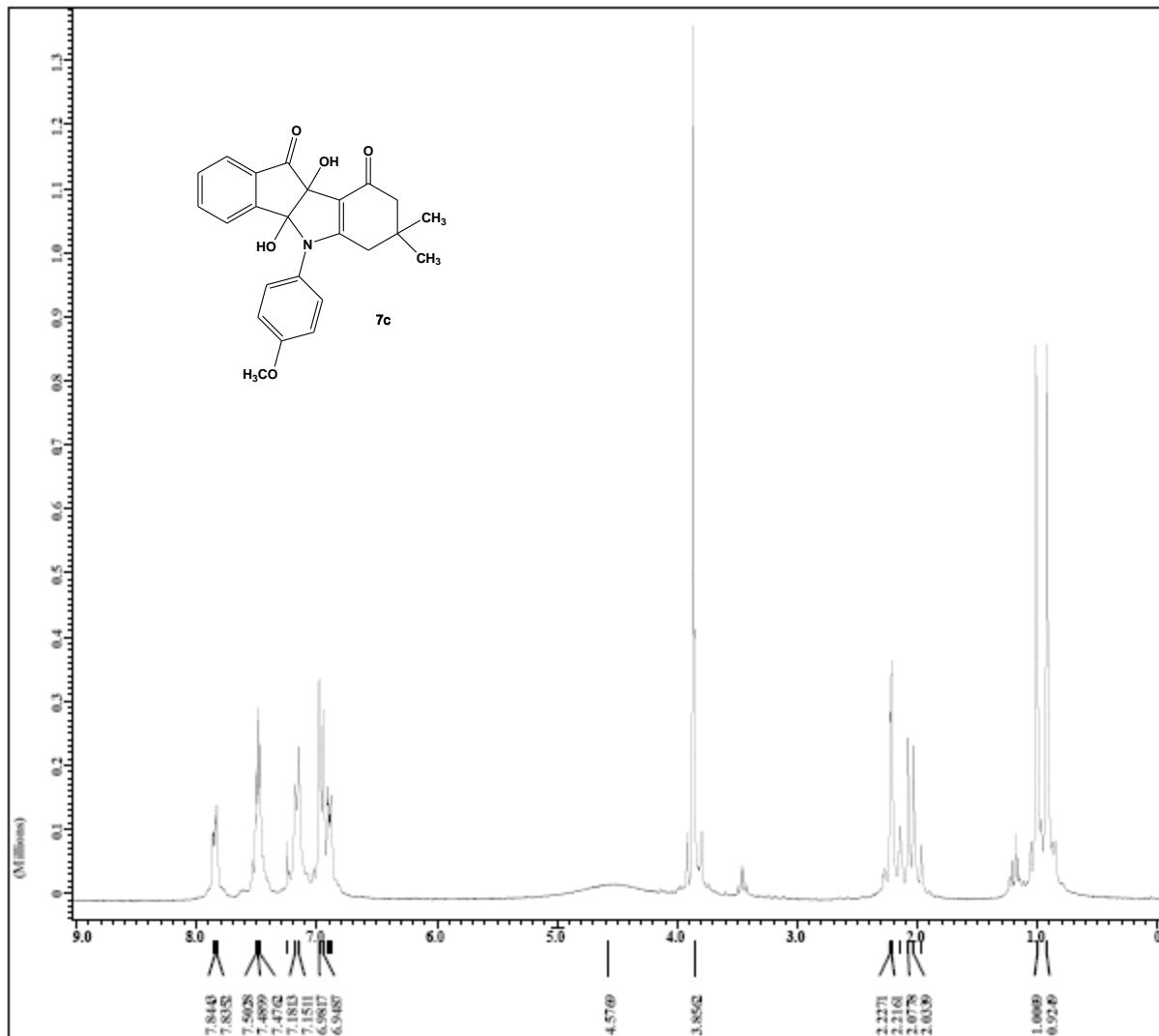
x_90_width = 7.8 [us]
 x_acq_time = 1.9267584 [s]
 x_angle = 30 [deg]
 x_pulse = 2.6 [us]
 initial_wait = 1 [s]
 phase_preset = 3 [us]
 recvr_gain = 15
 relaxation_delay = 1 [s]
 temp_gat = 21.3 [deg]
 unblank_time = 2 [us]



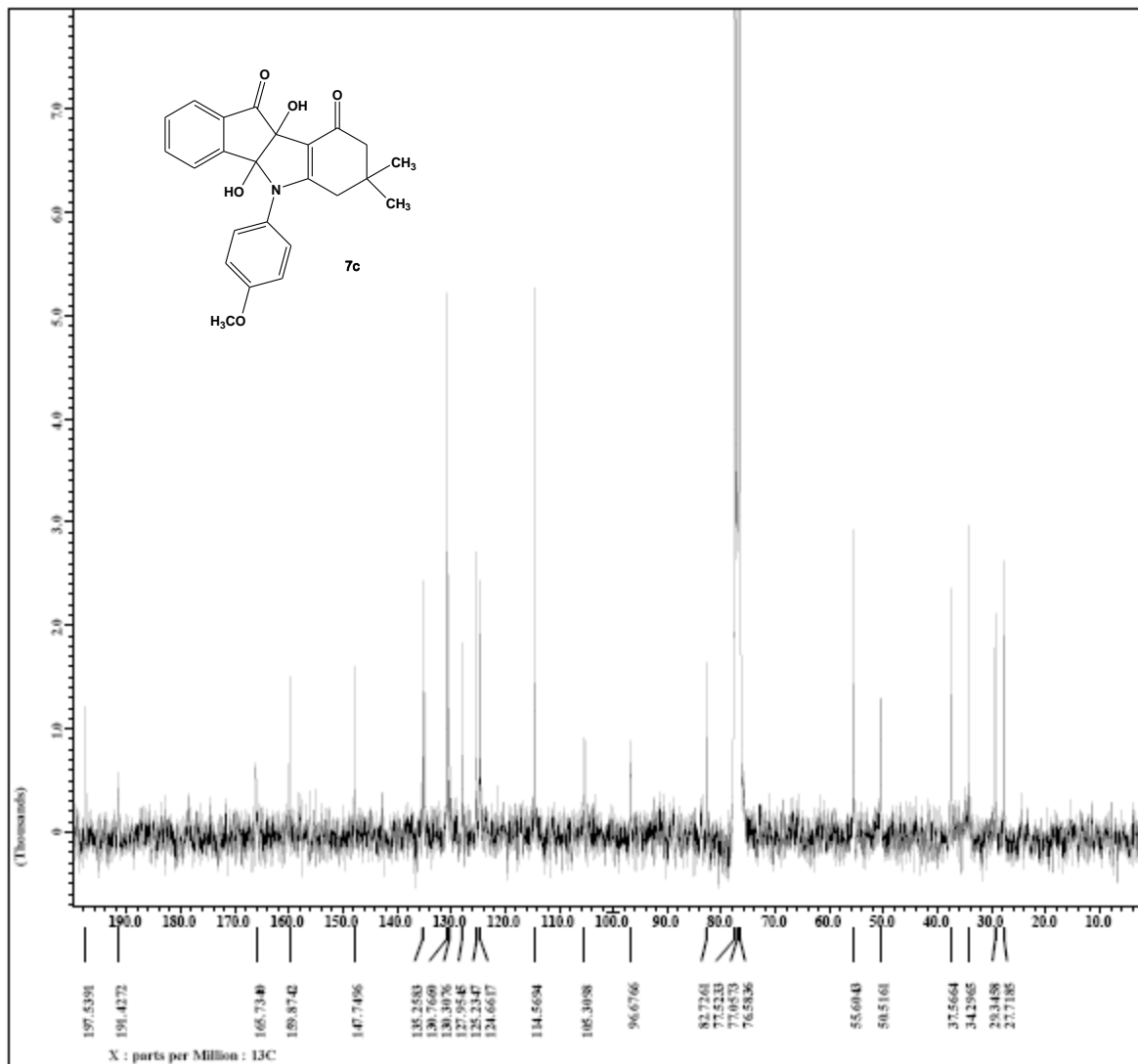
Filename = Jcharris2L202-1H-3.jd
 Author = runlab
 Experiment = single pulse.exp
 Sample_id = Jcharris2L202
 Solvent = CHLOROFORM-D
 Creation time = 30-DEC-2013 13:38:48
 Revision time = 2-MAR-2015 17:03:24
 Current_time = 2-MAR-2015 17:03:35

Content = Single Pulse Experiment
 Data_format = 1D COMPLEX
 Dim_size = 16384
 Dim_title = 1H
 Dim_units = [ppm]
 Dimensions = 1
 Site = Solipses+ 400
 Spectrometer = DELTA_NMR

Field_strength = 6.345446 [T] (270[MHz])
 F_acq_duration = 4.0419328 [s]
 F_domain = 1H
 F_freq = 270.16608844 [MHz]
 F_offset = 5 [ppm]
 F_points = 16384
 F_prescans = 0
 F_resolution = 0.24740639 [Hz]
 F_sweep = 4.05350628 [kHz]
 Clipped = FALSE
 Mod_return = 1
 Scans = 8
 Total_scans = 8
 F_90_width = 11.7 [us]
 F_acq_time = 4.0419328 [s]
 F_angle = 45 [deg]
 F_pulse = 5.85 [us]
 Initial_wait = 1 [s]
 Phase_preset = 3 [us]
 Recvr_gain = 15
 Relaxation_delay = 4 [s]
 Temp_set = 17.5 [dC]
 Unblank_time = 2 [us]



X : part: per Million : 1H

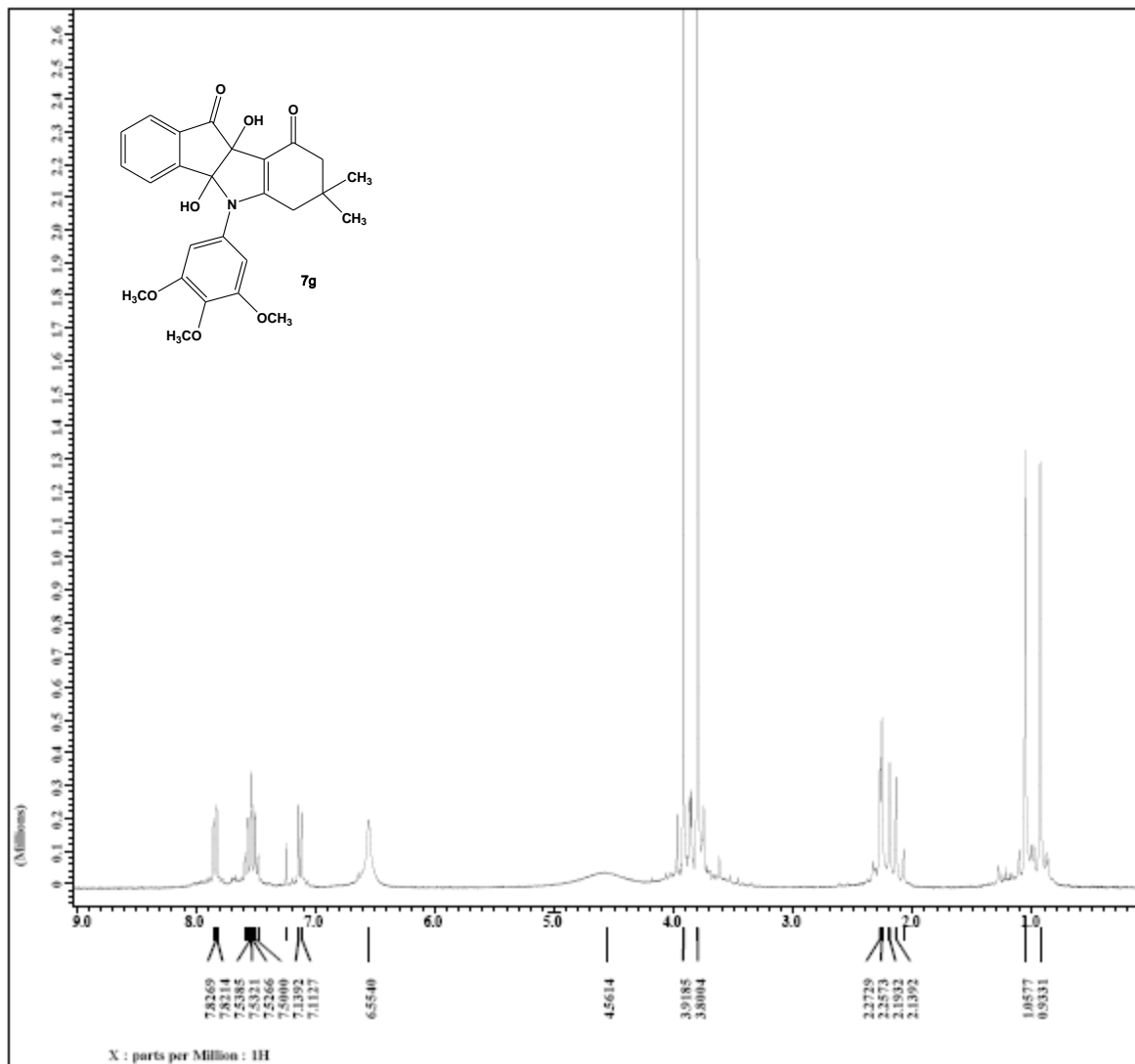


filename = jcharrison202-13c-3.j
 author = rmlab
 experiment = single pulse dec
 sample id = jcharrison202
 solvent = CDCl3
 creation time = 30-MAR-2013 20:08:57
 revision time = 2-MAR-2015 17:01:22
 current time = 2-MAR-2015 17:01:38

content = single pulse with exc
 data format = 1d cmv1mx
 bin size = 32768
 bin title = 13c
 bin units = [ppm]
 dimensions = x
 site = Eclipse+ 400
 spectrometer = MSL-400

field strength = 6.345446 [T] (270 [kHz])
 x acq duration = 1.9267584 [s]
 x domain = 13c
 x freq = 67.93330993 [kHz]
 x offset = 100 [ppm]
 x points = 32768
 x prescans = 4
 x resolution = 0.51900643 [Hz]
 x sweep = 17.00680272 [kHz]
 ifr domain = 1s
 ifr freq = 270.16608944 [kHz]
 ifr offset = 5 [ppm]
 clipped = FALSE
 mod return = 1
 scans = 7988
 total scans = 7988

x 90 width = 7.8 [us]
 x acq time = 1.9267584 [s]
 x angle = 30 [deg]
 x pulse = 2.6 [us]
 initial wait = 1 [s]
 phase preset = 3 [us]
 recvr gain = 15
 relaxation delay = 1 [s]
 temp gat = 26.7 [deg]
 unblank time = 2 [us]

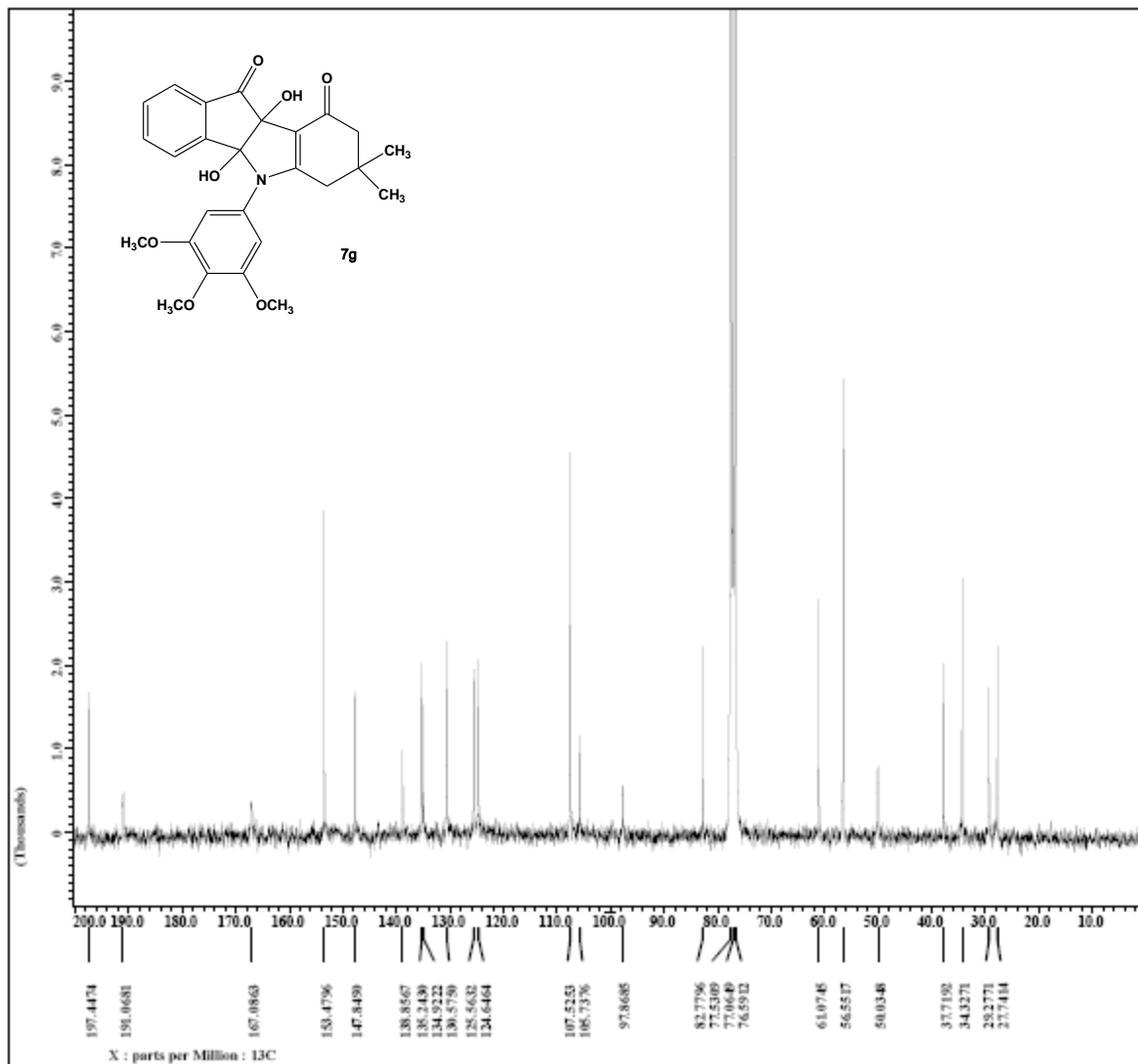


filename = jcharris01374-IN-5.jd
 author = rmlab
 experiment = single_pulse_exp
 sample_id = jcharris01374
 solvent = CDCl3
 creation_time = 3-MAR-2015 00:32:38
 revision_time = 3-MAR-2015 18:25:25
 current_time = 3-MAR-2015 18:25:26

content = single_pulse_experiment
 data_format = 1D_1D_NMR
 bin_size = 16384
 bin_title = 1D
 bin_units = [ppm]
 dimensions = 1
 site = Eclipse+ 400
 spectrometer = JEOL

field_strength = 6.345446 [T] (270 [kHz])
 x_acq_duration = 4.0419328 [s]
 x_domain = 1D
 x_freq = 270.16608944 [kHz]
 x_offset = 5 [ppm]
 x_points = 16384
 x_proscans = 0
 x_resolution = 0.24740639 [Hz]
 x_sweep = 4.05350628 [kHz]
 clipped = FALSE
 mod_return = 1
 scans = 8
 total_scans = 8

x_90_width = 11.7 [us]
 x_acq_time = 4.0419328 [s]
 x_angle = 45 [deg]
 x_pulse = 5.65 [us]
 initial_wait = 1 [s]
 phase_preset = 3 [us]
 recvr_gain = 15
 relaxation_delay = 4 [s]
 temp_get = 17.6 [deg]
 unblank_time = 2 [us]

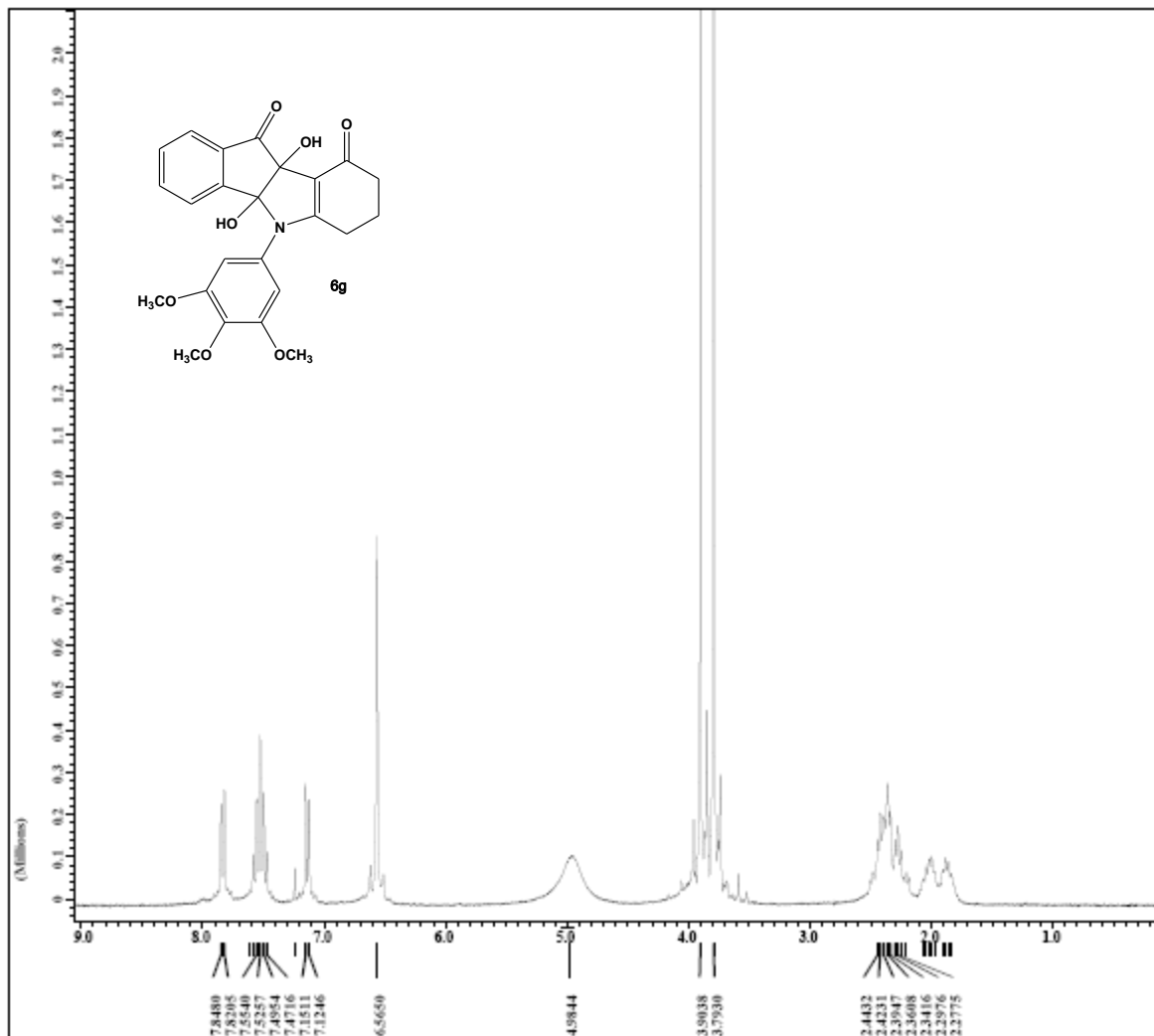


filename = Jcharrison374-13c-5.j
 Author = rmlab
 experiment = single pulse dec
 sample_id = Jcharrison374
 solvent = CDCl3
 creation_time = 3-MAR-2015 13:05:28
 revision_time = 4-MAR-2015 06:54:31
 current_time = 4-MAR-2015 06:54:55

content = single pulse with arc
 data_format = 1D 1D NMR
 data_size = 32768
 data_title = 13c
 data_units = [ppm]
 dimensions = 1
 site = Eclipse+ 400
 spectrometer = JEOL

field_strength = 6.345446 [T] (270 [kHz])
 x_acq_duration = 1.9267584 [s]
 x_domain = 13c
 x_freq = 67.93330993 [kHz]
 x_offset = 100 [ppm]
 x_points = 32768
 x_procs = 4
 x_resolution = 0.51900643 [Hz]
 x_sweep = 17.00680272 [kHz]
 ifr_domain = 13c
 ifr_freq = 270.16608944 [kHz]
 ifr_offset = 5 [ppm]
 clipped = FALSE
 mod_return = 1
 scans = 15416
 total_scans = 15416

x_90_width = 7.8 [us]
 x_acq_time = 1.9267584 [s]
 x_angle = 30 [deg]
 x_pulse = 2.6 [us]
 initial_wait = 1 [s]
 phase_reset = 3 [us]
 recvr_gain = 15
 relaxation_delay = 1 [s]
 temp_gat = 26 [deg]
 unblank_time = 2 [us]



X : parts per Million : 1H



```

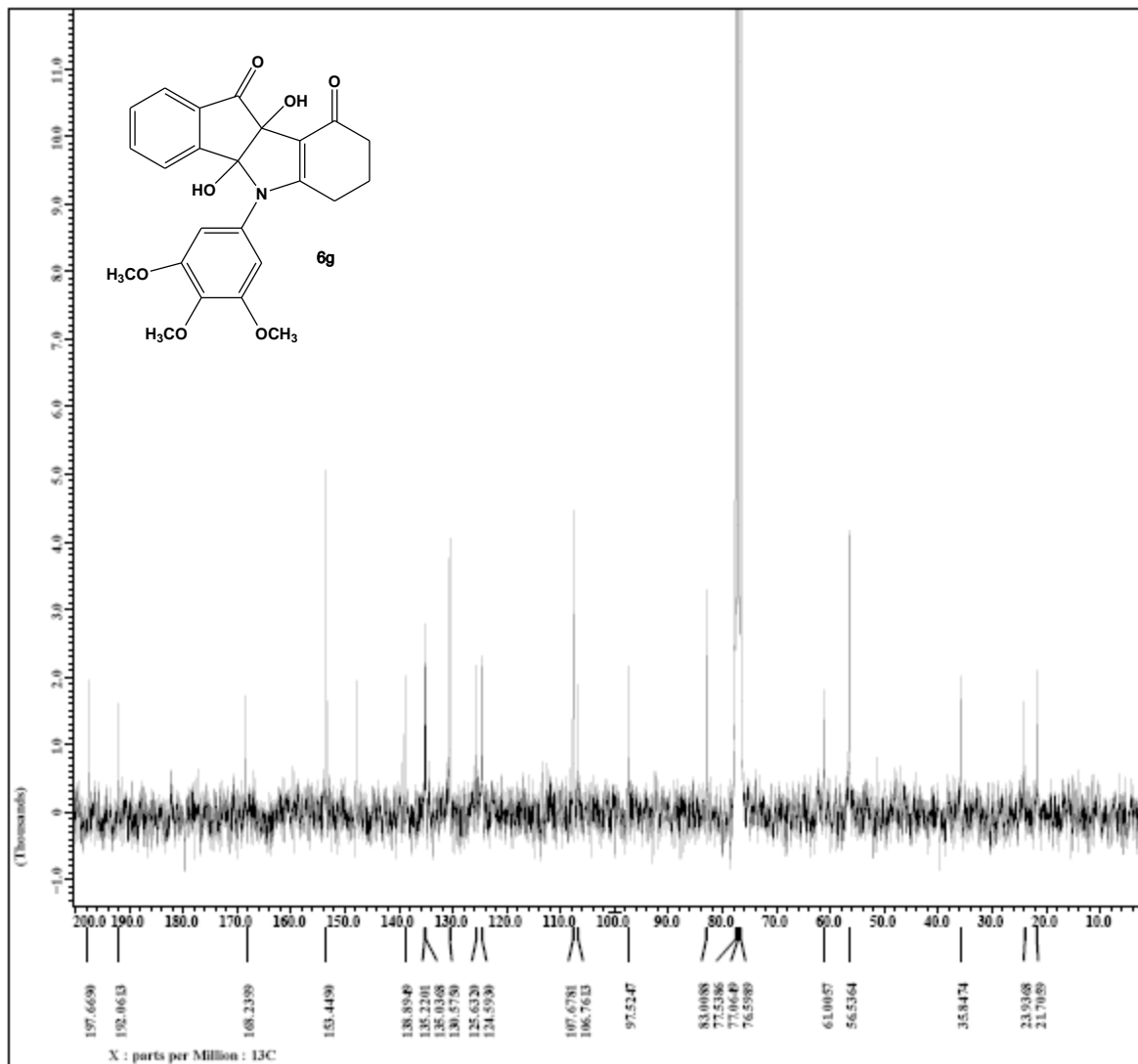
filename      = jcharris0366-1h-4.jd
author        = rmlab
experiment    = single_pulse.exp
sample_id     = jcharris0366
solvent       = CDCl3
creation_time  = 3-MAR-2015 20:14:18
revision_time  = 4-MAR-2015 14:04:04
current_time   = 4-MAR-2015 14:04:24

content       = single_pulse_experiment
data_format    = 1d_cmptlmx
bin_size      = 16384
bin_title     = 1h
bin_units     = [ppm]
dimensions    = x
site          = Eclipse+ 400
spectrometer   = DELTA_400

field_strength = 6.345446 [T] (270 [kHz])
x_acq_duration = 4.0419328 [s]
x_domain       = 1h
x_freq         = 270.16608944 [kHz]
x_offset       = 5 [ppm]
x_points       = 16384
x_proscans     = 0
x_resolution   = 0.24740639 [Hz]
x_sweep        = 4.05350628 [kHz]
clipped        = FALSE
mod_return     = 1
scans          = 8
total_scans    = 8

x_gd_width     = 11.7 [us]
x_acq_time     = 4.0419328 [s]
x_angle        = 45 [deg]
x_pulse        = 5.65 [us]
initial_wait   = 1 [s]
phase_preset   = 3 [us]
nucvr_gain     = 15
relaxation_delay = 4 [s]
temp_get       = 25 [degC]
unblank_time   = 2 [us]

```

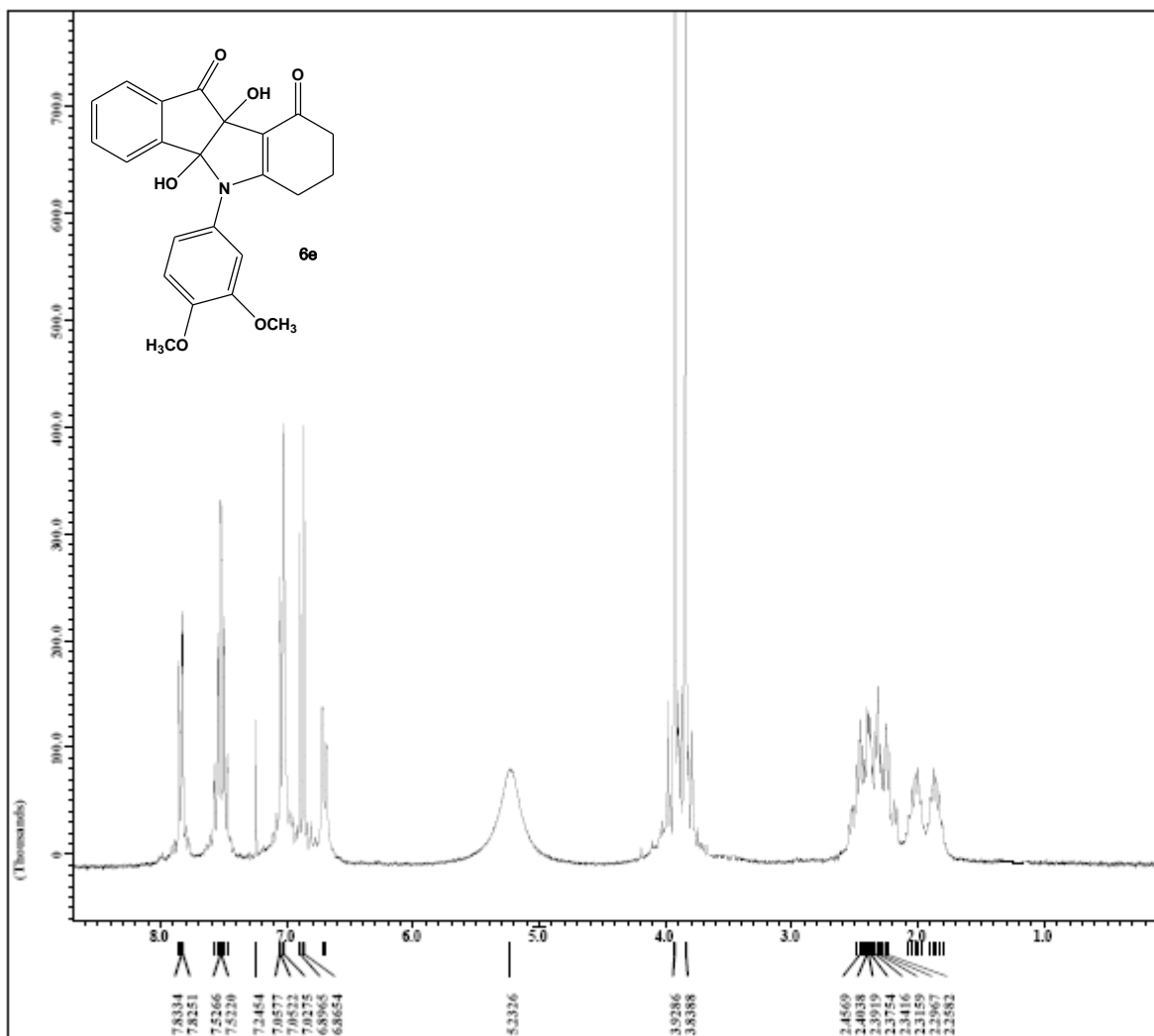


filename = jcharris0366-13c-3.j
 author = rmlab
 experiment = single pulse dec
 sample_id = jcharris0366
 solvent = CDCl3/FORM-D
 creation_time = 3-MAR-2015 20:12:52
 revision_time = 4-MAR-2015 14:02:03
 current_time = 4-MAR-2015 14:02:23

content = single pulse with arc
 data_format = 1d cmv16mx
 bin_size = 32768
 bin_title = 13c
 bin_units = [ppm]
 dimensions = x
 site = Eclipse+ 400
 spectrometer = Delta 400

field_strength = 6.345446 [T] (270 [kHz])
 x_acq_duration = 1.9267584 [s]
 x_domain = 13c
 x_freq = 67.93330993 [kHz]
 x_offset = 100 [ppm]
 x_points = 32768
 x_prescans = 4
 x_resolution = 0.51900643 [Hz]
 x_sweep = 17.00680272 [kHz]
 ifr_domain = 1s
 ifr_freq = 270.16608944 [kHz]
 ifr_offset = 5 [ppm]
 clipped = FALSE
 mod_return = 1
 scans = 8262
 total_scans = 8262

x_90_width = 7.8 [us]
 x_acq_time = 1.9267584 [s]
 x_angle = 30 [deg]
 x_pulse = 2.6 [us]
 initial_wait = 1 [s]
 phase_reset = 3 [us]
 recvr_gain = 15
 relaxation_delay = 1 [s]
 temp_gat = 25.7 [deg]
 unblank_time = 2 [us]



X : parts per Million : 1H

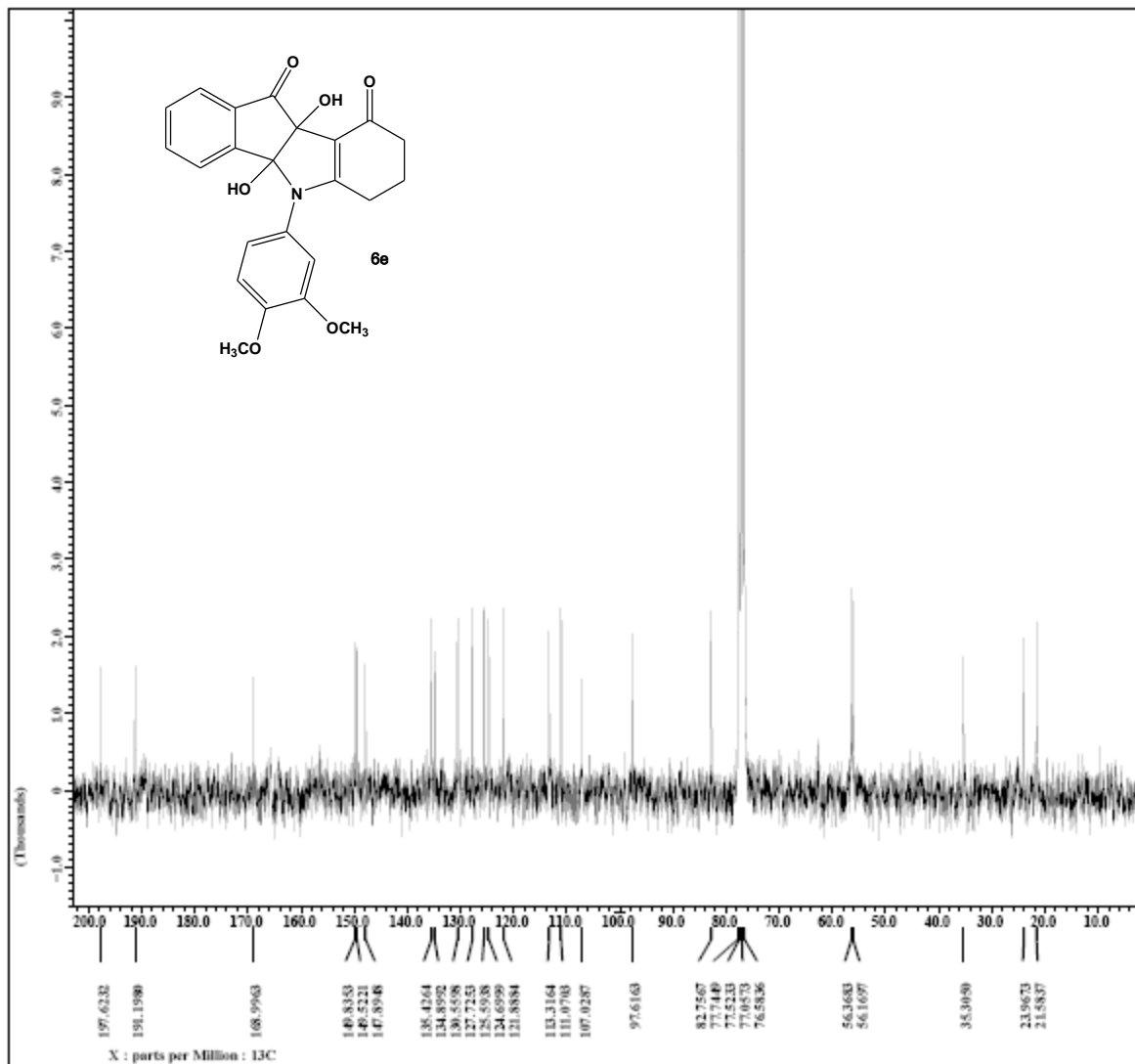


filename = jcharriseul367-in-4.jd
 Author = rmlab
 experiment = single pulse.exp
 sample_id = jcharriseul367
 solvent = CDCl3
 creation_time = 4-MAR-2015 22:18:41
 revision_time = 5-MAR-2015 16:08:22
 current_time = 5-MAR-2015 16:08:37

content = single pulse experiment
 data_format = 1D Complex
 bin_size = 16384
 bin_title = 1s
 bin_units = [ppm]
 dimensions = X
 site = mcp100-400
 spectrometer = mcp100-400

field_strength = 6.345446 [T] (270 [kHz])
 x_acq_duration = 4.0419328 [s]
 x_domain = 1s
 x_freq = 270.16608944 [kHz]
 x_offset = 5 [ppm]
 x_points = 16384
 x_prescans = 0
 x_resolution = 0.24740639 [Hz]
 x_sweep = 4.05350628 [kHz]
 mod_return = FALCON
 scans = 1
 total_scans = 16

x_90_width = 11.7 [us]
 x_acq_time = 4.0419328 [s]
 x_angle = 45 [deg]
 x_pulse = 5.65 [us]
 initial_wait = 1 [s]
 phase_reset = 3 [us]
 recvr_gain = 15
 relaxation_delay = 4 [s]
 ramp_get = 20 [dc]
 unblank_time = 2 [us]

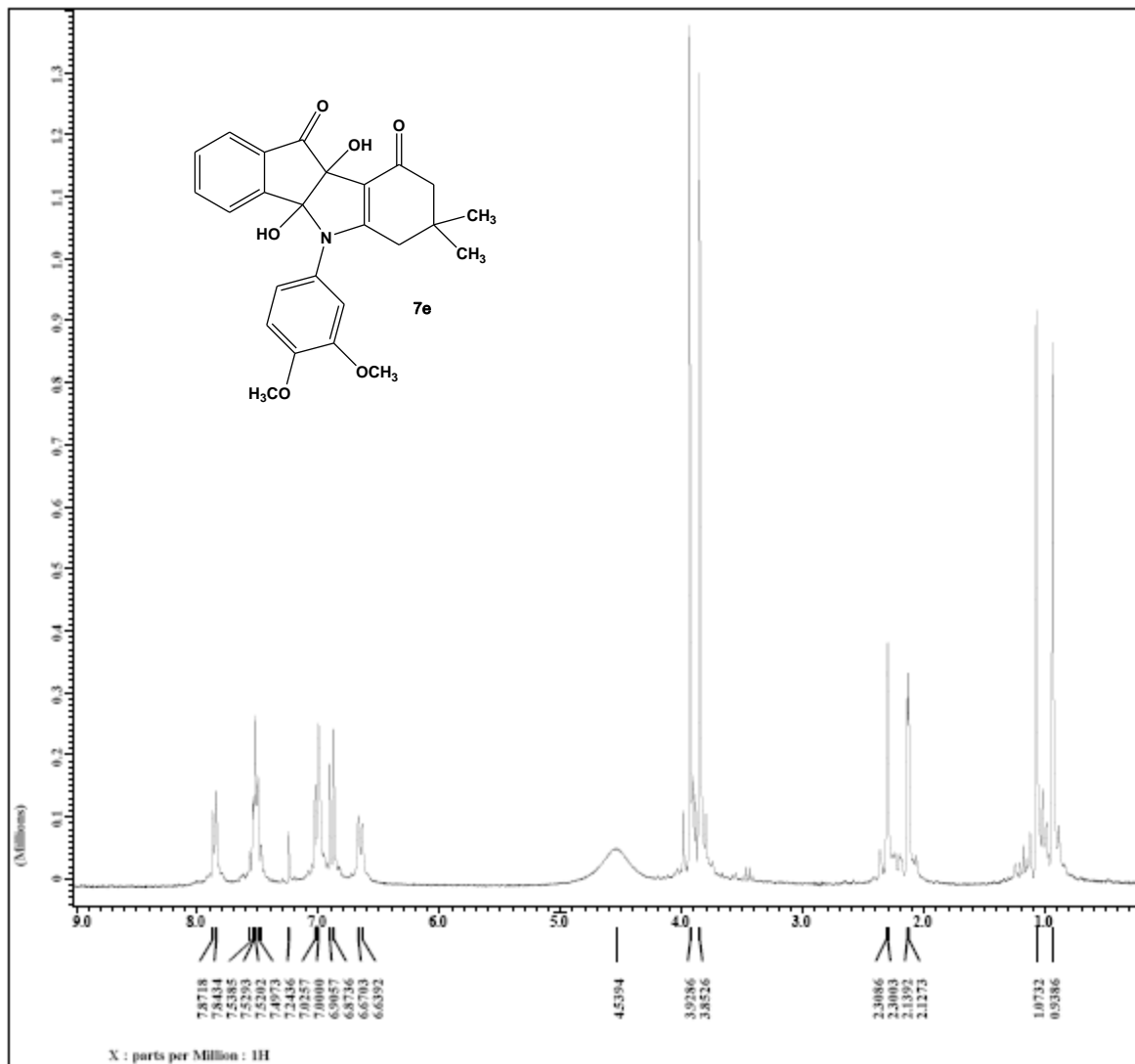


filename = JCHARRIS0367-13C-3.J
 author = rmlab
 experiment = single pulse dec
 sample id = JCHARRIS0367
 solvent = CDCl3/FORM-D
 creation time = 4-MAR-2015 22:07:59
 revision time = 5-MAR-2015 16:05:14
 current time = 5-MAR-2015 16:05:39

content = single pulse with exc
 data format = 1D COMPLEX
 bin size = 32768
 bin title = 13C
 bin units = [ppm]
 dimensions = x
 site = Eclipse+ 400
 spectrometer = DELTA 400

field strength = 6.345446 [T] (270 [kHz])
 x acq duration = 1.9267584 [s]
 x domain = 13C
 x freq = 67.93330993 [kHz]
 x offset = 100 [ppm]
 x points = 32768
 x prescans = 4
 x resolution = 0.51900643 [Hz]
 x sweep = 17.00680272 [kHz]
 ifr domain = 1H
 ifr freq = 270.16608944 [kHz]
 ifr offset = 5 [ppm]
 clipped = FALSE
 mod return = 1
 scans = 10000
 total scans = 10000

x 90 width = 7.8 [us]
 x acq time = 1.9267584 [s]
 x angle = 30 [deg]
 x pulse = 2.6 [us]
 initial wait = 1 [s]
 phase preset = 3 [us]
 recvr gain = 15
 relaxation delay = 1 [s]
 temp gat = 26.4 [deg]
 unblank time = 2 [us]

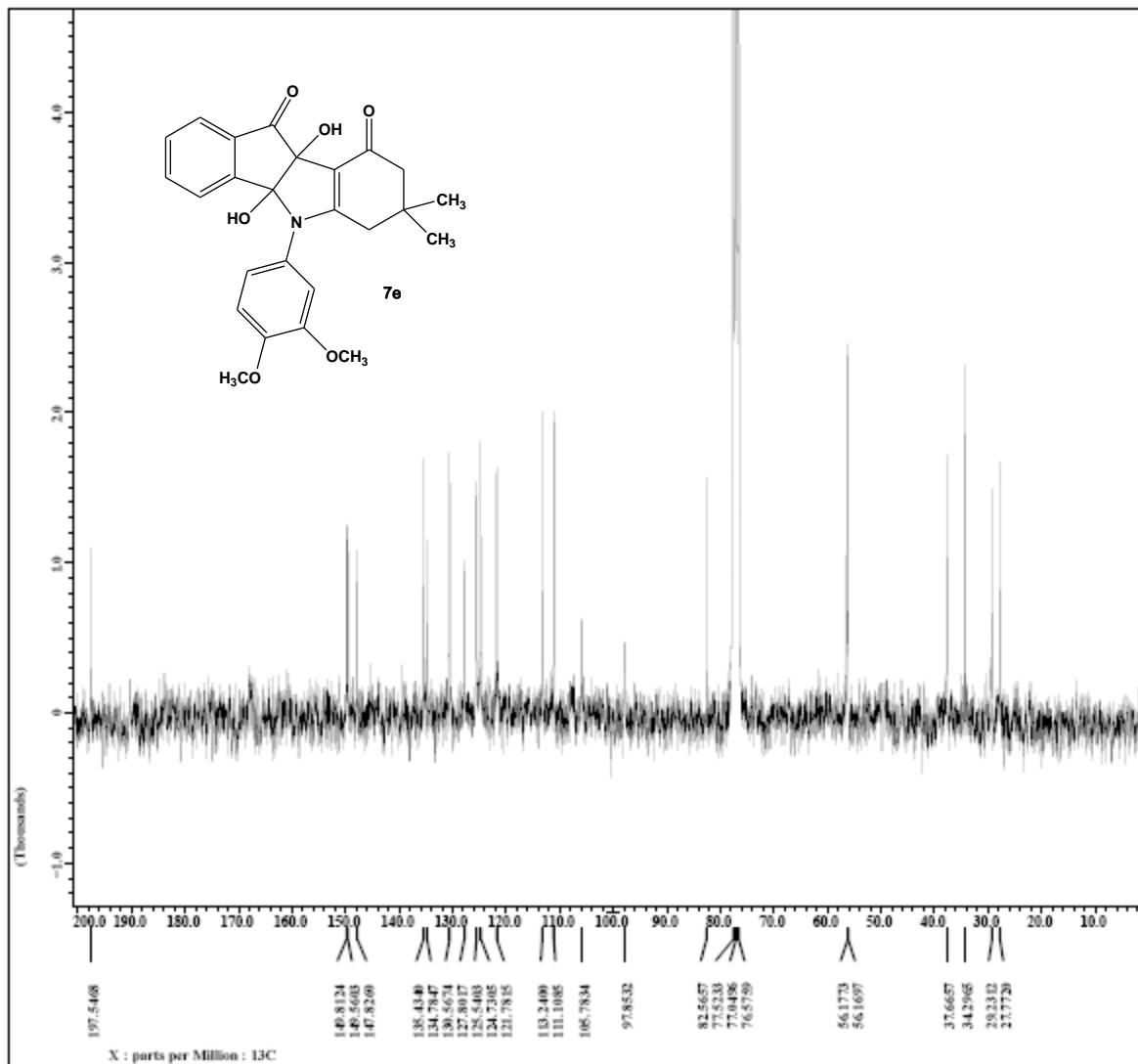


filename = jcharris0377-1h-5.jd
 author = rmlab
 experiment = single_pulse.exp
 sample_id = jcharris0377
 solvent = CDCl3
 creation_time = 5-MAR-2015 12:51:07
 revision_time = 6-MAR-2015 07:07:16
 current_time = 6-MAR-2015 07:07:25

content = single_pulse_experiment
 data_format = 1d_cmptmx
 bin_size = 16384
 bin_title = 1h
 bin_units = [ppm]
 dimensions = x
 site = Eclipse+ 400
 spectrometer = JEOL

field_strength = 6.345446 [T] (270 [kHz])
 x_acq_duration = 4.0419328 [s]
 x_domain = 1h
 x_freq = 270.16608944 [kHz]
 x_offset = 5 [ppm]
 x_points = 16384
 x_proscans = 0
 x_resolution = 0.24740639 [Hz]
 x_sweep = 4.05350628 [kHz]
 clipped = FALSE
 mod_return = 1
 scans = 16
 total_scans = 16

x_90_width = 11.7 [us]
 x_acq_time = 4.0419328 [s]
 x_angle = 45 [deg]
 x_pulse = 5.65 [us]
 initial_wait = 1 [s]
 phase_preset = 3 [us]
 recvr_gain = 15
 relaxation_delay = 4 [s]
 temp_get = 24.9 [deg]
 unblank_time = 2 [us]

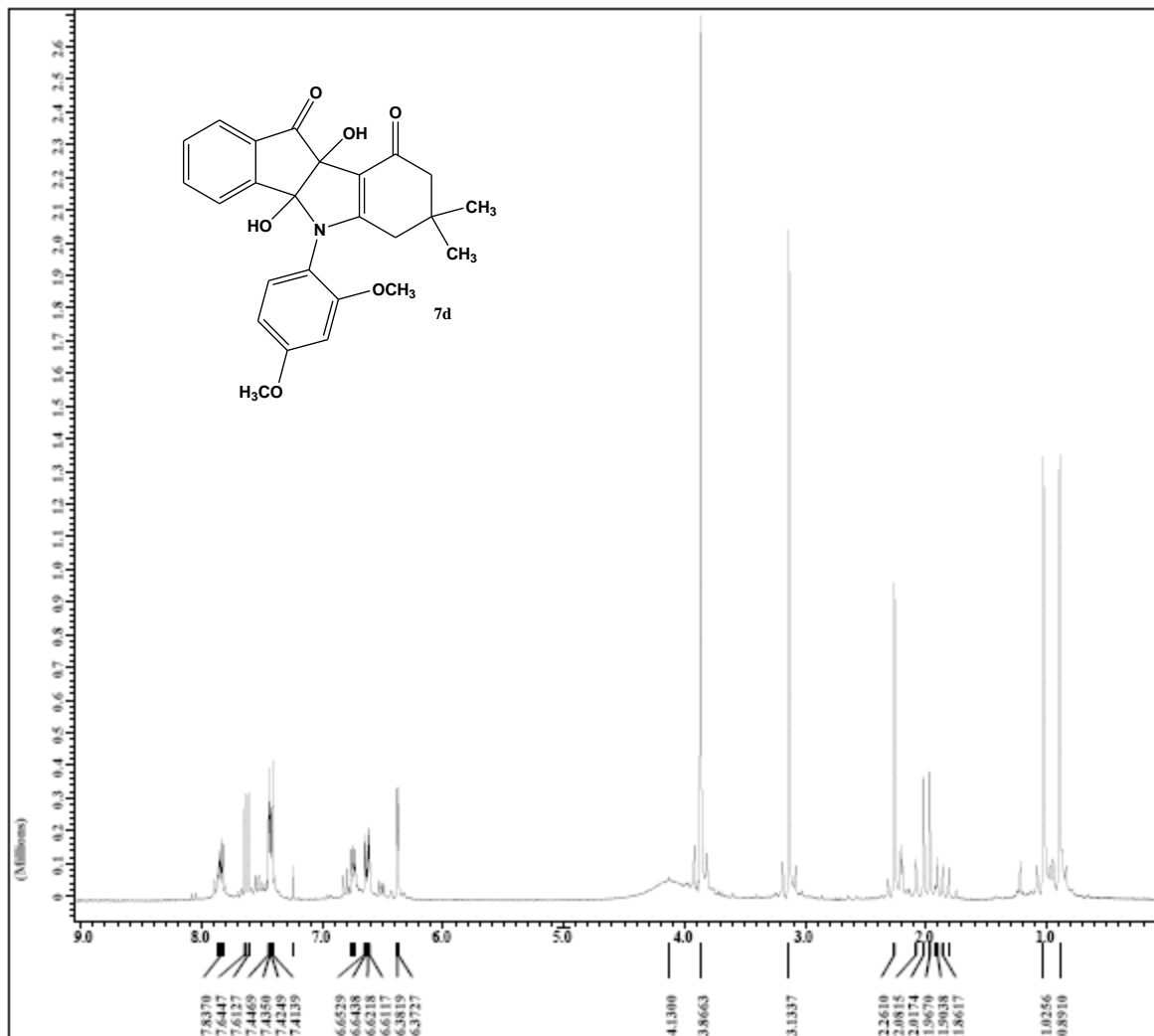


filename = jcharris0377-13c-3.j
 author = rmlab
 experiment = single pulse dsc
 sample id = jcharris0377
 solvent = CDCl3
 creation time = 5-MAR-2015 12:48:40
 revision time = 6-MAR-2015 07:05:20
 current time = 6-MAR-2015 07:05:28

content = single pulse with arc
 data format = 1d cmv1mx
 data size = 32768
 data title = 13c
 data units = [ppm]
 dimensions = x
 site = Eclipse+ 400
 spectrometer = Delta mm

field strength = 6.345446 [T] (270 [kHz])
 x acq duration = 1.9267584 [s]
 x domain = 13c
 x freq = 67.93330993 [kHz]
 x offset = 100 [ppm]
 x points = 32768
 x prescans = 4
 x resolution = 0.51900643 [Hz]
 x sweep = 17.00680272 [kHz]
 ifr domain = 1s
 ifr freq = 270.16608944 [kHz]
 ifr offset = 5 [ppm]
 clipped = FALSE
 mod return = 1
 scans = 16000
 total scans = 16000

x 90 width = 7.8 [us]
 x acq time = 1.9267584 [s]
 x angle = 30 [deg]
 x pulse = 2.6 [us]
 initial wait = 1 [s]
 phase preset = 3 [us]
 recvr gain = 15
 relaxation delay = 1 [s]
 temp gat = 26.7 [deg]
 unblank time = 2 [us]



X : parts per Million : 1H

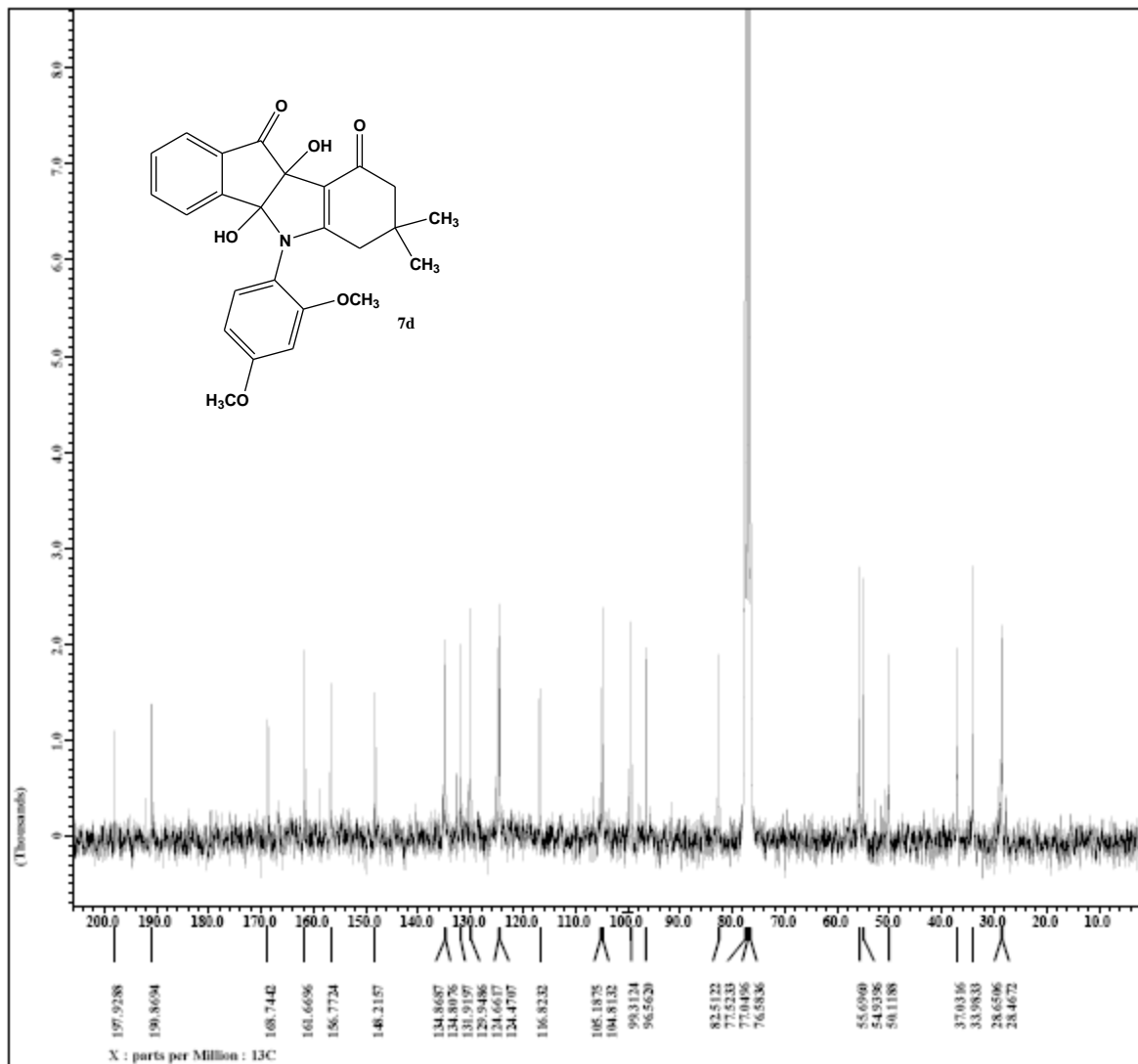


filename = JCHARRIS0377-IN-6.jd
 author = rmlab
 experiment = single_pulse_exp
 sample_id = JCHARRIS0377
 solvent = CDCl3
 creation_time = 5-MAR-2015 17:24:56
 revision_time = 6-MAR-2015 11:15:36
 current_time = 6-MAR-2015 11:15:39

content = single_pulse_experiment
 data_format = 1D_COSY_1H
 bin_size = 16384
 bin_title = 1H
 bin_units = [ppm]
 dimensions = 2
 site = Eclipse+ 400
 spectrometer = JEOL_400

field_strength = 6.345446 [T] (270 [kHz])
 x_acq_duration = 4.0419328 [s]
 x_domain = 1H
 x_freq = 270.16608944 [kHz]
 x_offset = 5 [ppm]
 x_points = 16384
 x_proscans = 0
 x_resolution = 0.24740639 [Hz]
 x_sweep = 4.05350628 [kHz]
 clipped = FALSE
 mod_return = 1
 scans = 16
 total_scans = 16

x_90_width = 11.7 [us]
 x_acq_time = 4.0419328 [s]
 x_angle = 45 [deg]
 x_pulse = 5.65 [us]
 initial_wait = 1 [s]
 phase_preset = 3 [us]
 recvr_gain = 15
 relaxation_delay = 4 [s]
 temp_get = 24.8 [deg]
 unblank_time = 2 [us]



filename = jcharris0367-13c-3.j
 author = rmlab
 experiment = single pulse dsc
 sample_id = jcharris0367
 solvent = CDCl3
 creation_time = 5-MAR-2015 17:22:23
 revision_time = 6-MAR-2015 11:10:37
 current_time = 6-MAR-2015 11:16:09

content = single pulse with arc
 data_format = 1d cmv1mx
 bin_size = 32768
 bin_title = 13c
 bin_units = [ppm]
 dimensions = x
 site = Eclipse+ 400
 spectrometer = Delta 400

field_strength = 6.345446 [T] (270 [kHz])
 x_acq_duration = 1.9267584 [s]
 x_domain = 13c
 x_freq = 67.9336993 [kHz]
 x_offset = 100 [ppm]
 x_points = 32768
 x_procscans = 4
 x_resolution = 0.51900643 [Hz]
 x_sweep = 17.00680272 [kHz]
 xfr_domain = 1s
 xfr_freq = 270.16608944 [kHz]
 xfr_offset = 5 [ppm]
 clipped = FALSE
 mod_return = 1
 scans = 4950
 total_scans = 4950

x_90_width = 7.8 [us]
 x_acq_time = 1.9267584 [s]
 x_angle = 30 [deg]
 x_pulse = 2.6 [us]
 initial_wait = 1 [s]
 phase_offset = 3 [us]
 recvr_gain = 15
 relaxation_delay = 1 [s]
 temp_gat = 26.7 [deg]
 unblank_time = 2 [us]